ornl

OAK RIDGE NATIONAL LABORATORY

UNION CARBIDE

NUREG/CR-2968
ORNL/TM-8509

# Experiment Data Report for Multirod Burst Test (MRBT) Bundle B-4

A. W. Longest
R. H. Chapman
J. L. Crowley

Prepared for the U.S. Nuclear Regulatory Commission
Office of Nuclear Regulatory Research
Under Interagency Agreements DOE 40-551-75 and 40-552-75

OPERATED BY
UNION CARBIDE CORPORATION
FOR THE UNITED STATES
DEPARTMENT OF ENERGY

Printed in the United States of America. Available from
National Technical Information Service
U.S. Department of Commerce
5285 Port Royal Road, Springfield, Virginia 22161

Available from
GPO Sales Program
Division of Technical Information and Document Control
U.S. Nuclear Regulatory Commission
Washington, D.C. 20555

NUREG/CR-2968
ORNL/TM-8509
Dist. Category R3

Contract No. W-7405-eng-26

Engineering Technology Division

# EXPERIMENT DATA REPORT FOR MULTIROD BURST TEST (MRBT) BUNDLE B-4

A. W. Longest R. H. Chapman
J. L. Crowley

Manuscript Completed — November 10, 1982
Date Published — December 1982

Prepared for the
U.S. Nuclear Regulatory Commission
Office of Nuclear Regulatory Research
Under Interagency Agreements DOE 40-551-75 and 40-552-75

NRC Fin No. B0120

Prepared by the
OAK RIDGE NATIONAL LABORATORY
Oak Ridge, Tennessee 37830
operated by
UNION CARBIDE CORPORATION
for the
DEPARTMENT OF ENERGY

# CONTENTS

## LIST OF FIGURES

# LIST OF TABLES

# FOREWORD

Examination, analysis, and interpretation of a bundle test take place over a long period of time, and our practice has been to report progress and results as they become available. Dissemination of the information in this manner results in its being disjointed and scattered throughout several publications. This presents some problems to the users in that one is never sure if the information at hand is the most recent. Our intention is to alleviate some of these problems by (1) publication of a data report on each bundle test and (2) publication of analytic and interpretative reports when sufficient information has been developed.

Consistent with this intention, the objective of this data report is to provide a reference source of information and results obtained during the B-4 test and from pretest and posttest examination of the test array. We believe the data presented herein, consisting of plots, tabulations, and photographs, are necessary for analysis and interpretation of the test. A decision was made that the data should be presented with a minimum of interpretation and that analysis or "second generation" data, such as comparative temperature vs time plots, should be excluded.

This report is derived from research performed by the Multirod Burst Test (MRBT) Program at Oak Ridge National Laboratory (ORNL). This research is sponsored by the Division of Accident Evaluation of the Nuclear Regulatory Commission, and the results are published routinely in a series of progress reports, topical reports and papers, quick-look reports, and data reports.

Progress reports published by the MRBT Program include:

| NUREG Report No. | ORNL Report No. | Period covered |
|---|---|---|
| | ORNL/TM-4729 | July–September 1974 |
| | ORNL/TM-4805 | October–December 1974 |
| | ORNL/TM-4914 | January–March 1975 |
| | ORNL/TM-5021 | April–June 1975 |
| | ORNL/TM-5154 | July–September 1975 |
| | ORNL/NUREG/TM-10 | October–December 1975 |
| | ORNL/NUREG/TM-36 | January–March 1976 |
| | ORNL/NUREG/TM-74 | April–June 1976 |
| | ORNL/NUREG/TM-77 | July–September 1976 |
| | ORNL/NUREG/TM-95 | October–December 1976 |
| | ORNL/NUREG/TM-108 | January–March 1977 |
| | ORNL/NUREG/TM-135 | April–June 1977 |
| NUREG/CR-0103 | ORNL/NUREG/TM-200 | July–December 1977 |
| NUREG/CR-0225 | ORNL/NUREG/TM-217 | January–March 1978 |
| NUREG/CR-0398 | ORNL/NUREG/TM-243 | April–June 1978 |
| NUREG/CR-0655 | ORNL/NUREG/TM-297 | July–December 1978 |
| NUREG/CR-0817 | ORNL/NUREG/TM-323 | January–March 1979 |
| NUREG/CR-1023 | ORNL/NUREG/TM-351 | April–June 1979 |
| NUREG/CR-1450 | ORNL/NUREG/TM-392 | July–December 1979 |
| NUREG/CR-1883 | ORNL/NUREG/TM-426 | January–June 1980 |
| NUREG/CR-1919 | ORNL/NUREG/TM-436 | July–December 1980 |

| | | |
|---|---|---|
| NUREG/CR-2366, Vol. 1 | ORNL/TM-8058 | January-June 1981 |
| NUREG/CR-2366, Vol. 2 | ORNL/TM-8190 | July-December 1981 |
| NUREG/CR-2911 | ORNL/TM-8485 | January-June 1982 |

Topical reports and papers pertaining to research and development carried out by this program are:


1. R. H. Chapman (comp.), *Characterization of Zircaloy-4 Tubing Procured for Fuel Cladding Research Programs*, ORNL/NUREG/TM-29 (July 1976).

2. W. E. Baucum and R. E. Dial, *An Apparatus for Spot Welding Sheathed Thermocouples to the Inside of Small-Diameter Tubes at Precise Locations*, ORNL/NUREG/TM-33 (August 1976).

3. W. A. Simpson, Jr., et al., *Infrared Inspection and Characterization of Fuel-Pin Simulators*, ORNL/NUREG/TM-55 (November 1976).

4. R. H. Chapman et al., *Effect of Creep Time and Heating Rate on Deformation of Zircaloy-4 Tubes Tested in Steam with Internal Heaters*, NUREG/CR-0343 (ORNL/NUREG/TM-245) (October 1978).

5. J. F. Mincey, *Steady-State Axial Pressure Losses Along the Exterior of Deformed Fuel Cladding: Multirod Burst Test (MRBT) Bundles B-1 and B-2*, NUREG/CR-1011 (ORNL/NUREG/TM-350) (January 1980).

6. R. W. McCulloch, P. T. Jacobs, and D. L. Clark, *Development of a Fabrication Procedure for the MRBT Fuel Simulator Based on the Use of Cold-Pressed Boron Nitride Preforms*, NUREG/CR-1111 (ORNL/NUREG/TM-362) (March 1980).

7. R. H. Chapman, J. V. Cathcart, and D. O. Hobson, "Status of Zircaloy Deformation and Oxidation Research at Oak Ridge National Laboratory," in *Proceedings of Specialists Meeting on the Behavior of Water Reactor Fuel Elements Under Accident Conditions, Spatind, Norway, September 13-16, 1976*, CSNI Report No. 13 (1977).

8. R. H. Chapman et al., "Zircaloy Cladding Deformation in a Steam Environment with Transient Heating," in *Proceedings of Fourth International Conference on Zirconium in the Nuclear Industry, Stratford-on-Avon, England, June 26-29, 1978*, ASTM STP 681 (1979).

9. R. T. Bailey, *Steady-State Pressure Losses for Multirod Burst Test (MRBT) Bundle B-5*, NUREG/CR-2597 (ORNL/Sub/80-40441/1) (April 1982).

10. R. L. Anderson, K. R. Carr, and T. G. Kollie, *Thermometry in the Multirod Burst Test Program*, NUREG/CR-2470 (ORNL/TM-8024) (March 1982).

11. A. W. Longest, J. L. Crowley, and R. H. Chapman, *Variations in Zircaloy-4 Cladding Deformation in Replicate LOCA Simulation Tests*, NUREG/CR-2810 (ORNL/TM-8413) (September 1982).

12. A. W. Longest, R. H. Chapman, and J. L. Crowley, "Boundary Effects on Zircaloy-4 Cladding Deformation in LOCA Simulation Tests," *Trans. Am. Nucl. Soc.* 41, 383 (1982).

13. R. H. Chapman, J. L. Crowley, and A. W. Longest, "Effect of Bundle Size on Cladding Deformation in LOCA Simulation Tests," paper presented at Sixth International Conference on Zirconium in the Nuclear Industry, Vancouver (B.C.), Canada, June 28–July 1, 1982.

The following limited-distribution quick-look and data reports have been issued by this program:

1. R. H. Chapman (comp.), *Quick-look Report on MRBT No. 1 4 x 4 Bundle Burst Test*, Internal Report ORNL/MRBT-2 (September 1977).

2. R. H. Chapman (comp.), *Quick-look Report on MRBT No. 2 4 x 4 Bundle Burst Test*, Internal Report ORNL/MRBT-3 (November 1977).

3. R. H. Chapman, *Quick-look Report on MRBT No. 3 4 x 4 Bundle Burst Test*, Internal Report ORNL/MRBT-4 (August 1978).

4. R. H. Chapman, *Quick-look Report on MRBT B-4 (6 x 6) Bundle Test*, Internal Report ORNL/MRBT-6 (February 1981).

5. R. H. Chapman et al., *Quick-look Report on MRBT B-5 (8 x 8) Bundle Test*, Internal Report ORNL/MRBT-5 (July 1980).

6. R. H. Chapman et al., *Quick-look Report on MRBT B-6 (8 x 8) Bundle Test*, Internal Report ORNL/MRBT-7 (January 1982).

7. R. H. Chapman et al., *Bundle B-1 Test Data*, ORNL/NUREG/TM-322 (June 1979).

8. R. H. Chapman et al., *Bundle B-2 Test Data*, ORNL/NUREG/TM-337 (August 1979).

9. R. H. Chapman et al., *Bundle B-3 Test Data*, ORNL/NUREG/TM-360 (January 1980).

# EXPERIMENT DATA REPORT FOR MULTIROD BURST TEST (MRBT) BUNDLE B-4

A. W. Longest R. H. Chapman
J. L. Crowley

## ABSTRACT

A compilation of bundle B-4 test data is presented. These data were obtained during the test and from pretest and posttest examination of the test array. They are presented in considerable detail but with minimum interpretation.

The B-4 test is the only 6 x 6 array in a series of 4 x 4, 6 x 6, and 8 x 8 bundle tests performed by the Multirod Burst Test Program at Oak Ridge National Laboratory. This research is sponsored by the Nuclear Regulatory Commission and is designed to investigate Zircaloy cladding deformation behavior under simulated light-water reactor loss-of-coolant accident conditions.

The specific objectives of the B-4 test were to investigate axial propagation of cladding ballooning as the result of rod-to-rod contact and to determine the effect of a relatively cold fuel pin simulator on the deformation behavior of its hotter neighbors under test conditions known to produce large deformation. These objectives were not realized, however, because the temperature transient did not proceed to the planned failure conditions. Electrical power to the bundle was lost when the bundle average cladding temperature was ~675°C. The bundle temperature slowly decreased (~0.2 K/s for ~380 s), and the tubes deformed (by creep) until pressure was vented from the tubes to terminate the test.

Significant deformation occurred (up to 18% average strain over the heated length), but none of the tubes burst. The bundle was disassembled, and deformation profiles of the individual tubes were measured. Although objectives of the test were not met, the data appear useful for model development and verification.

A brief description of the experiment and a summary of the test results are included with the detailed results of the B-4 test. Both graphical and tabular formats are used to show temperature and pressure data as functions of test time and strain data for the cladding in each of the fuel rod simulators. Photographic documentation is provided for both the overall bundle, before and after testing, and the 36 tubes as they were removed from the tested bundle for strain measurements.

The purpose of this report is to provide a background document for interpretative reports published previously and to be published in the future.

# 1. INTRODUCTION

This report presents, in detail, the experimental data for the B-4 test (the only 6 x 6 multirod burst test) conducted within the framework of the Multirod Burst Test Program at Oak Ridge National Laboratory. This work is sponsored by the Division of Accident Evaluation of the Nuclear Regulatory Commission and is designed to investigate Zircaloy cladding deformation behavior under simulated loss-of-coolant accident (LOCA) conditions. The report is intended primarily as a source document for B-4 test results, with a minimum amount of interpretation of the data. Because of this, it should be read in conjunction with other published results and interpretations.[1,2]

The objectives of the B-4 test were to investigate axial propagation of cladding ballooning as the result of rod-to-rod contact and to determine the effect of a relatively cold fuel pin simulator on the deformation behavior of its hotter neighbors under test conditions known to produce large deformation. Consistent with these objectives, initial conditions were established to cause the tubes to burst at ~800°C after ~90 s of heating at a rate of ~5 K/s, and the test was initiated. However, technical difficulties were encountered during the transient. After 60 s of heating and ~10 s after the onset of deformation, electrical power was terminated by the automatic control system; the bundle average cladding temperature at the time was ~675°C. While attempts were being made to restore power, the tubes continued to deform under near-isothermal creep conditions. These conditions continued for ~380 s, at which time the tubes were depressurized, and the test was terminated. Although significant deformation occurred, none of the tubes burst.

The loss of power was caused by a 0- to 60-s backup timer that was inadequately bypassed after it was used to terminate a short (15-s) power-bump checkout transient. Although an electrical bypass circuit was installed around the timer contacts in the primary shutdown circuit, a redundant shutdown circuit was not bypassed, and this caused termination of the transient after 60 s.

Although primary objectives of the test were not realized, the data appear useful for model development and verification, particularly with respect to "flat-topped" transients.

Following the format of the previous reports in this series,[3-5] a brief description of the test design and procedure will be given, followed by the test results.

# 2. TEST DESCRIPTION

## 2.1 Assembly

Figure 1 shows a simplified drawing of the B-4 test assembly. As indicated in Sect. B-B of the figure, the shroud was constructed of thin (0.13-mm-thick) stainless steel, with a highly reflective gold plating, and was backed by insulating material and a strong structure to withstand radial forces during the test transient. The shroud was spaced one-half of a coolant channel distance (1.75 mm) from the outer rod surfaces. This permitted some deformation of these simulators before contact with the shroud but prevented gross outward movement of the simulators. This design concept was also used in the B-5 (8 x 8) test, which was conducted prior to the B-4 test. The inlet steam arrangement was modified from a single nozzle on the north side, as used in the B-5 test, to diametrically opposed nozzles on the east and west sides of the bundle (Sect. A-A in the figure) to obtain a more uniform inlet temperature distribution than existed in B-5. As will be discussed later, this and other improvements were effective.

Figure 2 gives pertinent details of a typical fuel pin simulator, and Table 1 lists as-built data for the B-4 simulators. The fuel simulators (internal heaters) used in B-4 included those used in the earlier B-2 and B-3 tests (16 heaters each) plus an additional four from the original lot of simulators purchased from SEMCO for the 4 x 4 tests. The axial heat generation profiles of the simulators were characterized by pretest infrared (IR) scans.[6] The highest quality simulators were selected for the bundle interior positions.

The Zircaloy-4 tubes (10.92-mm OD by 0.635-mm wall thickness) used to fabricate the test assemblies came from the master lot of tubing purchased for use in several NRC-sponsored cladding research programs.[7] Serial numbers of the tubes are given in Table 1, and fabrication of the simulators and test array is discussed in Ref. 2.

Each fuel pin simulator was instrumented with a fast-response, strain-gage-type pressure transducer and four Inconel-sheathed (0.71-mm-OD) type K thermocouples with ungrounded junctions. The thermocouples were spot-welded to the inside of the Zircaloy-4 tubes, using a device developed specifically for this purpose.[8] Their positions are shown in Fig. 3, which also gives thermocouple identifications for use in subsequent figures (the nomenclature TE 10-4 identifies the No. 4 thermocouple in the No. 10 simulator). The axial locations of the thermocouples are also shown in Fig. 4. One thermocouple (TE 26-3) read ~20°C low throughout the transient; its reading is suspect.

Eight, 0.13-mm-diam bare-wire, type S thermocouples were spot-welded on the outside surface of the thin shroud surrounding the rod array. Two thermocouples were attached to each side at positions shown in Fig. 3 in an attempt to obtain information on both the axial and circumferential temperature distributions. The shroud thermocouple identifications are also given in the figure for use in subsequent temperature plots.

Five thermocouples (TE-320 through TE-324) were located in the tube matrix at the 107-cm elevation (centerline elevation of the steam inlet nozzles) to obtain inlet steam temperature measurements. Five thermocouples (TE-325 through TE-329) were similarly dispersed in the tube matrix near the bottom of the heated zone (at the 3-cm elevation) to obtain outlet steam temperature measurements in the bundle at this elevation. Figure 5 shows the identifications and locations. These thermocouples were 0.71-mm-diam, stainless steel-sheathed, type K with ungrounded junctions.

A detailed description of the temperature measurement systems and a comprehensive analysis of the errors and uncertainties associated with the measurements have been reported previously.*

Millivolt signals from the pressure transducers, thermocouples, and electrical power measuring instruments were recorded on magnetic tape by a computer-controlled data acquisition system (CCDAS) for subsequent analysis. Calibration corrections, programmed into the computer system, were automatically applied to the millivolt signals before printout of the data.

## 2.2 Operations

It was planned that the powered portion of the test would be terminated by any of three actions: (1) CCDAS action resulting from a signal that 32 of the 36 simulators had burst, (2) CCDAS action resulting when 75 simulator thermocouples had exceeded the upper temperature limit (50°C above the anticipated burst temperature) on each of three successive data scans, or (3) operator override. The powered phase of the test was terminated prematurely by a timer circuit that was not effectively bypassed as discussed earlier.

Heatup of the test assembly was initiated early in the afternoon of Jan. 14, 1981; the temperature was near 200°C at the end of the work shift. Power adjustments to the vessel heaters were made to maintain the temperature near this value during the next 12 h to avoid temperature cycling the test assembly. About 4:00 AM on January 15, power to the vessel heaters was increased, and superheated steam was admitted to the vessel in the approach to the initial test temperature. Throughout this phase of operation, periodic leak checks indicated the simulator seals were performing very well (i.e., <10 kPa pressure loss per min at 8600 kPa and ~330°C).

After thermal equilibration (~330°C) of the test assembly was attained, the simulators were pressurized to ~5300 kPa, and a short power run (~15-s transient) was conducted at 12:30 PM to ascertain that the data acquisition system (DAS) and all the instrumentation were functioning properly and that the performance of the test components was as expected. Simulator 27 was earmarked at this time to be the unheated one. Other than omitting the fuse from its electrical circuit and setting its initial pressure level at 500 kPa (to preclude deformation), this simulator was identical to the others. Examination and evaluation of the quick-look data from this short transient, which increased the temperature of the simulators to ~410°C, indicated voltage adjustments were not needed to achieve the desired heating rate of 5 to 6 K/s.

Simulator 16 developed a severe leak during the time (~5 h) between the pretest power-bump and the test. The magnitude of the leak was such that for deformation to be comparable to the other simulators, it would be necessary to test the simulator at constant pressure by inflow of helium at a rate equal to the leak. Rather than degrade the quality of the deformation data by this expediency, a decision was made to select No. 16 (instead of No. 27) as the unpressurized (actual pressure of 560 kPa) and unheated simulator. All the remaining simulators were leak tight (leak rates of <10 kPa/min at 9300 kPa and 332°C) and were tested in the usual manner (i.e., with the individual isolation valves to the supply header closed to provide a constant gas inventory in each simulator during the transient).

Superheated steam entered the array on the east and west sides at the 107-cm elevation (Fig. 1) and flowed downward through the bundle during the test at a mass flux of ~279 $g/s \cdot m^2$. Inlet steam conditions of ~327°C and ~305 kPa (absolute) resulted in a Reynolds number of ~132 at the inlet end of the bundle. These inlet conditions remained essentially constant throughout the transient, although a small perturbation (lasting 10 to 15 s) occurred about 140 s after power-off, as will be discussed later.

Following stabilization of the bundle temperature at ~332°C, all the fuel simulators except No. 16 were pressurized simultaneously to ~9100 kPa (differential above the external coolant pressure) and isolated from the supply header. Pressure in the unheated simulator (No. 16) was set at ~560 kPa (differential) to preclude deformation. With these initial conditions established, the test transient was initiated. The tubes were expected to burst at ~800°C after ~90 s of heating at a rate of ~5 K/s. However, after 60 s of heating and about 10 s after the onset of deformation, electrical power to the bundle was terminated by the automatic control system; the bundle average cladding temperature at the time was ~675°C. Hurried attempts to diagnose the cause of the outage and to restore power were unsuccessful. The bundle temperature slowly decreased (~0.2 K/s), and the tubes continued to deform under near-isothermal creep conditions during this time. After ~380 s the tubes were depressurized to preclude further deformation.

With conditions stabilized after depressurization, quick-look evaluation of the recorded pressure data revealed that none of the tubes had burst, but appreciable deformation had occurred. Repressurizing the tubes and continuing the test to burst conditions would only render the data uninterpretable, because the initial conditions (i.e., the extent and distribution of the deformation in each tube at restart) would be unknown. Furthermore, this would prevent realization of a primary objective of the test (i.e., determination of the effect of a relatively cold rod on the deformation behavior of its neighbors). Consequently, a decision was made to terminate the test at this point so that it could be analyzed and interpreted in view of the reasonably well-defined test conditions.

## 3. SUMMARY OF TEST RESULTS

Tables 2–5 summarize pertinent data from the B-4 test. Initial pressure conditions (~9090 kPa) were selected to cause the tubes to burst at a temperature of ~800°C had the test been completed as planned. As indicated in Table 2, the initial temperature was ~332°C, and the temperature distribution in the bundle was very uniform (see Figs. 3 and 4 for thermocouple locations). The average temperature indicated by the eight shroud thermocouples was 335°C. Average indicated steam inlet temperature was 326°C, and the average outlet temperature was 335°C. The latter value indicates slight heating of the small steam flow (1.15 g/s) as it flowed downward through the test assembly.

Table 2 also lists the temperature indicated by each of the thermocouples at the time of maximum pressure for the respective simulators (5 to 10 s before power–off). The point of maximum simulator internal pressure occurs when the opposing effects of temperature increase and tube expansion are equal and indicates the onset of appreciable deformation. The spread in temperatures in a given simulator is not unusual, considering the location of the thermocouples and the power distribution of the fuel simulators as determined from the pretest IR characterization scans.

Simulator temperatures reached maximum values in the interval between 1 and 3 s after power–off (Table 3) and decreased steadily thereafter at ~0.2 K/s. The data of Tables 2 and 3 together indicate conditions were very uniform during the powered portion of the transient and to the point of maximum simulator temperatures.

Table 4 gives the simulator temperatures at the time of depressurization (vent) for the respective simulators (381–401 s after power–off). The indicated cladding temperature variations along each simulator and from simulator to simulator show the axial and radial temperature distributions were highly nonuniform near the end of the test.

Table 5 lists some of the volume-related data for the B-4 tubes. The initial gas volumes were quite uniform among the tubes – ranging from 47.8 to 51.7 $cm^3$, about twice that of a full-length reactor fuel rod. Of the total initial volume (at room temperature), about 13% is in the heated portion of the annulus between the fuel simulator and the inside diameter of the Zircaloy tube, 10% is in the unheated portion of the annulus, 33% is in the pressure transducer and connecting tube, and 44% is distributed in the end regions (mostly at the upper end) of the fuel pin simulator. At any given time during the test, all these volumes have different temperatures (the major volumes remain at or near room temperature), ranging from room temperature to cladding temperature, and one cannot calculate accurately the fractional volume increase from the pressure decrease in a straightforward manner. Instead, we calculated the volume increase from the tube deformation profiles (assuming circular cross sections).

# 4. DETAILED TEST RESULTS

This section presents, in a number of subsections, the detailed results of the B-4 test. The purpose of this presentation is to provide a fairly complete reference source of uninterpreted data.

## 4.1 Transient Results

### 4.1.1 Bundle behavior

The information contained in this section was obtained during the course of the B-4 test transient. The data were recorded by the DAS in the continuous scan mode (i.e., each sensor was sampled every 0.025 s) over a period of ~10 min. Each rod was instrumented with four thermocouples attached to the interior surface at various elevations (see Fig. 4) above the bottom of the heated zone. In addition, the heated shroud was monitored by eight thermocouples attached to its outer surface. These locations were shown previously in Fig. 3.

Superheated steam entered the array through two inlet nozzles located on the east and west sides of the bundle (Fig. 1) at the 107-cm elevation and flowed downward through the bundle at a mass flux of 279 $g/s \cdot m^2$, equivalent to an inlet Reynolds number of ~132 at the top of the heated zone (91.5-cm elevation). Apparently the nozzle arrangement and other modifications made after the preceding B-5 test, such as a steam distribution baffle just below the inlet (Fig. 1) to minimize flow channeling and additional heaters on the vessel closure flange to minimize heat losses from the flange via axial conduction along the simulators, were effective in producing a fairly uniform inlet steam temperature distribution in the matrix. This is illustrated in Fig. 5, which shows a schematic of the array with the locations, identifications, and temperature readings of the steam inlet and outlet thermocouples 1 s before power-on. The measurements indicate the temperature distribution was fairly uniform at the inlet and very uniform at the outlet. Also, the steam average temperature increased about 9°C while passing through the bundle.

Figures 6–15 present temperatures measured 1 s before power-on in the format of a schematic layout of the bundle at each of the instrumented sections. The layout represents the tube by eight dots, positioned at possible thermocouple azimuthal angles (Fig. 3), centered about the rod position number. An asterisk replaces a dot, indicating the azimuthal position of a thermocouple, if the junction is in the plane for which the particular map applies; the temperature measured by the thermocouple at the time is printed below the schematic representation of the tube. The respective row and column average temperatures are printed on the right and at the bottom of the layout. The cross section and bundle average temperatures, the elevation of the section, and other pertinent information are also included in the format. The thermocouples in simulator 16 (unheated) and those located at the grid elevations are excluded from the bundle average temperature. Also, if a particular thermocouple indicates a temperature 25°C greater or less than the section average, that reading is excluded (and noted in the format) from the average.

The maps provide considerable data and greatly facilitate interpretation and evaluation of local and overall temperature distributions. As evident, the initial radial and axial temperature distributions were very uniform, indicating uniform distribution of the steam. Compare, for example, data in Fig. 6 for the 84-cm elevation with the inlet steam temperatures (at the 107-cm elevation) in Fig. 5. Also, compare Fig. 15 with Fig. 5 for the radial distributions at the lower end of the heated zone.

The overall radial temperature distribution may be visualized somewhat easier in the temperature map depicted in Fig. 16. The temperature given in the map for each simulator is the average of the thermocouple measurements for that simulator without regard to elevation, excluding measurements obtained from thermocouples at the grid elevations. Asterisk locations (and number) in the schematic representation of the simulators denote the azimuthal position of the thermocouples whose measurements comprise the average. Row and column averages are printed on the right side and at the bottom of the map, respectively, to facilitate visualization of uniformity.

Initial pressures are presented in a similar format in Fig. 17. Again the column of numbers on the right and the row of numbers at the bottom of the figure represent the row and column average pressures, respectively.

With these initial conditions established, the transient was initiated. A number of plots and data maps will be presented to illustrate the significant features of the test as it progressed and to provide an indication of the general conditions prevailing at the time of important events. A parameter TAV-10 will be plotted in a number of these figures to represent the bundle average temperature. This parameter is in reality the average of six thermocouples (TE 9-3, TE 14-2, TE 15-1, TE 21-3, TE 23-1, and TE 26-1) at the 38-cm elevation (see Fig. 3 for relative positions) that were electronically averaged and recorded during the test to facilitate visualization of the bundle temperature as a function of time. Because of the way this average temperature was derived, it differs slightly (≲10°C) from the average calculated posttest from individual measurements. This small discrepancy is unimportant for quick-look characterization.

Figure 18 shows TAV-10 and the applied voltage during the powered portion of the transient; the average heating rate during this time was ~5.7 K/s. The temperature measured by TE 16-3 on the unpressurized and unpowered simulator (at the same elevation as the thermocouples used to obtain TAV-10) is also shown for reference. Internal pressure (differential) measured on a corner (No. 1) and a central (No. 21) simulator are included to illustrate pressure behavior of exterior and interior simulators, respectively. Maximum pressure was encountered in all the pressurized simulators 5 to 10 s before power-off, indicating the onset of deformation had taken place. Pressure (Fig. 19) and temperature (Figs. 20–30) measurements made ~0.2 s before power-off show conditions were very uniform at the time power was terminated; the effect of the unpowered simulator (No. 16) appears negligible up to this time.

Figure 31 shows the temperature behavior, as characterized by TAV-10 and TE 16-3, during the time attempts were being made to restore electrical power to the bundle. As evident, the temperature reached a maximum ~2 s after power-off (Fig. 18) and decreased steadily thereafter (~0.15 K/s based on TAV-10 and ~0.23 K/s based on overall bundle average temperature, with the latter value reflecting development of axial and radial temperature gradients during this time). The temperature of the unpowered rod increased at a rate of ~1.7 K/s during the first 100 s of unpowered operation and at a reduced rate thereafter until it reached essential equilibrium with TAV-10 ~300 s after power-off.

The figure also shows the pressure behavior of the first (No. 1) and last (No. 25) simulators to be depressurized and of the simulator (No. 14) that exhibited the greatest pressure decrease before depressurization. Because the temperature decrease before venting was moderate, the predominant cause of the observed pressure decrease was creep deformation.

The first simulator (No. 1) was vented to the supply header at ~441.5 s from power-on and the last (No. 25) at ~461.5 s, creating conditions that precluded further deformation. About 30 s after venting the simulators to the header and each other (at a common pressure of ~3620 kPa), the header was vented to ~800 kPa, and the bundle was allowed to continue cooling without disturbing the inlet steam conditions.

Discussion of the short temperature perturbation evident ~200 s after power-on in Fig. 31 will be deferred to a later point.

Pressures measured ~0.7 s before the first simulator was vented are shown in Fig. 32. Because the pressures changed very little from the time of these measurements to that of venting the individual simulators, the pressures are very good estimates of those existing at the time of venting (Table 4). Because the final pressure can be correlated with deformation, the map provides an indication of how the deformation is distributed with respect to simulator position. As would be expected, the exterior simulators have less deformation than the interior ones, with the corner simulators having the least deformation.

Also, deformation is greater in the lower left triangular half of the bundle formed by simulators at the No. 1, No. 31, and No. 36 positions than in the upper right half. This may be an effect of the unpowered simulator (No. 16) in the upper right half.

Temperature measurements made at the same time (i.e., ~0.7 s before venting of the No. 1 tube and ~380 s after power-off) are shown in Figs. 33-42. The axial and radial temperature distributions were highly nonuniform as may be deduced by comparison of (1) the individual measurements and averages within a section, (2) the various section averages with the bundle average, and (3) the simulator averages in the radial temperature map given in Fig. 43.

Thermocouples were attached to the outside surface of the (electrically) unheated shroud to obtain information about shroud axial and azimuthal temperature variations. As indicated in Fig. 3, two thermocouples were located at each of four elevations, with one of the two thermocouples being positioned directly opposite a simulator and the other being positioned between two simulators. Because the shroud was very thin (~0.13 mm thick), significant variations might be expected from the thermocouple measurements. Figure 44, which compares shroud temperature measurements at the 76-cm elevation during the powered portion of the transient with cladding temperature measurements obtained from simulators in the vicinity of the shroud thermocouples (Fig. 3), confirms this expectation. The figure shows that the thermocouple (TE 91-2) located opposite the simulator thermocouple (TE 32-3) indicated a much higher temperature than that indicated by the thermocouple midway between two simulators. In fact, ~33 s after power-on, the shroud thermocouple (TE 91-2) reading indicated an increased heating rate as if the simulator and shroud were in contact. The matched simulator thermocouple (TE 32-3) showed a decreased heating rate at the same time, as if local cooling conditions had changed. Posttest visual examination of the shroud panel showed significant temperature variations existed during the transient as revealed by the degree of oxidation evident on the unplated backside of the stainless steel surface.

The shroud thermocouples at three of the four instrumented elevations showed this general behavior. Although this may be interpreted as evidence that the simulators bowed outward to contact the closely spaced shroud during the test, the timing (well before the onset of deformation) and uniformity of deformation suggest that the thin shroud panel buckled (locally) inward and touched the simulators.

Figure 45 shows measurements obtained from the same sensors over a much longer time span. The perturbation ~200 s after power-on was very pronounced on the shroud and simulator thermocouples at this elevation. The perturbation was caused by partial opening of steam valves upstream and downstream of the test vessel by action of interlocks during an attempt to restore power to the bundle; Fig. 46 will facilitate explanation of the event.

The steam flow rate is controlled by a small valve downstream of the vessel, and the steam pressure in the vessel, indicated by PE 301 in the figure, is controlled by a pressure regulator upstream of the vessel. After the tubes burst (in a normal burst test), a large downstream valve opens to relieve the vessel pressure, and a large upstream valve opens simultaneously to admit a large flow of steam from the building supply to cool the bundle. Actuation of these valves is controlled through interlock circuits that require the proper sequence of events. In an attempt to reinitialize the sequence for start-up of the electrical power generator, the valves were opened partially as indicated in Fig. 46 by the sharp decrease in vessel pressure (PE 301) at ~195 s after power-on and closed 12 to 15 s later.

Measurements by the inlet and outlet steam thermocouples, of which an example of each (locations given in Fig. 5) is plotted in the figure, indicated significant temperature changes as a result of the sudden increase in steam flow. The first response was an increase in temperature caused by a reduction in residence time in the steam inlet line (i.e., less sensible heat loss from the highly superheated steam as it passed through the line). Shortly thereafter the superheated steam was displaced by a larger flow of saturated (or only slightly superheated) steam, causing the inlet steam temperature to decrease to ~125°C. This relatively cold steam provided good cooling conditions for a few seconds. Shortly thereafter, the vessel pressure, steam flow rate, and inlet temperatures returned to their original values and were maintained at these values until well after the test was terminated.

The short period of rapid cooling caused significant perturbation of the simulator pressures (differential) and cladding temperatures as shown by the plots presented in the next section.

### 4.1.2 Fuel pin simulator pressure and temperature plots

Individual pressure (differential) and temperature curves for the simulators are shown in Figs. 47–82. An arrow is located on the abscissa in the figures to mark the time at which power was terminated. These curves were computer-plotted at 0.2-s intervals from the magnetic data storage tapes. Each of the figures is comprised of four temperature plots (corresponding to the four thermocouples attached to the individual simulator cladding ID) and one pressure curve. Thermocouple identification in the figures follows the numbering scheme shown in Figs. 3 and 4.

Except for unpressurized (actual pressure of ~560 kPa) and unheated simulator No. 16 (Fig. 62), the vent time for each simulator can be detected by the sudden drop in the pressure curve. The point of maximum pressure (see Table 2) is an indication that the onset of deformation has taken place. Subsequent plastic deformation caused a continuing decrease in pressure until venting occurred.

## 4.2 Pretest and Posttest Results

The information contained in this section was obtained from the pretest and posttest examinations of the B-4 test array. Some information, such as the simulator IR scans, resulted from quality assurance efforts made to characterize the test components. Other information, such as bundle disassembly photographs, were obtained as a step in the posttest examination of the bundle. The results are presented in considerable detail, because we believe the data are extremely important to the interpretation of the test in terms of deformation behavior and distribution.

### 4.2.1 Pretest bundle photographs

Although not directly applicable to the interpretation of the B-4 test, selected photographs of the bundle assembly are included in this section for general interest. Various details of the construction and monitoring instrumentation may be seen.

A view of the B-4 array before installation of the shroud around the bundle is shown in Fig. 83. As described earlier the 6 x 6 bundle design is basically a scaled-down version of the preceding 8 x 8 bundle (B-5) design. A close-fitting shroud of the same design as the one used in B-5 was used to simulate the radial restraint in a nuclear fuel assembly. The shroud was spaced one-half of a coolant channel distance (1.75 mm) from the outer rod surfaces. A view with three sides of the shroud assembled around the bundle is shown in Fig. 84. Details of the shroud panels are shown in Fig. 85. The completely assembled bundle is shown in Fig. 86.

In scaling down the B-5 design, several changes were made in an attempt to improve performance. These included improving the steam distribution at the bundle inlet and outlet. Instead of one steam inlet on the north side of the shroud, the flow was directed to two sides (east and west), as can be seen in Fig. 86. Additionally, a flow distribution baffle (Fig. 83) with 12.3-mm-diam holes for the 10.92-mm-diam rods was positioned between the steam inlet and the uppermost grid. A steam deflector

(Fig. 83) was added to minimize impingement of hot steam on the lower seal glands of the fuel pin simulators.

Figure 87 shows a typical shroud thermocouple attachment. Each thermocouple was formed by making a ball junction (~0.4-mm diam) on the end of 0.13-mm-diam type S wires. The ball was then spot-welded to the back side of the thin shroud reflector strip. The mass of the thermocouple was kept small to minimize thermal shunting, this is, cooling of the reflector at the point of attachment by the thermocouple itself. An even smaller type S wire (0.076-mm diam) was used in B-5 but was found to be difficult to work with and too fragile for this particular application. The small thermocouple wires exited through an insulator at the center of a plug, as shown in Fig. 88. The wires were spliced (Fig. 88) to 0.25-mm-diam bare wires exiting a sheathed type S thermocouple having a glass end seal to prevent ingress of moisture. A protective cover was installed over the area where the thermocouple wires exited the shroud panel (Fig. 86).

A view of the lower end of the bundle showing the outlet steam thermocouples is shown in Fig. 89. All the steam thermocouples were 0.71-mm-diam stainless steel-sheathed Type K with insulated junctions. The junction end was centered within the flow channel with a ceramic spacer.

#### 4.2.2 Posttest bundle photographs and general examination results

Following cooldown, the assembly was removed from the test vessel and partially disassembled to facilitate photography and dimensional measurements for documentation.

Because none of the tubes burst, posttest leak checks were made on all the simulators; two had developed leaks. One of these (No. 16) developed a leak prior to the test. Posttest examination revealed the leak to be at the brazed seal joining the copper electrical lead to the stainless steel portion of the ceramic insulated seal gland at the lower end of the fuel pin simulator. (Figure 2 indicates a Swagelok ferrule and gland-type seal, but it has been our practice to make this seal by silver brazing.) The leak in the other simulator (No. 22) developed during posttest cooldown. Posttest examination showed the leak location to be at the multipin Teflon seal at the insulating gland at the upper end of the simulator (Fig. 2). Both of these simulators leaked at locations not previously identified as troublesome points.

Visual observations confirmed that deformation was moderate and uniformly distributed over the heated length as expected from the test conditions. Figure 90 shows an overall view of the west face of the test array after removal of the shroud and internal heaters. The west face of the shroud, shown below the bundle, is located in its correct axial position relative to the bundle. One of the steam inlet nozzles is visible in the shroud near the upper end of the bundle.

Posttest views of the four faces of the bundle are shown in Fig. 91; the meter scale is positioned so that the 0-cm mark is at the bottom and the 91.5-cm mark is at the top of the heated length. Deformation uniformity is evident in the photographs. However, localized ballooning of simulator No. 14 (an interior simulator) is obvious, particularly in the east and west face views at the 49-cm mark. This is the simulator with the greatest volume increase (Table 5). Two close-up views of this region of the bundle are shown in Fig. 92 as viewed from the west face at slightly different camera angles. These views indicate the ballooned region is symmetrical and not in contact with the No. 8 simulator. However, one cannot see through the bundle from the north face in this region, indicating that the ballooned portion is perhaps in contact with the neighboring simulators (Nos. 13 and 15).

Because deformation was modest and uniformly distributed, a decision was made to forgo flow characterization of the test array and to disassemble the bundle to permit direct measurement of the strain profile of the individual tubes. Disassembly was accomplished by slitting the grids to facilitate removal of a layer of tubes as a unit. A photograph was taken of the remaining portion of the bundle each time a layer of tubes was removed. This operation started on the south side of the bundle (i.e., tubes 31-36 were removed first) and progressed northward. Figure 93 presents a composite of the photographs, showing the bundle as each layer of tubes was uncovered. Except for tube No. 14, deformation in all the tubes (No. 16 was not pressurized and, hence, undeformed) is uniformly distributed. Figure 94 shows an enlarged portion of the ballooned region of tube No. 14.

The tubes were freed from the tube layer subassemblies for strain profile measurements. The results are given in the next section.

Axial shrinkage occurs with circumferential strain in tests, such as this one, conducted in the alpha temperature region. Axial shrinkage data (Fig. 95) are reasonably consistent with the other data, indicating greater shrinkage (and greater circumferential strain) on the average on the interior simulators compared with the exterior ones.

#### 4.2.3 Strain data and tube strain profiles

Circumferential strain measurements were made on the individual B-4 tubes at 20-mm intervals, using a modified-planimeter-wheel mechanism developed for single rod tests. This mechanism, described previously,[10] is capable of resolving a circumference of 75 mm into 1000 parts to give a resolution of 0.075 mm. Table 6 tabulates the strains obtained in this way at each axial position for each tube; the values are given in percentage increase of original tube circumference. A measure of the accuracy is also evident by the data for tube No. 16, which did not deform. The maximum observed strain was 50% at the 48-cm elevation in simulator No. 14, which is also the elevation with the maximum total deformation (sum of all tubes).

The strain data were used to plot axial profiles of the individual tubes; these are presented in Figs. 96-131. The pretest IR characterization scans of the fuel simulators (internal heaters) and the pretest axial positions of the thermocouples are also shown for reference purposes.

All the deformation profiles have certain characteristics, more or less independent of the characteristics of the individual fuel simulators. These include strains of 2 to 6% in the region of the grids (centered about the 10- and 66-cm pretest elevations) and maximum strains of 2 to 7% in the region between the bottom of the heated zone and the lower grid.

Most tubes exhibited maximum strains of 5 to 15% in the region between the upper grid and the top of the heated zone. Strain in this region is strongly influenced by the cooling effect of the inlet steam.

Strains in the region between grids are rather uniform as expected from the test conditions, except for tube No. 14. As mentioned earlier, tube No. 14 exhibited the greatest volume increase (Table 5) and was the only tube with a large localized balloon (Fig. 109). Tube No. 16 (unpressurized and unpowered) showed no significant strain (Fig. 111) as expected.

The deformation profiles correlate reasonably well with the pretest IR characterization scans, considering that (1) the grids have a strong restraining effect over 10 to 15 cm of length, (2) the characterization scans are for a single angular orientation but circumferential temperature gradients are known to exist in the SEMCO fuel simulators, and (3) the characterization scans are for a heating rate of ~40 K/s whereas the test was conducted at a heating rate of ~5.7 K/s (powered portion) with most of the deformation occurring under near-isothermal conditions after power was terminated. The large localized balloon on tube No. 14 (Fig. 109) corresponds to a high peak in the IR scan; power was off while most of the deformation was occurring, as indicated by the pressure trace in Fig. 60.

Excessive ballooning over an extended length is a concern in LOCA analyses. For the tubes and spacing (10.92-mm OD on a 14.43-mm-square pitch; 1.32 pitch-to-diameter ratio) used in our tests, adjacent tubes will touch with 32% uniform expansion. As evident from the deformation profiles, only tube No. 14 experienced strains greater than this value and those strains exceeding 32% are over a length of only approximately eight (original) tube diameters (Fig. 109).

Another important characterization of tube deformation is the volume increase over the heated length. This parameter is closely related to flow resistance, because the volume increase takes into account deformation along the length of the tube. The volume increase was calculated for each of the tubes from the strain data given in Table 6 by using the equation for the volume of a cone frustum to estimate the subvolume for each length interval between strain measurements, summing these subvolumes over the heated length, and subtracting the original volume from the sum. The results of this analysis are included with other characteristics of the test presented earlier in Table 5.

#### 4.2.4 Coolant channel flow area restriction

As evident from the deformation profiles for the individual tubes, overall bundle deformation was moderate. The total expansion for all tubes at each axial position is normally of interest because it determines the coolant channel flow area restriction. This parameter was calculated on the basis of a rod-centered unit cell, using the equation

$$B = 100 \times \frac{\sum_{n=1}^{n=N} (A_{d,n} - A_o)}{N\,(p^2 - A_o)} ,$$

where

$B$ = percentage restriction in coolant channel flow area,
$A_{d,n}$ = outside area of deformed tube ($mm^2$),
$A_o$ = outside area of original tube ($mm^2$),
$p$ = tube-to-tube pitch in square array (mm),
$N$ = number of tubes in square array.

With this definition, B is 0% for no deformation and 100% if all the tubes deform into a square whose sides are of length p (completely filling the open area). For the case of uniform ballooning such that the tubes just come into contact (i.e., 32% strain for the dimensions appropriate to this test), B is 61%.

The deformed tube areas were calculated from the strain data given in Table 5, assuming the tube cross sections are circular. Table 7 gives the deformed tube areas $A_{d,n}$ for each tube at each axial position. The areas were used in the above equation to calculate the coolant channel flow area restriction at each position.

Flow area restriction calculations were performed for the entire 6 x 6 array and for the inner 4 x 4 array. These results are tabulated in Table 8 and plotted in Fig. 132. The cross-sectional area occupied by the grids (~100 $mm^2$) was not included in the calculation; including this area would slightly increase the restriction at the grid locations centered about elevations 10.3 and 65.4 cm. The pretest elevation of the upper grid was 66.0 cm; axial shrinkage during the test accounts for the difference in pretest and posttest locations.

The maximum loss in flow area occurred at the 48-cm elevation and amounted to 21.2% for the entire 6 x 6 array and 30.7% for the inner 4 x 4 array. These data agree with the previous observations that the deformation was moderate and uniformly distributed in the region between the two interior grids and that the interior simulators deformed more than the exterior ones.

## ACKNOWLEDGMENTS

Data presented in this report reflect the combined effort of a number of people over an extended period of time, spanning fabrication, testing, and pretest and posttest examination of the test array.

We wish to acknowledge the contribution of W. A. Bird for his careful attention to all the instrumentation and control aspects of the test; E. L. Biddle, J. N. Money, and C. Cross for assembly of the test array and for the many other necessary support tasks; F. R. Gibson for programming and operating the CCDAS and for processing the strain data; the Fuel Pin Simulator Development Group, under the leadership of R. W. McCulloch, for development and procurement of the fuel simulators; and the many other groups and individuals who had a part in the test.

## REFERENCES

1. A. W. Longest, *Multirod Burst Test Program Prog. Rep. January—June 1981*, NUREG/CR-2366, Vol. 1 (ORNL/TM-8058).

2. R. H. Chapman, *Multirod Burst Test Program Prog. Rep. July—December 1980*, NUREG/CR-1919 (ORNL/NUREG/TM-436).

3. R. H. Chapman et al., *Bundle B-1 Test Data*, ORNL/NUREG/TM-322 (June 1979).

4. R. H. Chapman et al., *Bundle B-2 Test Data*, ORNL/NUREG/TM-337 (August 1979).

5. R. H. Chapman et al., *Bundle B-3 Test Data*, ORNL/NUREG/TM-360 (January 1980).

6. W. A. Simpson, Jr., et al., *Infrared Inspection and Characterization of Fuel-Pin Simulators*, ORNL/NUREG/TM-55 (November 1976).

7. R. H. Chapman, *Characterization of Zircaloy-4 Tubing Procured for Fuel Cladding Research Programs*, ORNL/NUREG/TM-29 (July 1976).

8. W. E. Baucum and R. E. Dial, *An Apparatus for Spot Welding Sheathed Thermocouples to the Inside of Small Diameter Tubes at Precise Locations*, ORNL/NUREG/TM-33 (August 1976).

9. R. L. Anderson, K. R. Carr, and T. G. Kollie, *Thermometry in the Multirod Burst Test Program*, NUREG/CR-2470 (ORNL/TM-8024) (March 1982).

10. R. H. Chapman, *Multirod Burst Test Program Prog. Rep. April—June 1976*, ORNL/NUREG/TM-74.

Table 1. As-built data for fuel pin simulators in B-4 test

| Bundle position No. | Zircaloy tube serial No. | Internal fuel simulator[a] | | Fuel pin simulator gas volume[b] ($cm^3$) |
|---|---|---|---|---|
| | | Serial No. | Element resistance (Ω) | |
| 1 | 0725 | 2828052 | 4.13 | 48.5 |
| 2 | 0173 | 2828072 | 4.08 | 49.5 |
| 3 | 0839 | 2828068 | 4.07 | 48.3 |
| 4 | 0099 | 2828057 | 4.15 | 50.6 |
| 5 | 0825 | 2828083 | 4.04 | 47.8 |
| 6 | 0180 | 2828070 | 4.02 | 49.0 |
| 7 | 0181 | 2828056 | 4.02 | 50.3 |
| 8 | 0826 | 2828067 | 4.10 | 48.5 |
| 9 | 0182 | 2828044 | 4.08 | 49.8 |
| 10 | 0734 | 2828050 | 4.17 | 49.6 |
| 11 | 0100 | 2828046 | 4.06 | 51.5 |
| 12 | 0729 | 2828058 | 4.01 | 49.9 |
| 13 | 0736 | 2828051 | 4.18 | 50.4 |
| 14 | 0096 | 2828060 | 4.09 | 51.7 |
| 15 | 0827 | 2828081 | 4.09 | 48.1 |
| 16 | 0090 | 2828047 | 4.07 | 50.5 |
| 17 | 0730 | 2828049 | 4.18 | 49.1 |
| 18 | 0183 | 2828082 | 4.07 | 50.2 |
| 19 | 0184 | 2828080 | 4.04 | 49.2 |
| 20 | 0831 | 2828048 | 4.15 | 50.3 |
| 21 | 0185 | 2828071 | 4.04 | 50.3 |
| 22 | 0735 | 2828035 | 4.03 | 51.0 |
| 23 | 0198 | 2828078 | 4.15 | 49.9 |
| 24 | 0728 | 2828045 | 4.07 | 50.1 |
| 25 | 0832 | 2828076 | 4.12 | 47.9 |
| 26 | 0098 | 2828055 | 4.04 | 51.2 |
| 27 | 0833 | 2828086 | 4.18 | 47.9 |
| 28 | 0199 | 2828069 | 4.15 | 51.0 |
| 29 | 0834 | 2828064A | 4.05 | 48.6 |
| 30 | 0089 | 2828061 | 4.08 | 50.8 |
| 31 | 0097 | 2828062 | 4.01 | 49.8 |
| 32 | 0835 | 2828039 | 4.05 | 48.3 |
| 33 | 0206 | 2828073 | 4.12 | 49.6 |
| 34 | 0836 | 2828084 | 4.04 | 49.0 |
| 35 | 0201 | 2828079 | 4.05 | 49.8 |
| 36 | 0844 | 2828085 | 4.10 | 48.0 |

[a]All 64 fuel simulators were fabricated by SEMCO.

[b]Fuel pin simulator gas volume measured at room temperature before installation into bundle; the volume measured includes a pressure transducer and connecting tube identical to the facility hookup for each simulator.

Table 2. Summary of B-4 initial conditions and conditions at time of maximum pressures

| RCD NO. | INITIAL CONDITIONS: DIFFERENTIAL PRESSURE (KPA) | INITIAL CONDITIONS: TEMPERATURES (DEG C) TE-1 | TE-2 | TE-3 | TE-4 | AVG | CONDITIONS AT TIME OF MAXIMUM PRESSURES: DIFFERENTIAL PRESSURE (KPA) | TEMPERATURES (DEG C) TE-1 | TE-2 | TE-3 | TE-4 | AVG | TIME[a] (SEC) |
|---|---|---|---|---|---|---|---|---|---|---|---|---|---|
| 1 | 9095 | 332 | 332 | 331 | 330 | 331 | 9528 | 669 | 669 | 662 | 663 | 666 | 60.70 |
| 2 | 9077 | 330 | 329 | 330 | 335 | 331 | 9467 | 645 | 652 | 653 | 658 | 652 | 56.95 |
| 3 | 9091 | 329 | 328 | 331 | 330 | 330 | 9480 | 627 | 635 | 635 | 635 | 633 | 54.15 |
| 4 | 9091 | 330 | 332 | 330 | 330 | 331 | 9497 | 653 | 654 | 648 | 655 | 652 | 58.50 |
| 5 | 9099 | 334 | 333 | 334 | 332 | 333 | 9499 | 663 | 674 | 675 | 670 | 670 | 60.70 |
| 6 | 9076 | 333 | 335 | 335 | 336 | 335 | 9456 | 637 | 642 | 645 | 650 | 643 | 55.50 |
| 7 | 9105 | 335 | 333 | 335 | 334 | 334 | 9474 | 636 | 634 | 634 | 640 | 636 | 52.70 |
| 8 | 9088 | 335 | 333 | 332 | 334 | 333 | 9506 | 647 | 644 | 645 | 645 | 645 | 53.65 |
| 9 | 9079 | 334 | 335 | 333 | 329 | 333 | 9445 | 647 | 641 | 641 | 637 | 641 | 54.15 |
| 10 | 9078 | 330 | 328 | 331 | 331 | 329 | 9468 | 624 | 640 | 644 | 642 | 637 | 55.65 |
| 11 | 9064 | 330 | 331 | 330 | 331 | 331 | 9463 | 635 | 631 | 629 | 632 | 632 | 52.50 |
| 12 | 9064 | 330 | 331 | 330 | 332 | 331 | 9462 | 641 | 656 | 651 | 618 | 642 | 56.15 |
| 13 | 9091 | 331 | 330 | 330 | 332 | 331 | 9462 | 652 | 647 | 651 | 633 | 646 | 57.50 |
| 14 | 9095 | 331 | 331 | 331 | 331 | 331 | 9502 | 653 | 653 | 648 | 641 | 649 | 55.10 |
| 15 | 9094 | 334 | 331 | 334 | 331 | 333 | 9473 | 635 | 636 | 634 | 627 | 633 | 53.00 |
| 16[b] | 562 | 331 | 331 | 331 | 331 | 331 | | | | | | | |
| 17 | 9067 | 328 | 329 | 332 | 331 | 330 | 9456 | 641 | 644 | 649 | 653 | 647 | 57.10 |
| 18 | 9056 | 330 | 332 | 331 | 331 | 331 | 9441 | 647 | 650 | 645 | 645 | 647 | 56.95 |
| 19 | 9106 | 332 | 332 | 331 | 331 | 331 | 9475 | 636 | 645 | 641 | 644 | 642 | 55.60 |
| 20 | 9120 | 335 | 334 | 335 | 331 | 334 | 9518 | 645 | 644 | 640 | 642 | 643 | 53.75 |
| 21 | 9110 | 331 | 329 | 332 | 332 | 331 | 9482 | 644 | 643 | 649 | 639 | 644 | 54.10 |
| 22 | 9101 | 328 | 332 | 332 | 332 | 331 | 9478 | 639 | 647 | 650 | 628 | 641 | 55.50 |
| 23 | 9064 | 331 | 330 | 332 | 332 | 331 | 9448 | 636 | 642 | 638 | 629 | 636 | 53.75 |
| 24 | 9052 | 332 | 333 | 331 | 331 | 332 | 9444 | 635 | 644 | 640 | 642 | 640 | 55.05 |
| 25 | 9111 | 334 | 335 | 335 | 337 | 335 | 9475 | 657 | 654 | 654 | 634 | 650 | 57.80 |
| 26 | 9116 | 332 | 332 | 315 | 332 | 328 | 9516 | 644 | 641 | 607 | 644 | 634 | 53.45 |
| 27 | 9112 | 331 | 331 | 329 | 328 | 330 | 9484 | 641 | 630 | 635 | 632 | 634 | 53.80 |
| 28 | 9113 | 329 | 330 | 332 | 331 | 331 | 9506 | 649 | 656 | 641 | 653 | 650 | 56.25 |
| 29 | 9098 | 331 | 331 | 330 | 329 | 330 | 9489 | 634 | 634 | 631 | 629 | 632 | 52.45 |
| 30 | 9063 | 332 | 331 | 332 | 330 | 331 | 9435 | 659 | 643 | 644 | 647 | 648 | 56.75 |
| 31 | 9098 | 333 | 331 | 329 | 332 | 331 | 9473 | 633 | 641 | 644 | 647 | 641 | 56.65 |
| 32 | 9084 | 335 | 333 | 334 | 333 | 334 | 9469 | 630 | 653 | 624 | 658 | 641 | 56.30 |
| 33 | 9107 | 333 | 334 | 334 | 333 | 334 | 9472 | 649 | 653 | 651 | 644 | 649 | 56.85 |
| 34 | 9118 | 333 | 330 | 331 | 331 | 331 | 9477 | 653 | 642 | 650 | 654 | 650 | 56.70 |
| 35 | 9117 | 331 | 332 | 330 | 331 | 331 | 9464 | 649 | 641 | 648 | 650 | 647 | 57.50 |
| 36 | 9093 | 336 | 331 | 333 | 329 | 332 | 9450 | 638 | 641 | 647 | 634 | 640 | 57.40 |

[a] Time from power-on.

[b] Simulator No. 16 was unpressurized (~560 kPa) and unheated (electrically) during the test.

Table 3. Summary of B-4 conditions 2.25 s after power-off

| ROD NO. | DIFFERENTIAL PRESSURE (KPA) | TEMPERATURE (DEG C) TE-1 | TE-2 | TE-3 | TE-4 | AVG | ROD NO. | DIFFERENTIAL PRESSURE (KPA) | TEMPERATURE (DEG C) TE-1 | TE-2 | TE-3 | TE-4 | AVG |
|---|---|---|---|---|---|---|---|---|---|---|---|---|---|
| 1 | 9444 | 672 | 672 | 666 | 666 | 669 | 2 | 9403 | 666 | 675 | 675 | 681 | 574 |
| 3 | 9410 | 665 | 672 | 674 | 673 | 671 | 4 | 9453 | 657 | 669 | 663 | 669 | 667 |
| 5 | 9393 | 665 | 677 | 679 | 673 | 674 | 6 | 9399 | 667 | 672 | 675 | 678 | 573 |
| 7 | 9380 | 682 | 681 | 676 | 686 | 681 | 8 | 9398 | 639 | 635 | 687 | 636 | 687 |
| 9 | 9347 | 686 | 679 | 681 | 676 | 691 | 10 | 9388 | 652 | 670 | 673 | 672 | 667 |
| 11 | 9378 | 682 | 679 | 678 | 691 | 680 | 12 | 9385 | 668 | 634 | 677 | 646 | 669 |
| 13 | 9396 | 673 | 666 | 672 | 650 | 665 | 14 | 9395 | 688 | 638 | 683 | 672 | 683 |
| 15 | 9386 | 579 | 682 | 680 | 669 | 677 | 16[a] | 550 | 403 | 416 | 407 | 411 | 409 |
| 17 | 9396 | 664 | 667 | 672 | 677 | 670 | 18 | 9382 | 668 | 674 | 667 | 568 | 669 |
| 19 | 9411 | 667 | 677 | 671 | 676 | 672 | 20 | 9408 | 690 | 688 | 678 | 686 | 686 |
| 21 | 9378 | 684 | 683 | 689 | 680 | 684 | 22 | 9380 | 669 | 678 | 680 | 655 | 670 |
| 23 | 9362 | 676 | 683 | 679 | 665 | 676 | 24 | 9374 | 667 | 678 | 674 | 674 | 673 |
| 25 | 9417 | 677 | 673 | 671 | 652 | 668 | 26 | 9403 | 637 | 636 | 656 | 589 | 679 |
| 27 | 9386 | 683 | 668 | 676 | 674 | 675 | 28 | 9425 | 678 | 634 | 668 | 681 | 678 |
| 29 | 9385 | 685 | 684 | 681 | 678 | 682 | 30 | 9376 | 683 | 669 | 664 | 669 | 671 |
| 31 | 9407 | 657 | 664 | 668 | 670 | 665 | 32 | 9393 | 554 | 680 | 651 | 685 | 668 |
| 33 | 9405 | 673 | 675 | 672 | 565 | 671 | 34 | 9403 | 676 | 605 | 675 | 676 | 673 |
| 35 | 9406 | 669 | 660 | 666 | 672 | 557 | 36 | 9398 | 655 | 662 | 666 | 652 | 659 |

[a] Simulator No. 16 was unpressurized (~560 kPa) and unheated (electrically) during the test.

Table 4. Summary of B-4 conditions at time of vent

| ROD NO. | APPROXIMATE VENT CONDITIONS: DIFFERENTIAL PRESSURE (KPA) | TEMPERATURES (DEG C): TE-1 | TE-2 | TE-3 | TE-4 | AVG | VENT[a] TIME (SEC) |
|---|---|---|---|---|---|---|---|
| 1 | 8824 | 508 | 548 | 570 | 572 | 550 | 441.46 |
| 2 | 8514 | 590 | 513 | 594 | 587 | 571 | 443.15 |
| 3 | 8513 | 595 | 513 | 599 | 599 | 576 | 444.40 |
| 4 | 8573 | 560 | 591 | 596 | 597 | 586 | 446.05 |
| 5 | 8610 | 547 | 592 | 590 | 507 | 559 | 447.20 |
| 6 | 8798 | 575 | 544 | 569 | 540 | 557 | 448.45 |
| 7 | 8303 | 586 | 597 | 550 | 565 | 574 | 449.94 |
| 8 | 7739 | 607 | 617 | 578 | 618 | 605 | 451.79 |
| 9 | 7808 | 617 | 585 | 621 | 516 | 585 | 453.34 |
| 10 | 8268 | 591 | 509 | 613 | 617 | 582 | 455.34 |
| 11 | 8189 | 564 | 598 | 604 | 608 | 593 | 453.99 |
| 12 | 8491 | 504 | 587 | 591 | 576 | 564 | 452.99 |
| 13 | 8295 | 602 | 522 | 605 | 581 | 577 | 451.64 |
| 14 | 7142 | 610 | 625 | 625 | 570 | 607 | 448.45 |
| 15 | 7991 | 631 | 586 | 618 | 630 | 616 | 446.40 |
| 16[b] | | | | | | | |
| 17 | 8393 | 510 | 568 | 610 | 614 | 576 | 448.65 |
| 18 | 8514 | 596 | 596 | 509 | 593 | 574 | 450.54 |
| 19 | 8375 | 600 | 594 | 567 | 604 | 591 | 452.34 |
| 20 | 7727 | 628 | 619 | 575 | 524 | 587 | 453.64 |
| 21 | 7434 | 618 | 580 | 631 | 631 | 615 | 455.04 |
| 22 | 7945 | 517 | 624 | 629 | 613 | 595 | 457.03 |
| 23 | 7998 | 617 | 573 | 605 | 568 | 591 | 458.98 |
| 24 | 8516 | 511 | 560 | 597 | 591 | 565 | 460.68 |
| 25 | 8472 | 596 | 594 | 515 | 588 | 573 | 461.48 |
| 26 | 7707 | 608 | 609 | 544 | 605 | 592 | 459.78 |
| 27 | 7630 | 624 | 570 | 616 | 520 | 582 | 459.68 |
| 28 | 7866 | 575 | 622 | 568 | 609 | 594 | 457.38 |
| 29 | 7954 | 612 | 607 | 608 | 514 | 585 | 457.33 |
| 30 | 8607 | 555 | 586 | 578 | 587 | 577 | 458.03 |
| 31 | 8820 | 534 | 563 | 570 | 575 | 561 | 456.93 |
| 32 | 8528 | 575 | 587 | 554 | 600 | 579 | 455.93 |
| 33 | 8476 | 601 | 604 | 606 | 564 | 594 | 455.83 |
| 34 | 8462 | 604 | 513 | 603 | 595 | 579 | 457.33 |
| 35 | 8618 | 582 | 588 | 588 | 553 | 578 | 459.28 |
| 36 | 8925 | 525 | 499 | 557 | 559 | 535 | 460.83 |

[a]Time from power-on.

[b]Simulator No. 16 was unpressurized (~560 kPa) and unheated (electrically) during the test.

Table 5. Summary of B-4 test results related to volume changes

| Rod No. | Initial gas volume[a] (cm³) | Approximate vent conditions: Pressure (kPa) | Approximate vent conditions: Maximum measured temperature (°C) | Approximate vent conditions: Maximum strain (%) | Initial-to-vent pressure ratio | Vent-to-initial gas volume ratio[b] | Volume increase of tube over heated length[c] (%) | Average strain[d] (%) |
|---|---|---|---|---|---|---|---|---|
| 1 | 48.5 | 8825 | 572 | 6.3 | 1.031 | 1.14 | 7.9 | 3.9 |
| 2 | 49.5 | 8515 | 594 | 10.5 | 1.066 | 1.21 | 12.4 | 6.0 |
| 3 | 48.3 | 8515 | 599 | 9.8 | 1.068 | 1.22 | 12.5 | 6.1 |
| 4 | 50.6 | 8575 | 597 | 9.4 | 1.060 | 1.20 | 11.9 | 5.8 |
| 5 | 47.8 | 8610 | 592 | 7.8 | 1.057 | 1.19 | 10.6 | 5.2 |
| 6 | 49.0 | 8800 | 575 | 6.3 | 1.032 | 1.14 | 7.9 | 3.9 |
| 7 | 50.3 | 8305 | 597 | 13.3 | 1.097 | 1.27 | 16.0 | 7.7 |
| 8 | 48.5 | 7740 | 618 | 19.8 | 1.174 | 1.42 | 24.0 | 11.3 |
| 9 | 49.8 | 7810 | 621 | 19.0 | 1.163 | 1.41 | 24.2 | 11.4 |
| 10 | 49.6 | 8270 | 617 | 11.8 | 1.098 | 1.28 | 16.4 | 7.9 |
| 11 | 51.5 | 8190 | 608 | 12.2 | 1.107 | 1.29 | 17.8 | 8.5 |
| 12 | 49.9 | 8490 | 591 | 9.8 | 1.067 | 1.21 | 12.2 | 5.9 |
| 13 | 50.4 | 8295 | 605 | 13.1 | 1.096 | 1.27 | 15.8 | 7.6 |
| 14 | 51.7 | 7140 | 625 | 50.1 | 1.273 | 1.65 | 39.2 | 18.0 |
| 15 | 48.1 | 7990 | 631 | 15.3 | 1.138 | 1.36 | 20.5 | 9.8 |
| 16 | 50.5 | *e* | *e* | 0 | *e* | 1.0 | 0 | 0 |
| 17 | 49.1 | 8395 | 614 | 11.3 | 1.080 | 1.25 | 14.6 | 7.0 |
| 18 | 50.2 | 8515 | 596 | 9.8 | 1.064 | 1.22 | 13.1 | 6.3 |
| 19 | 49.2 | 8375 | 604 | 12.0 | 1.087 | 1.25 | 14.7 | 7.1 |
| 20 | 50.3 | 7725 | 628 | 19.8 | 1.180 | 1.44 | 26.0 | 12.2 |
| 21 | 50.3 | 7435 | 631 | 30.3 | 1.225 | 1.54 | 31.6 | 14.7 |
| 22 | 51.0 | 7945 | 629 | 19.0 | 1.146 | 1.38 | 22.5 | 10.7 |
| 23 | 49.9 | 8000 | 617 | 14.4 | 1.133 | 1.35 | 20.6 | 9.8 |
| 24 | 50.1 | 8515 | 597 | 8.7 | 1.063 | 1.20 | 11.9 | 5.8 |
| 25 | 47.9 | 8470 | 596 | 9.8 | 1.075 | 1.24 | 13.2 | 6.4 |
| 26 | 51.2 | 7705 | 609 | 19.8 | 1.183 | 1.44 | 26.4 | 12.4 |
| 27 | 47.9 | 7630 | 624 | 20.9 | 1.194 | 1.47 | 26.4 | 12.4 |
| 28 | 51.0 | 7865 | 622 | 19.4 | 1.159 | 1.40 | 23.8 | 11.3 |
| 29 | 48.6 | 7955 | 608 | 15.7 | 1.144 | 1.38 | 21.4 | 10.2 |
| 30 | 50.8 | 8605 | 586 | 8.5 | 1.053 | 1.19 | 11.3 | 5.5 |
| 31 | 49.8 | 8820 | 575 | 6.3 | 1.032 | 1.14 | 8.3 | 4.1 |
| 32 | 48.3 | 8530 | 600 | 10.9 | 1.065 | 1.23 | 12.9 | 6.2 |
| 33 | 49.6 | 8475 | 606 | 12.4 | 1.074 | 1.24 | 13.9 | 6.7 |
| 34 | 49.0 | 8460 | 604 | 12.6 | 1.078 | 1.25 | 14.3 | 6.9 |
| 35 | 49.8 | 8620 | 588 | 8.9 | 1.058 | 1.21 | 12.2 | 5.9 |
| 36 | 48.0 | 8925 | 559 | 5.2 | 1.019 | 1.11 | 6.3 | 3.1 |

[a]Measured at room temperature; includes fuel pin simulator, pressure transducer, and connecting tube.

[b]Includes fuel pin simulator, pressure transducer, and connecting tube; calculated from volume increase of tube over heated length (91 cm) and measured initial gas volume.

[c]Calculated from the circumferential strain measurements by using the equation for the volume of a cone frustum to estimate the subvolume for each length interval between strain measurements, summing these subvolumes over the heated length, and subtracting the original volume from the sum.

[d]Average (or equivalent) strain over heated length ($\bar{\varepsilon}$) was calculated from the volume increase over the heated length ($\Delta V$) using the equation $\bar{\varepsilon} = \sqrt{1 + \Delta V/V_o} - 1$, where $V_o$ is the original heated-length volume.

[e]Simulator No. 16 was unpressurized (~560 kPa) and unheated (electrically) during the test.

Table 6. Strain in tubes of B-4 test

| ELEVATION[a] (CM) | Circumferential strain (%) of tube No. 1 | 2 | 3 | 4 | 5 | 6 | 7 | 8 | 9 | 10 | 11 | 12 | 13 | 14 | 15 | 16 | 17 | 18 |
|---|---|---|---|---|---|---|---|---|---|---|---|---|---|---|---|---|---|---|
| 0.0 | 0.0 | 0.9 | 0.0 | 0.0 | 0.0 | 0.2 | 0.0 | 0.7 | 0.4 | 0.2 | 0.2 | 0.2 | 0.7 | 0.0 | 0.2 | 0.0 | 0.2 | 0.2 |
| 2.0 | 0.7 | 0.7 | 0.4 | 0.4 | 1.1 | 0.7 | 1.3 | 1.3 | 1.1 | 1.3 | 1.3 | 0.9 | 1.5 | 1.3 | 1.3 | 0.0 | 1.1 | 0.9 |
| 4.0 | 1.7 | 2.0 | 1.7 | 2.4 | 2.4 | 2.2 | 2.3 | 3.9 | 3.7 | 3.3 | 3.9 | 2.6 | 3.1 | 4.1 | 3.5 | 0.0 | 2.8 | 2.4 |
| 6.0 | 2.4 | 3.7 | 3.1 | 3.7 | 3.7 | 2.8 | 4.5 | 5.4 | 5.7 | 4.6 | 5.4 | 3.9 | 5.0 | 5.9 | 6.1 | 0.2 | 4.1 | 3.9 |
| 8.0 | 2.6 | 3.5 | 3.3 | 3.7 | 3.5 | 2.5 | 4.4 | 5.4 | 5.7 | 4.4 | 5.2 | 3.7 | 4.6 | 5.9 | 5.2 | 0.2 | 4.4 | 4.1 |
| 10.0 | 2.4 | 2.8 | 2.4 | 2.5 | 2.4 | 2.0 | 4.4 | 5.2 | 5.4 | 4.4 | 4.8 | 3.3 | 4.4 | 5.7 | 5.2 | 0.2 | 4.1 | 3.7 |
| 12.0 | 3.3 | 4.4 | 3.9 | 4.1 | 4.1 | 3.3 | 5.7 | 7.0 | 6.5 | 5.7 | 5.7 | 4.1 | 5.4 | 7.2 | 6.1 | 0.2 | 5.2 | 5.0 |
| 14.0 | 4.4 | 5.7 | 5.0 | 5.2 | 5.0 | 3.7 | 10.0 | 10.5 | 9.8 | 7.8 | 8.3 | 5.4 | 9.6 | 13.7 | 9.6 | 0.2 | 7.4 | 5.9 |
| 16.0 | 4.6 | 6.5 | 6.1 | 6.1 | 5.4 | 3.9 | 12.3 | 12.9 | 12.6 | 9.4 | 9.8 | 6.8 | 12.0 | 18.1 | 11.8 | 0.0 | 8.9 | 7.8 |
| 18.0 | 5.0 | 7.6 | 7.0 | 7.6 | 6.5 | 4.1 | 12.9 | 14.2 | 13.9 | 10.7 | 10.5 | 7.6 | 11.5 | 19.2 | 13.3 | 0.0 | 10.2 | 8.9 |
| 20.0 | 3.5 | 7.3 | 7.6 | 8.3 | 6.5 | 3.7 | 9.3 | 16.4 | 15.5 | 11.1 | 11.1 | 7.2 | 8.5 | 19.0 | 13.9 | 0.0 | 10.7 | 7.8 |
| 22.0 | 3.9 | 6.5 | 6.8 | 7.0 | 6.1 | 3.7 | 9.5 | 14.4 | 15.7 | 11.3 | 11.3 | 6.5 | 8.3 | 19.6 | 14.4 | 0.0 | 10.9 | 7.4 |
| 24.0 | 3.9 | 7.4 | 7.6 | 7.6 | 6.3 | 3.5 | 11.5 | 15.5 | 17.0 | 11.3 | 11.8 | 7.8 | 10.2 | 23.7 | 14.8 | 0.0 | 11.1 | 8.5 |
| 26.0 | 5.0 | 8.9 | 8.9 | 8.5 | 7.0 | 3.5 | 13.3 | 15.3 | 16.8 | 11.8 | 12.0 | 8.1 | 12.9 | 26.8 | 15.3 | 0.0 | 11.3 | 8.5 |
| 28.0 | 4.8 | 7.8 | 7.8 | 7.6 | 6.8 | 4.4 | 12.9 | 15.9 | 17.0 | 11.1 | 11.8 | 7.2 | 13.1 | 27.0 | 15.3 | 0.0 | 10.9 | 7.6 |
| 30.0 | 4.1 | 6.5 | 6.8 | 7.4 | 6.3 | 3.5 | 9.3 | 14.8 | 15.7 | 10.5 | 11.5 | 8.1 | 11.1 | 24.5 | 15.3 | 0.2 | 10.2 | 8.3 |
| 32.0 | 3.3 | 6.1 | 7.0 | 6.5 | 6.5 | 3.9 | 8.1 | 13.9 | 15.0 | 10.2 | 11.5 | 7.8 | 9.4 | 23.7 | 15.0 | 0.2 | 9.8 | 7.8 |
| 34.0 | 3.9 | 7.2 | 7.6 | 7.2 | 5.9 | 3.7 | 9.4 | 14.4 | 15.3 | 10.2 | 11.1 | 7.2 | 11.1 | 25.5 | 15.0 | 0.0 | 9.4 | 6.8 |
| 36.0 | 3.9 | 7.8 | 7.6 | 7.2 | 6.3 | 4.1 | 10.7 | 14.4 | 14.6 | 10.2 | 11.1 | 7.2 | 11.5 | 24.4 | 13.9 | 0.0 | 9.6 | 7.6 |
| 38.0 | 4.1 | 6.5 | 5.9 | 5.9 | 5.9 | 4.1 | 10.0 | 14.4 | 15.3 | 10.5 | 10.9 | 7.8 | 10.9 | 23.5 | 14.6 | 0.0 | 9.4 | 8.3 |
| 40.0 | 4.1 | 7.4 | 6.3 | 5.9 | 5.9 | 4.5 | 8.3 | 14.4 | 15.5 | 10.7 | 11.3 | 8.1 | 9.2 | 23.3 | 14.8 | -0.2 | 9.6 | 8.5 |
| 42.0 | 4.4 | 8.5 | 7.8 | 7.2 | 7.2 | 4.5 | 8.5 | 15.9 | 17.6 | 11.3 | 11.5 | 8.3 | 11.8 | 25.7 | 14.8 | 0.0 | 9.4 | 7.8 |
| 44.0 | 4.6 | 8.7 | 8.1 | 7.6 | 6.8 | 5.2 | 10.2 | 18.1 | 19.3 | 11.3 | 11.5 | 8.5 | 12.4 | 31.2 | 13.9 | 0.4 | 9.6 | 7.8 |
| 46.0 | 5.2 | 8.1 | 7.4 | 6.8 | 6.8 | 5.2 | 10.9 | 19.6 | 17.9 | 11.8 | 12.0 | 9.4 | 12.4 | 40.1 | 13.9 | 0.0 | 9.8 | 9.4 |
| 48.0 | 4.1 | 8.3 | 8.1 | 8.5 | 7.4 | 5.9 | 12.0 | 19.8 | 18.7 | 11.5 | 12.2 | 8.7 | 11.1 | 50.1 | 13.9 | 0.2 | 9.8 | 9.4 |
| 50.0 | 4.6 | 10.5 | 9.8 | 9.4 | 7.8 | 5.3 | 10.7 | 18.7 | 19.0 | 11.3 | 12.2 | 9.2 | 11.1 | 44.0 | 14.2 | 0.0 | 9.6 | 9.6 |
| 52.0 | 5.2 | 9.6 | 8.9 | 7.3 | 6.8 | 6.1 | 10.0 | 17.2 | 17.2 | 11.1 | 12.2 | 9.8 | 10.9 | 32.7 | 13.3 | -0.2 | 9.4 | 9.8 |
| 54.0 | 5.2 | 8.3 | 7.0 | 6.8 | 6.8 | 5.9 | 11.1 | 15.3 | 15.7 | 10.5 | 11.8 | 8.9 | 9.2 | 24.4 | 13.9 | -0.2 | 9.2 | 8.5 |
| 56.0 | 5.4 | 9.2 | 8.5 | 8.1 | 7.0 | 5.7 | 8.5 | 15.0 | 14.4 | 10.0 | 10.9 | 8.3 | 6.8 | 19.0 | 10.7 | 0.0 | 8.3 | 8.1 |
| 58.0 | 3.9 | 7.6 | 7.2 | 7.4 | 7.2 | 5.2 | 6.9 | 12.9 | 12.4 | 9.2 | 10.2 | 8.1 | 7.0 | 14.6 | 9.6 | 0.0 | 7.0 | 7.6 |
| 60.0 | 4.1 | 6.1 | 5.7 | 5.7 | 5.9 | 5.4 | 6.3 | 10.5 | 10.0 | 7.8 | 8.5 | 6.1 | 5.0 | 11.3 | 7.8 | -0.2 | 6.5 | 5.7 |
| 62.0 | 3.7 | 5.4 | 5.4 | 5.2 | 5.0 | 4.1 | 5.2 | 7.6 | 7.6 | 6.3 | 6.3 | 5.2 | 4.1 | 8.7 | 6.3 | 0.0 | 5.9 | 5.4 |
| 64.0 | 1.5 | 3.5 | 4.1 | 3.9 | 4.1 | 2.4 | 4.1 | 5.7 | 5.7 | 4.6 | 4.8 | 3.7 | 3.7 | 5.2 | 4.8 | -0.2 | 3.7 | 3.7 |
| 66.0 | 2.4 | 3.7 | 3.9 | 3.7 | 3.7 | 2.8 | 3.9 | 6.5 | 5.7 | 5.0 | 4.8 | 3.5 | 5.9 | 6.1 | 5.0 | 0.2 | 4.1 | 3.3 |
| 68.0 | 4.1 | 4.4 | 4.8 | 4.9 | 5.0 | 3.3 | 6.5 | 9.9 | 7.6 | 6.3 | 6.3 | 5.0 | 6.5 | 8.9 | 6.8 | 0.0 | 5.2 | 5.0 |
| 70.0 | 5.0 | 6.8 | 6.3 | 6.3 | 6.3 | 3.7 | 8.1 | 12.2 | 10.2 | 7.6 | 8.3 | 5.7 | 6.8 | 13.5 | 8.5 | 0.2 | 6.5 | 5.7 |
| 72.0 | 5.9 | 7.5 | 7.2 | 7.2 | 6.1 | 5.0 | 11.1 | 13.5 | 11.5 | 8.7 | 9.2 | 6.3 | 7.4 | 15.7 | 9.4 | 0.2 | 7.2 | 6.8 |
| 74.0 | 6.3 | 6.3 | 7.0 | 6.1 | 6.5 | 4.8 | 10.5 | 13.7 | 12.0 | 8.7 | 9.4 | 7.4 | 7.2 | 15.5 | 9.6 | -0.2 | 7.2 | 7.8 |
| 76.0 | 5.7 | 7.0 | 7.0 | 5.2 | 6.5 | 4.9 | 8.3 | 13.5 | 11.1 | 8.5 | 9.4 | 6.8 | 7.0 | 15.9 | 9.4 | 0.2 | 7.0 | 6.5 |
| 78.0 | 6.1 | 8.1 | 7.8 | 7.0 | 6.1 | 3.9 | 9.2 | 14.2 | 10.2 | 7.8 | 8.5 | 5.0 | 7.4 | 15.9 | 8.5 | 0.0 | 6.3 | 4.1 |
| 80.0 | 6.1 | 7.8 | 6.8 | 7.0 | 5.4 | 4.1 | 8.7 | 10.5 | 9.2 | 7.2 | 8.1 | 5.2 | 7.2 | 13.3 | 7.4 | -0.2 | 5.7 | 4.6 |
| 82.0 | 5.9 | 6.1 | 6.5 | 5.9 | 5.0 | 3.1 | 7.5 | 9.5 | 7.4 | 6.1 | 6.8 | 4.6 | 5.4 | 10.2 | 6.1 | -0.2 | 5.2 | 4.4 |
| 84.0 | 4.6 | 4.1 | 3.7 | 3.9 | 4.1 | 3.1 | 6.5 | 6.3 | 5.2 | 4.4 | 5.4 | 3.5 | 5.2 | 6.8 | 4.8 | -0.2 | 3.9 | 3.3 |
| 86.0 | 3.7 | 2.8 | 2.8 | 2.6 | 2.0 | 2.2 | 4.1 | 3.9 | 2.6 | 2.8 | 3.5 | 3.3 | 3.3 | 3.9 | 3.1 | 0.0 | 2.4 | 2.4 |
| 88.0 | 2.4 | 0.9 | 1.5 | 1.5 | 1.3 | 1.3 | 1.5 | 1.7 | 1.7 | 1.5 | 1.5 | 1.5 | 1.3 | 1.1 | 1.7 | -0.2 | 1.5 | 0.9 |
| 90.0 | 0.9 | 0.2 | 0.2 | 0.4 | 0.4 | 0.0 | 0.4 | 0.7 | 0.0 | 0.2 | 0.2 | 0.2 | 0.4 | 0.2 | 0.4 | -0.2 | 0.4 | -0.2 |
| 92.0 | 0.2 | -0.2 | -0.2 | 0.0 | 0.0 | 0.0 | 0.2 | 0.2 | -0.2 | 0.2 | 0.0 | 0.0 | 0.2 | -0.4 | 0.0 | 0.0 | 0.2 | -0.4 |

[a]Above bottom of heated zone.

Table 6 (continued)

| ELEVATION[a] (CM) | Circumferential strain (%) of tube No. 19 | 20 | 21 | 22 | 23 | 24 | 25 | 26 | 27 | 28 | 29 | 30 | 31 | 32 | 33 | 34 | 35 | 35 |
|---|---|---|---|---|---|---|---|---|---|---|---|---|---|---|---|---|---|---|
| 0.0 | 0.2 | 0.2 | 0.4 | 0.2 | 0.2 | 0.4 | 0.2 | 0.4 | 0.4 | 0.2 | 0.2 | 0.2 | 0.2 | 0.7 | 0.2 | 0.2 | 0.0 | 0.4 |
| 2.0 | 0.9 | 1.1 | 1.5 | 1.3 | 0.9 | 0.9 | 0.9 | 1.7 | 1.5 | 1.3 | 1.3 | 0.9 | 0.9 | 1.3 | 0.7 | 0.9 | 0.4 | 0.7 |
| 4.0 | 2.4 | 4.1 | 4.4 | 3.3 | 3.3 | 2.2 | 2.4 | 5.0 | 4.4 | 3.7 | 3.7 | 2.0 | 2.2 | 3.5 | 2.4 | 2.6 | 2.0 | 1.7 |
| 6.0 | 4.1 | 5.7 | 6.5 | 5.0 | 4.8 | 3.5 | 3.7 | 7.2 | 6.3 | 5.4 | 5.2 | 3.1 | 2.4 | 4.1 | 2.6 | 3.1 | 2.4 | 2.4 |
| 8.0 | 4.1 | 5.7 | 6.3 | 5.2 | 5.0 | 3.9 | 3.9 | 5.5 | 6.3 | 5.7 | 5.0 | 3.3 | 2.4 | 3.9 | 3.3 | 3.3 | 2.8 | 2.2 |
| 10.0 | 3.1 | 5.4 | 5.9 | 5.2 | 4.8 | 3.5 | 4.4 | 5.9 | 6.1 | 5.4 | 4.8 | 3.1 | 2.2 | 3.3 | 2.8 | 3.3 | 2.4 | 2.0 |
| 12.0 | 5.2 | 7.2 | 7.4 | 6.5 | 5.9 | 4.8 | 4.8 | 7.8 | 7.2 | 6.8 | 5.9 | 3.9 | 3.1 | 4.4 | 3.9 | 4.1 | 3.1 | 2.5 |
| 14.0 | 7.4 | 12.0 | 12.2 | 10.7 | 9.2 | 5.4 | 8.1 | 14.2 | 11.5 | 10.7 | 9.6 | 4.8 | 5.2 | 7.2 | 6.5 | 6.1 | 4.8 | 3.3 |
| 16.0 | 10.5 | 16.1 | 16.6 | 14.2 | 11.5 | 7.0 | 9.5 | 13.0 | 15.3 | 14.4 | 12.6 | 6.3 | 6.3 | 9.2 | 9.2 | 8.9 | 6.5 | 3.5 |
| 18.0 | 10.7 | 17.9 | 19.2 | 17.0 | 12.9 | 8.1 | 9.8 | 13.8 | 17.0 | 16.1 | 14.6 | 7.0 | 5.2 | 8.1 | 8.7 | 8.5 | 6.8 | 3.9 |
| 20.0 | 8.5 | 17.9 | 20.0 | 18.3 | 13.1 | 7.2 | 8.3 | 13.0 | 17.0 | 17.2 | 15.5 | 6.8 | 4.8 | 8.3 | 9.2 | 8.5 | 6.8 | 3.5 |
| 22.0 | 8.1 | 18.1 | 21.1 | 19.0 | 13.1 | 7.4 | 7.6 | 18.5 | 17.4 | 18.5 | 15.7 | 7.0 | 4.4 | 9.4 | 12.0 | 11.1 | 8.1 | 3.9 |
| 24.0 | 10.0 | 18.5 | 22.4 | 19.0 | 13.5 | 8.3 | 8.7 | 18.3 | 18.3 | 18.7 | 15.7 | 7.4 | 4.8 | 9.8 | 12.4 | 11.8 | 8.3 | 3.9 |
| 26.0 | 12.0 | 19.2 | 23.3 | 18.5 | 13.5 | 7.8 | 9.5 | 17.6 | 19.0 | 18.5 | 14.8 | 7.4 | 4.8 | 8.9 | 10.2 | 10.0 | 7.6 | 3.5 |
| 28.0 | 11.8 | 19.8 | 23.5 | 17.9 | 13.5 | 7.4 | 9.3 | 17.0 | 19.8 | 19.2 | 13.9 | 7.4 | 5.4 | 10.0 | 11.3 | 11.5 | 8.3 | 3.7 |
| 30.0 | 9.8 | 18.7 | 23.7 | 16.3 | 13.5 | 7.8 | 8.3 | 17.2 | 20.5 | 19.4 | 13.3 | 7.4 | 5.4 | 10.9 | 12.0 | 12.4 | 8.9 | 3.7 |
| 32.0 | 8.7 | 17.6 | 24.8 | 15.9 | 13.7 | 7.2 | 8.7 | 17.2 | 20.0 | 18.3 | 12.4 | 7.0 | 5.0 | 8.9 | 9.8 | 12.6 | 8.3 | 4.1 |
| 34.0 | 10.0 | 17.0 | 27.5 | 15.5 | 13.5 | 6.3 | 8.7 | 17.6 | 20.3 | 16.8 | 12.0 | 6.3 | 5.4 | 8.7 | 9.2 | 9.6 | 7.2 | 3.9 |
| 36.0 | 10.5 | 17.9 | 30.3 | 15.9 | 13.7 | 7.2 | 8.9 | 17.2 | 20.9 | 16.3 | 12.6 | 7.0 | 5.0 | 9.8 | 10.2 | 10.9 | 8.1 | 3.3 |
| 38.0 | 8.5 | 17.4 | 28.3 | 15.9 | 13.9 | 7.8 | 7.8 | 15.8 | 20.3 | 16.1 | 13.1 | 7.2 | 5.0 | 8.9 | 10.0 | 10.7 | 7.6 | 3.5 |
| 40.0 | 7.8 | 16.8 | 25.1 | 15.5 | 13.9 | 8.1 | 7.2 | 15.9 | 18.7 | 15.9 | 13.5 | 7.2 | 5.0 | 7.4 | 8.3 | 8.9 | 7.2 | 3.3 |
| 42.0 | 8.7 | 17.2 | 23.7 | 15.0 | 13.5 | 7.2 | 7.8 | 15.1 | 18.1 | 16.3 | 13.5 | 6.8 | 5.4 | 8.9 | 10.0 | 10.5 | 8.1 | 3.7 |
| 44.0 | 9.8 | 17.9 | 23.1 | 15.0 | 13.7 | 7.2 | 8.9 | 17.2 | 17.4 | 15.7 | 13.7 | 7.2 | 5.4 | 9.2 | 10.9 | 11.3 | 8.9 | 4.1 |
| 46.0 | 10.7 | 18.3 | 22.7 | 13.9 | 13.9 | 8.7 | 8.9 | 17.6 | 16.6 | 15.0 | 13.7 | 7.8 | 5.0 | 8.3 | 8.7 | 9.2 | 7.8 | 3.9 |
| 48.0 | 11.3 | 18.7 | 22.7 | 14.5 | 13.9 | 8.5 | 9.4 | 17.9 | 15.6 | 15.0 | 13.7 | 8.1 | 5.0 | 7.4 | 7.8 | 8.5 | 7.0 | 3.7 |
| 50.0 | 9.4 | 18.1 | 22.2 | 14.5 | 14.4 | 8.5 | 7.4 | 17.6 | 17.6 | 15.5 | 14.4 | 7.4 | 5.0 | 8.9 | 9.2 | 10.0 | 8.3 | 3.3 |
| 52.0 | 10.0 | 17.6 | 21.1 | 14.2 | 13.9 | 8.7 | 8.7 | 17.9 | 17.9 | 15.5 | 14.8 | 8.5 | 5.4 | 9.2 | 9.8 | 10.7 | 8.9 | 4.4 |
| 54.0 | 10.7 | 16.3 | 19.0 | 12.9 | 13.1 | 7.8 | 9.2 | 17.6 | 17.6 | 14.6 | 13.7 | 7.8 | 5.7 | 7.4 | 8.3 | 8.7 | 8.7 | 4.1 |
| 56.0 | 9.2 | 14.2 | 15.6 | 12.0 | 12.0 | 7.4 | 7.8 | 15.7 | 17.0 | 13.9 | 13.1 | 7.0 | 5.7 | 8.1 | 8.5 | 9.4 | 7.6 | 4.1 |
| 58.0 | 7.0 | 11.5 | 13.5 | 10.2 | 10.2 | 7.4 | 7.2 | 13.1 | 14.8 | 12.2 | 11.3 | 7.2 | 5.4 | 7.6 | 8.7 | 9.4 | 8.3 | 5.0 |
| 60.0 | 6.5 | 9.4 | 10.5 | 8.1 | 8.7 | 5.9 | 6.5 | 10.5 | 11.3 | 9.6 | 9.6 | 5.7 | 5.2 | 5.5 | 6.5 | 6.5 | 6.1 | 4.1 |
| 62.0 | 4.8 | 7.2 | 7.6 | 5.9 | 6.5 | 4.8 | 5.0 | 7.6 | 8.1 | 7.4 | 7.0 | 4.4 | 4.1 | 4.8 | 4.6 | 5.0 | 4.1 | 3.5 |
| 64.0 | 3.5 | 5.0 | 5.7 | 4.5 | 5.0 | 3.5 | 3.7 | 5.9 | 5.9 | 5.2 | 5.4 | 2.4 | 3.1 | 3.7 | 3.5 | 3.7 | 3.3 | 3.1 |
| 66.0 | 3.5 | 5.7 | 6.1 | 5.0 | 5.9 | 3.7 | 3.5 | 5.3 | 5.9 | 5.7 | 6.1 | 3.5 | 2.8 | 3.7 | 3.3 | 3.7 | 2.8 | 2.0 |
| 68.0 | 5.2 | 7.5 | 8.3 | 6.8 | 7.6 | 5.2 | 5.0 | 8.3 | 7.8 | 5.2 | 8.1 | 5.4 | 3.7 | 4.8 | 4.6 | 5.0 | 4.4 | 3.7 |
| 70.0 | 6.3 | 10.5 | 11.1 | 8.5 | 10.2 | 5.9 | 5.7 | 10.0 | 10.5 | 9.4 | 10.9 | 6.5 | 4.4 | 4.8 | 4.8 | 5.2 | 4.8 | 3.9 |
| 72.0 | 8.1 | 11.5 | 12.9 | 9.5 | 11.1 | 6.8 | 6.5 | 11.1 | 11.3 | 10.5 | 12.6 | 7.6 | 4.4 | 6.1 | 6.1 | 5.7 | 6.8 | 4.6 |
| 74.0 | 5.9 | 11.1 | 12.9 | 9.4 | 11.1 | 7.4 | 5.4 | 11.3 | 11.3 | 10.5 | 12.0 | 8.5 | 4.4 | 5.2 | 5.2 | 5.0 | 5.2 | 5.2 |
| 76.0 | 6.3 | 11.1 | 12.4 | 9.2 | 10.7 | 6.1 | 5.9 | 11.1 | 11.3 | 10.2 | 10.9 | 6.8 | 3.9 | 5.2 | 5.0 | 5.0 | 5.2 | 4.4 |
| 78.0 | 6.5 | 10.2 | 10.9 | 8.5 | 8.9 | 4.8 | 5.7 | 10.7 | 11.1 | 9.5 | 10.0 | 6.3 | 3.7 | 5.7 | 5.4 | 5.2 | 5.9 | 4.8 |
| 80.0 | 5.0 | 9.8 | 9.2 | 7.6 | 7.8 | 4.8 | 5.0 | 10.0 | 10.0 | 8.7 | 8.9 | 5.2 | 4.1 | 5.0 | 5.0 | 4.6 | 5.0 | 3.7 |
| 82.0 | 4.1 | 8.1 | 7.8 | 6.5 | 6.5 | 4.1 | 4.4 | 8.9 | 8.1 | 7.6 | 7.8 | 4.4 | 3.7 | 5.0 | 4.1 | 4.1 | 4.8 | 3.5 |
| 84.0 | 4.4 | 6.1 | 5.7 | 5.0 | 5.0 | 3.3 | 4.4 | 7.0 | 5.9 | 5.7 | 6.1 | 3.9 | 3.5 | 3.3 | 3.1 | 3.3 | 3.1 | 3.3 |
| 86.0 | 2.8 | 3.7 | 3.5 | 3.5 | 3.3 | 2.5 | 2.8 | 4.1 | 3.9 | 3.9 | 4.1 | 2.6 | 2.8 | 3.1 | 2.4 | 2.6 | 2.2 | 2.5 |
| 88.0 | 1.1 | 1.5 | 1.7 | 2.0 | 1.1 | 1.5 | 1.5 | 2.0 | 1.7 | 2.2 | 2.0 | 1.7 | 1.5 | 1.5 | 1.1 | 1.3 | 1.1 | 1.7 |
| 90.0 | 0.0 | 0.2 | 0.2 | 0.0 | 0.2 | 0.2 | 0.2 | 0.4 | 0.4 | 0.4 | 0.4 | 0.4 | 0.2 | 0.4 | 0.2 | 0.2 | -0.2 | 0.7 |
| 92.0 | 0.0 | 0.2 | 0.2 | 0.2 | 0.0 | 0.0 | -0.2 | -0.2 | 0.0 | 0.2 | 0.0 | 0.2 | -0.2 | 0.4 | -0.2 | 0.0 | -0.2 | 0.2 |

[a]Above bottom of heated zone.

Table 7. Deformed tube areas in B-4 test

| ELEVATION[a] (CM) | Outside area (mm²) of tube No. 1 | 2 | 3 | 4 | 5 | 6 | 7 | 8 | 9 | 10 | 11 | 12 | 13 | 14 | 15 | 16 | 17 | 18 |
|---|---|---|---|---|---|---|---|---|---|---|---|---|---|---|---|---|---|---|
| 0.0 | 93 | 95 | 93 | 93 | 93 | 94 | 93 | 94 | 94 | 94 | 94 | 94 | 94 | 93 | 94 | 93 | 94 | 94 |
| 2.0 | 94 | 94 | 94 | 94 | 95 | 94 | 96 | 96 | 95 | 96 | 96 | 95 | 96 | 96 | 96 | 93 | 95 | 95 |
| 4.0 | 96 | 97 | 96 | 98 | 98 | 97 | 99 | 101 | 100 | 99 | 101 | 98 | 99 | 101 | 100 | 93 | 99 | 98 |
| 6.0 | 98 | 100 | 99 | 100 | 100 | 99 | 102 | 104 | 104 | 102 | 104 | 101 | 103 | 105 | 105 | 94 | 101 | 101 |
| 8.0 | 98 | 100 | 99 | 100 | 100 | 98 | 102 | 104 | 104 | 102 | 103 | 100 | 102 | 105 | 103 | 94 | 102 | 101 |
| 10.0 | 98 | 99 | 98 | 98 | 98 | 97 | 102 | 103 | 104 | 102 | 102 | 99 | 102 | 104 | 103 | 94 | 101 | 100 |
| 12.0 | 99 | 102 | 101 | 101 | 101 | 99 | 104 | 107 | 106 | 104 | 104 | 101 | 104 | 107 | 105 | 94 | 103 | 103 |
| 14.0 | 102 | 104 | 103 | 103 | 103 | 100 | 113 | 114 | 112 | 108 | 109 | 104 | 112 | 121 | 112 | 94 | 108 | 105 |
| 16.0 | 102 | 105 | 105 | 105 | 104 | 101 | 119 | 119 | 118 | 112 | 112 | 106 | 117 | 130 | 117 | 93 | 111 | 108 |
| 18.0 | 103 | 108 | 107 | 108 | 106 | 101 | 119 | 122 | 121 | 114 | 114 | 108 | 116 | 133 | 120 | 93 | 113 | 111 |
| 20.0 | 100 | 108 | 108 | 109 | 106 | 100 | 112 | 122 | 124 | 115 | 115 | 107 | 110 | 132 | 121 | 93 | 114 | 108 |
| 22.0 | 101 | 106 | 106 | 107 | 105 | 100 | 112 | 122 | 125 | 116 | 116 | 106 | 109 | 134 | 122 | 93 | 115 | 108 |
| 24.0 | 101 | 108 | 108 | 108 | 105 | 100 | 115 | 124 | 128 | 116 | 117 | 108 | 113 | 143 | 123 | 93 | 115 | 110 |
| 26.0 | 103 | 111 | 111 | 110 | 107 | 100 | 120 | 126 | 127 | 117 | 117 | 109 | 119 | 150 | 124 | 93 | 116 | 110 |
| 28.0 | 102 | 108 | 108 | 108 | 106 | 102 | 119 | 125 | 128 | 115 | 117 | 107 | 119 | 151 | 124 | 93 | 115 | 108 |
| 30.0 | 101 | 106 | 106 | 108 | 105 | 100 | 112 | 123 | 125 | 114 | 116 | 109 | 115 | 145 | 124 | 94 | 113 | 109 |
| 32.0 | 99 | 105 | 107 | 105 | 106 | 101 | 109 | 121 | 123 | 113 | 116 | 108 | 112 | 143 | 123 | 94 | 112 | 108 |
| 34.0 | 101 | 107 | 108 | 107 | 105 | 100 | 112 | 122 | 124 | 113 | 115 | 107 | 115 | 147 | 123 | 93 | 112 | 106 |
| 36.0 | 101 | 108 | 108 | 107 | 105 | 101 | 114 | 122 | 123 | 113 | 115 | 107 | 116 | 144 | 121 | 93 | 112 | 108 |
| 38.0 | 101 | 105 | 105 | 105 | 105 | 101 | 113 | 122 | 124 | 114 | 115 | 108 | 115 | 142 | 123 | 93 | 112 | 109 |
| 40.0 | 101 | 108 | 105 | 105 | 105 | 102 | 109 | 122 | 124 | 114 | 116 | 109 | 111 | 142 | 123 | 93 | 112 | 110 |
| 42.0 | 102 | 110 | 108 | 107 | 107 | 102 | 110 | 125 | 129 | 116 | 116 | 109 | 117 | 148 | 123 | 93 | 112 | 108 |
| 44.0 | 102 | 110 | 109 | 108 | 106 | 103 | 113 | 130 | 131 | 116 | 116 | 110 | 118 | 161 | 121 | 94 | 112 | 108 |
| 46.0 | 103 | 109 | 108 | 106 | 106 | 103 | 115 | 134 | 130 | 117 | 117 | 112 | 118 | 183 | 121 | 93 | 112 | 112 |
| 48.0 | 101 | 109 | 109 | 110 | 108 | 105 | 117 | 134 | 132 | 116 | 117 | 110 | 115 | 211 | 121 | 94 | 112 | 112 |
| 50.0 | 102 | 114 | 112 | 112 | 108 | 105 | 114 | 132 | 132 | 116 | 117 | 111 | 115 | 194 | 122 | 93 | 112 | 112 |
| 52.0 | 103 | 112 | 111 | 108 | 106 | 105 | 113 | 128 | 128 | 115 | 117 | 112 | 115 | 164 | 120 | 93 | 112 | 112 |
| 54.0 | 103 | 109 | 107 | 105 | 106 | 105 | 115 | 126 | 125 | 114 | 117 | 111 | 111 | 144 | 121 | 93 | 111 | 110 |
| 56.0 | 104 | 111 | 110 | 109 | 107 | 104 | 110 | 123 | 122 | 113 | 115 | 109 | 106 | 132 | 114 | 93 | 109 | 109 |
| 58.0 | 101 | 108 | 107 | 108 | 107 | 103 | 105 | 119 | 118 | 111 | 113 | 109 | 107 | 123 | 112 | 93 | 107 | 108 |
| 60.0 | 101 | 105 | 104 | 104 | 105 | 104 | 105 | 114 | 113 | 108 | 110 | 105 | 103 | 115 | 108 | 93 | 106 | 104 |
| 62.0 | 100 | 104 | 104 | 103 | 103 | 101 | 103 | 108 | 108 | 105 | 105 | 103 | 101 | 110 | 105 | 93 | 105 | 104 |
| 64.0 | 96 | 100 | 101 | 101 | 101 | 98 | 101 | 104 | 104 | 102 | 102 | 100 | 100 | 103 | 102 | 93 | 100 | 100 |
| 66.0 | 98 | 100 | 101 | 100 | 100 | 99 | 101 | 106 | 104 | 103 | 102 | 100 | 105 | 105 | 103 | 94 | 101 | 99 |
| 68.0 | 101 | 102 | 102 | 102 | 103 | 99 | 105 | 111 | 108 | 105 | 105 | 103 | 106 | 111 | 106 | 93 | 103 | 103 |
| 70.0 | 103 | 105 | 105 | 105 | 105 | 100 | 109 | 117 | 113 | 108 | 109 | 104 | 106 | 120 | 110 | 94 | 106 | 104 |
| 72.0 | 105 | 108 | 107 | 107 | 105 | 103 | 115 | 120 | 116 | 110 | 111 | 105 | 108 | 125 | 112 | 94 | 107 | 106 |
| 74.0 | 105 | 105 | 107 | 105 | 106 | 102 | 114 | 121 | 117 | 110 | 112 | 108 | 107 | 124 | 112 | 93 | 107 | 108 |
| 76.0 | 104 | 107 | 107 | 103 | 105 | 102 | 109 | 120 | 115 | 110 | 112 | 106 | 107 | 125 | 112 | 94 | 107 | 106 |
| 78.0 | 105 | 109 | 108 | 107 | 105 | 101 | 111 | 122 | 113 | 108 | 110 | 103 | 108 | 125 | 110 | 93 | 105 | 101 |
| 80.0 | 105 | 108 | 106 | 107 | 104 | 101 | 110 | 114 | 111 | 107 | 109 | 103 | 107 | 120 | 108 | 93 | 104 | 102 |
| 82.0 | 105 | 105 | 106 | 105 | 103 | 99 | 108 | 110 | 108 | 105 | 106 | 102 | 104 | 113 | 105 | 93 | 103 | 102 |
| 84.0 | 102 | 101 | 100 | 101 | 101 | 99 | 105 | 105 | 103 | 102 | 104 | 100 | 103 | 106 | 102 | 93 | 101 | 99 |
| 86.0 | 100 | 99 | 99 | 98 | 97 | 97 | 101 | 101 | 98 | 99 | 100 | 99 | 99 | 101 | 99 | 93 | 98 | 98 |
| 88.0 | 98 | 95 | 96 | 96 | 96 | 95 | 95 | 96 | 95 | 96 | 96 | 96 | 96 | 95 | 96 | 93 | 96 | 95 |
| 90.0 | 95 | 94 | 94 | 94 | 94 | 93 | 94 | 94 | 93 | 94 | 94 | 94 | 94 | 94 | 94 | 93 | 94 | 93 |
| 92.0 | 94 | 93 | 93 | 93 | 93 | 93 | 94 | 94 | 93 | 94 | 93 | 93 | 94 | 92 | 93 | 93 | 94 | 92 |

[a] Above bottom of heated zone.

Table 7 (continued)

| ELEVATION[a] (CM) | Outside area (mm²) of tube No. 19 | 20 | 21 | 22 | 23 | 24 | 25 | 25 | 27 | 28 | 29 | 30 | 31 | 32 | 33 | 34 | 35 | 36 |
|---|---|---|---|---|---|---|---|---|---|---|---|---|---|---|---|---|---|---|
| 0.0 | 94 | 94 | 94 | 94 | 94 | 94 | 94 | 94 | 94 | 94 | 94 | 94 | 94 | 94 | 94 | 94 | 93 | 94 |
| 2.0 | 95 | 95 | 96 | 96 | 95 | 95 | 95 | 96 | 96 | 96 | 96 | 95 | 95 | 96 | 94 | 95 | 94 | 94 |
| 4.0 | 98 | 101 | 102 | 99 | 99 | 97 | 98 | 103 | 102 | 100 | 100 | 97 | 97 | 103 | 98 | 98 | 97 | 96 |
| 6.0 | 101 | 104 | 106 | 103 | 102 | 100 | 100 | 107 | 105 | 104 | 103 | 99 | 98 | 101 | 98 | 99 | 98 | 98 |
| 8.0 | 101 | 104 | 105 | 103 | 103 | 101 | 101 | 106 | 105 | 104 | 103 | 99 | 98 | 101 | 99 | 99 | 99 | 97 |
| 10.0 | 99 | 104 | 105 | 103 | 102 | 100 | 102 | 105 | 105 | 104 | 102 | 99 | 97 | 99 | 99 | 99 | 98 | 97 |
| 12.0 | 103 | 107 | 109 | 105 | 105 | 102 | 102 | 108 | 107 | 105 | 105 | 101 | 99 | 102 | 101 | 101 | 99 | 98 |
| 14.0 | 108 | 117 | 117 | 114 | 111 | 104 | 109 | 122 | 116 | 114 | 112 | 102 | 103 | 107 | 106 | 105 | 102 | 99 |
| 16.0 | 114 | 126 | 127 | 122 | 116 | 107 | 112 | 132 | 124 | 122 | 118 | 105 | 105 | 111 | 111 | 111 | 106 | 100 |
| 18.0 | 114 | 130 | 133 | 123 | 119 | 109 | 112 | 134 | 128 | 126 | 123 | 107 | 103 | 109 | 110 | 110 | 105 | 101 |
| 20.0 | 110 | 130 | 135 | 131 | 119 | 107 | 109 | 132 | 128 | 128 | 124 | 106 | 102 | 109 | 111 | 110 | 106 | 100 |
| 22.0 | 109 | 130 | 137 | 132 | 119 | 108 | 109 | 131 | 129 | 131 | 125 | 107 | 102 | 112 | 117 | 115 | 109 | 101 |
| 24.0 | 113 | 131 | 140 | 132 | 120 | 109 | 110 | 131 | 131 | 132 | 125 | 108 | 102 | 112 | 118 | 117 | 109 | 101 |
| 26.0 | 117 | 133 | 142 | 131 | 120 | 108 | 112 | 129 | 132 | 131 | 123 | 108 | 102 | 111 | 113 | 113 | 108 | 100 |
| 28.0 | 117 | 134 | 142 | 133 | 120 | 108 | 112 | 126 | 134 | 133 | 121 | 108 | 104 | 113 | 116 | 116 | 109 | 100 |
| 30.0 | 112 | 132 | 143 | 127 | 120 | 108 | 109 | 128 | 135 | 133 | 120 | 108 | 104 | 115 | 117 | 118 | 111 | 100 |
| 32.0 | 110 | 129 | 146 | 125 | 121 | 107 | 110 | 128 | 135 | 131 | 118 | 107 | 103 | 111 | 112 | 118 | 109 | 101 |
| 34.0 | 113 | 128 | 152 | 124 | 120 | 105 | 110 | 129 | 135 | 127 | 117 | 105 | 104 | 110 | 111 | 112 | 107 | 101 |
| 36.0 | 114 | 130 | 159 | 125 | 121 | 107 | 111 | 128 | 136 | 126 | 118 | 107 | 103 | 112 | 113 | 115 | 109 | 99 |
| 38.0 | 110 | 129 | 154 | 125 | 121 | 108 | 108 | 127 | 135 | 126 | 119 | 107 | 103 | 111 | 113 | 114 | 108 | 100 |
| 40.0 | 108 | 127 | 146 | 124 | 121 | 109 | 107 | 125 | 132 | 125 | 120 | 107 | 103 | 108 | 109 | 111 | 107 | 99 |
| 42.0 | 110 | 128 | 143 | 123 | 120 | 107 | 108 | 126 | 130 | 125 | 120 | 106 | 104 | 111 | 113 | 114 | 109 | 100 |
| 44.0 | 112 | 130 | 141 | 123 | 121 | 107 | 111 | 128 | 129 | 125 | 121 | 107 | 104 | 111 | 115 | 116 | 111 | 101 |
| 46.0 | 114 | 131 | 140 | 121 | 121 | 110 | 111 | 129 | 127 | 123 | 121 | 108 | 103 | 109 | 110 | 111 | 108 | 101 |
| 48.0 | 116 | 132 | 140 | 123 | 121 | 110 | 112 | 130 | 127 | 123 | 121 | 109 | 103 | 108 | 108 | 110 | 107 | 100 |
| 50.0 | 112 | 130 | 139 | 123 | 122 | 110 | 108 | 129 | 129 | 124 | 122 | 108 | 103 | 111 | 111 | 113 | 109 | 99 |
| 52.0 | 113 | 129 | 137 | 122 | 121 | 110 | 110 | 130 | 130 | 124 | 123 | 110 | 104 | 111 | 112 | 114 | 111 | 102 |
| 54.0 | 114 | 126 | 132 | 119 | 119 | 109 | 111 | 129 | 129 | 123 | 121 | 108 | 104 | 108 | 109 | 110 | 110 | 101 |
| 56.0 | 111 | 122 | 127 | 117 | 117 | 108 | 108 | 125 | 128 | 121 | 119 | 107 | 104 | 109 | 110 | 112 | 108 | 101 |
| 58.0 | 107 | 116 | 120 | 113 | 113 | 108 | 107 | 119 | 123 | 117 | 117 | 107 | 104 | 109 | 110 | 112 | 109 | 103 |
| 60.0 | 106 | 112 | 114 | 109 | 110 | 105 | 105 | 114 | 116 | 112 | 112 | 104 | 103 | 106 | 106 | 106 | 105 | 101 |
| 62.0 | 102 | 107 | 108 | 105 | 106 | 102 | 103 | 108 | 109 | 108 | 107 | 102 | 101 | 102 | 102 | 103 | 101 | 100 |
| 64.0 | 100 | 103 | 104 | 102 | 103 | 100 | 100 | 105 | 105 | 103 | 104 | 98 | 99 | 100 | 100 | 100 | 99 | 99 |
| 66.0 | 100 | 104 | 105 | 103 | 105 | 100 | 100 | 105 | 105 | 104 | 105 | 100 | 99 | 100 | 99 | 100 | 99 | 97 |
| 68.0 | 103 | 108 | 109 | 105 | 108 | 103 | 103 | 109 | 108 | 103 | 109 | 104 | 100 | 102 | 102 | 103 | 102 | 100 |
| 70.0 | 105 | 114 | 115 | 110 | 113 | 105 | 104 | 113 | 114 | 112 | 115 | 106 | 102 | 102 | 102 | 103 | 102 | 101 |
| 72.0 | 109 | 115 | 119 | 112 | 115 | 105 | 105 | 115 | 116 | 114 | 118 | 108 | 102 | 105 | 105 | 104 | 106 | 102 |
| 74.0 | 105 | 115 | 119 | 112 | 115 | 108 | 104 | 116 | 116 | 114 | 117 | 110 | 102 | 103 | 103 | 103 | 103 | 103 |
| 76.0 | 105 | 115 | 118 | 111 | 114 | 105 | 105 | 115 | 116 | 113 | 115 | 106 | 101 | 103 | 103 | 103 | 103 | 102 |
| 78.0 | 105 | 113 | 115 | 110 | 111 | 102 | 104 | 114 | 115 | 112 | 113 | 105 | 100 | 104 | 104 | 103 | 105 | 102 |
| 80.0 | 103 | 112 | 111 | 108 | 108 | 102 | 103 | 113 | 113 | 110 | 111 | 103 | 101 | 103 | 103 | 102 | 103 | 100 |
| 82.0 | 101 | 109 | 108 | 105 | 106 | 101 | 102 | 111 | 109 | 108 | 108 | 102 | 100 | 103 | 101 | 101 | 102 | 100 |
| 84.0 | 102 | 105 | 104 | 103 | 103 | 99 | 102 | 107 | 105 | 104 | 105 | 101 | 100 | 99 | 99 | 99 | 99 | 99 |
| 86.0 | 99 | 100 | 100 | 100 | 99 | 98 | 99 | 101 | 101 | 101 | 101 | 98 | 99 | 99 | 98 | 98 | 97 | 98 |
| 88.0 | 95 | 96 | 96 | 97 | 95 | 95 | 95 | 97 | 96 | 97 | 97 | 96 | 96 | 95 | 95 | 96 | 95 | 96 |
| 90.0 | 93 | 94 | 94 | 93 | 94 | 94 | 94 | 94 | 94 | 94 | 94 | 94 | 94 | 94 | 94 | 94 | 93 | 94 |
| 92.0 | 93 | 94 | 94 | 94 | 93 | 93 | 93 | 93 | 93 | 94 | 93 | 94 | 93 | 94 | 93 | 93 | 93 | 94 |

[a] Above bottom of heated zone.

Table 8. Coolant channel flow area restriction in B-4 test

| ELEVATION[a] (CM) | 6X6 ARRAY (%) | 4X4 ARRAY (%) |
|---|---|---|
| 0.0 | 0.4 | 0.4 |
| 2.0 | 1.7 | 2.0 |
| 4.0 | 4.8 | 6.0 |
| 6.0 | 7.1 | 8.8 |
| 8.0 | 7.0 | 8.6 |
| 10.0 | 6.4 | 8.3 |
| 12.0 | 8.5 | 10.4 |
| 14.0 | 13.1 | 17.0 |
| 16.0 | 16.9 | 22.3 |
| 18.0 | 18.5 | 25.0 |
| 20.0 | 18.2 | 25.8 |
| 22.0 | 18.6 | 26.5 |
| 24.0 | 19.9 | 27.8 |
| 26.0 | 20.5 | 28.4 |
| 28.0 | 20.5 | 28.3 |
| 30.0 | 19.7 | 27.4 |
| 32.0 | 18.8 | 26.6 |
| 34.0 | 18.8 | 26.8 |
| 36.0 | 19.4 | 27.1 |
| 38.0 | 18.8 | 26.7 |
| 40.0 | 18.1 | 26.0 |
| 42.0 | 19.1 | 26.6 |
| 44.0 | 20.0 | 27.7 |
| 46.0 | 20.5 | 28.9 |
| 48.0 | 21.2 | 30.7 |
| 50.0 | 21.1 | 29.8 |
| 52.0 | 20.2 | 27.4 |
| 54.0 | 18.5 | 25.0 |
| 56.0 | 17.0 | 22.2 |
| 58.0 | 15.0 | 18.8 |
| 60.0 | 12.1 | 15.0 |
| 62.0 | 9.4 | 11.2 |
| 64.0 | 6.7 | 8.1 |
| 66.0 | 7.1 | 8.8 |
| 68.0 | 9.7 | 11.7 |
| 70.0 | 12.4 | 15.9 |
| 72.0 | 14.2 | 18.0 |
| 74.0 | 13.9 | 17.9 |
| 76.0 | 13.3 | 17.5 |
| 78.0 | 12.8 | 16.3 |
| 80.0 | 11.5 | 14.2 |
| 82.0 | 9.8 | 11.9 |
| 84.0 | 7.5 | 8.7 |
| 86.0 | 5.0 | 5.4 |
| 88.0 | 2.4 | 2.6 |
| 90.0 | 0.4 | 0.4 |
| 92.0 | 0.0 | 0.1 |

[a]Above bottom of heated zone.

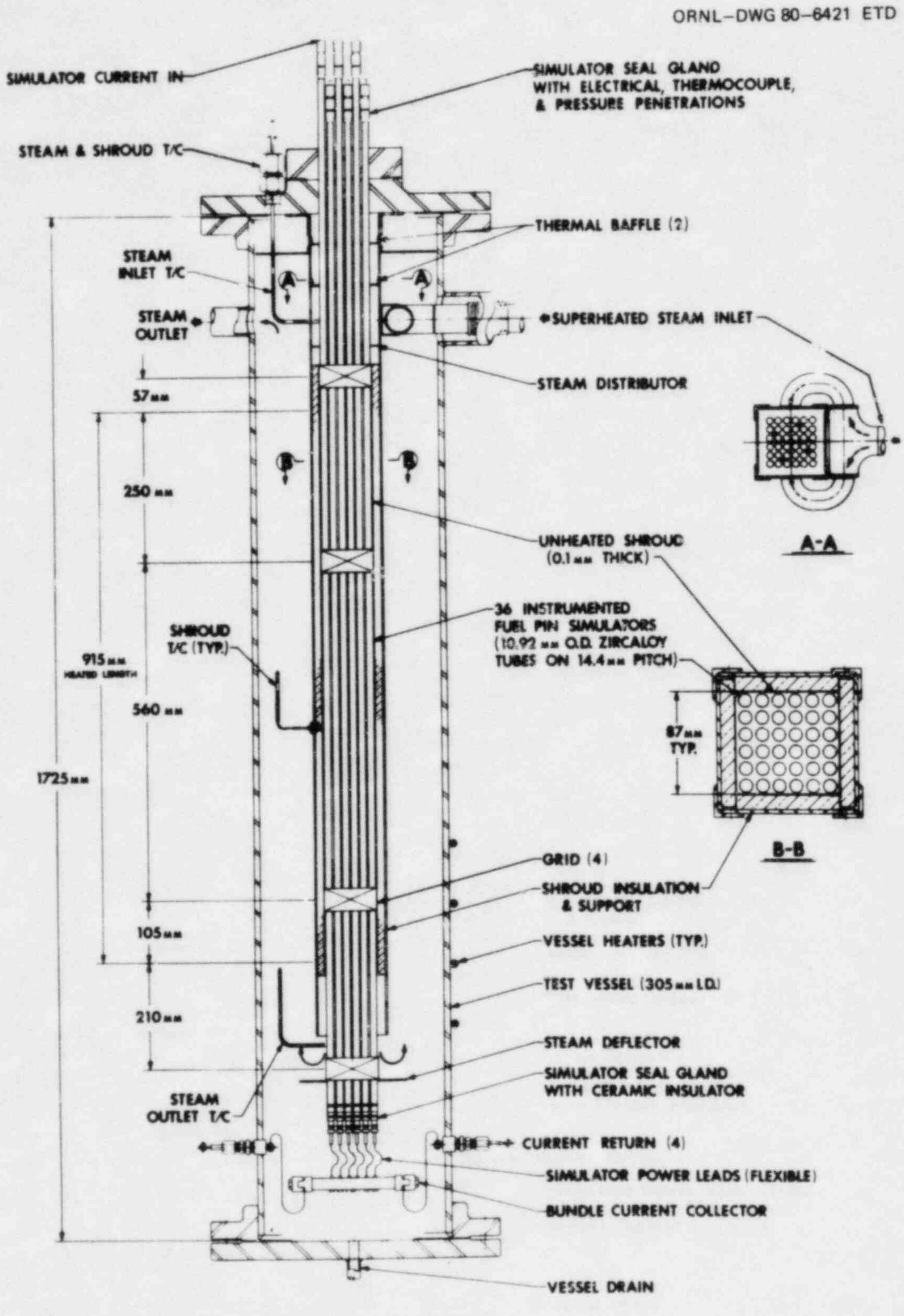


Fig. 1. Schematic of B-4 test assembly.

ORNL–DWG 77–8293

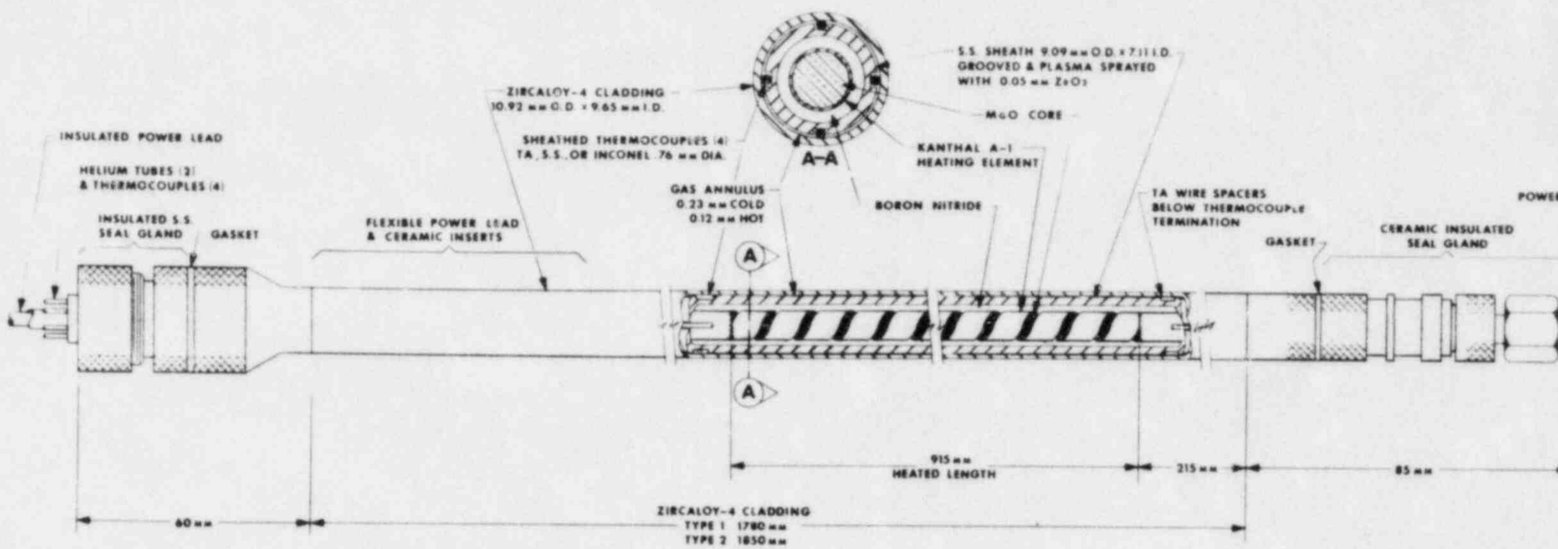


Fig. 2. Typical fuel pin simulator.

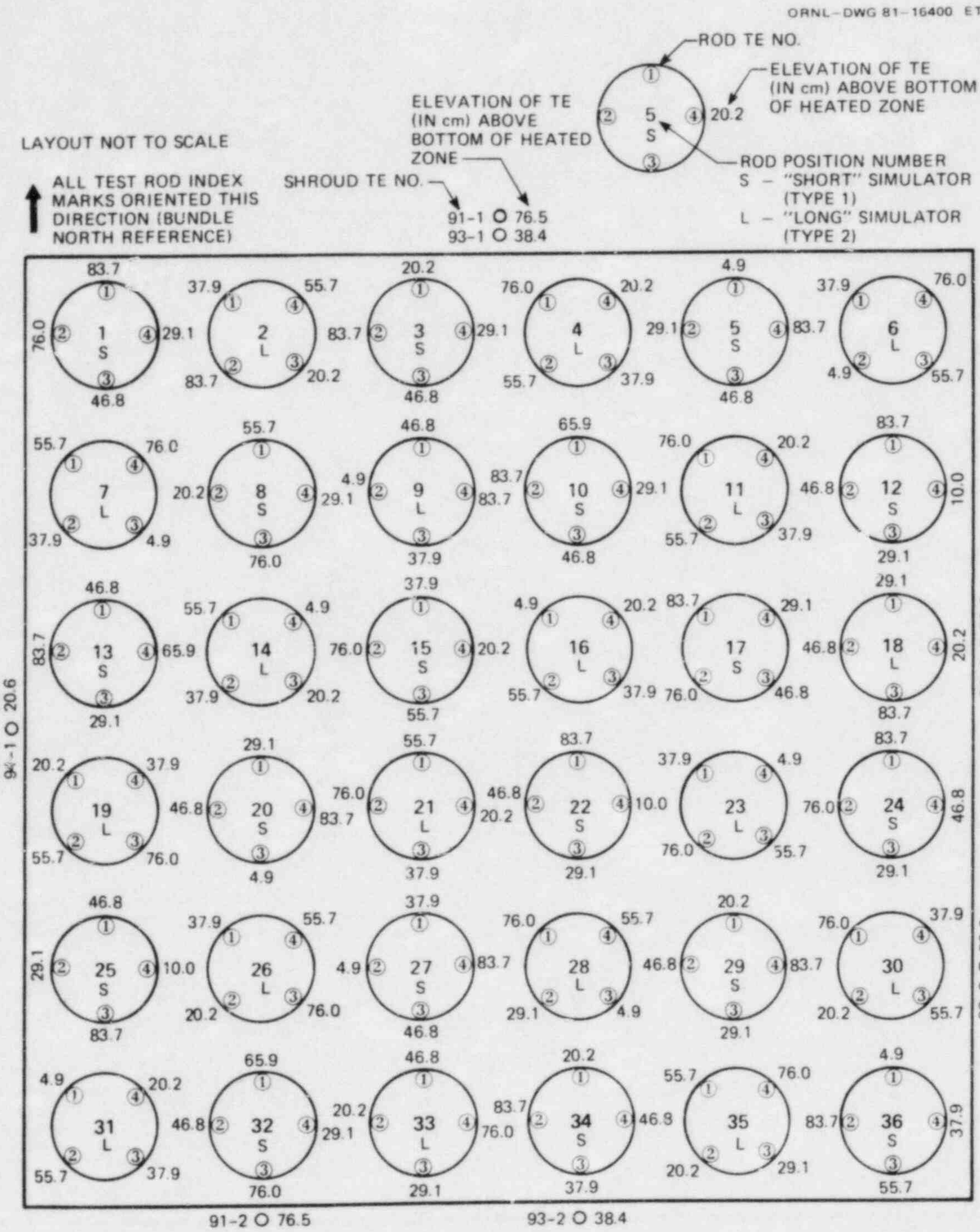


Fig. 3. As-built thermocouple locations and identifications in B-4 test (plan view).

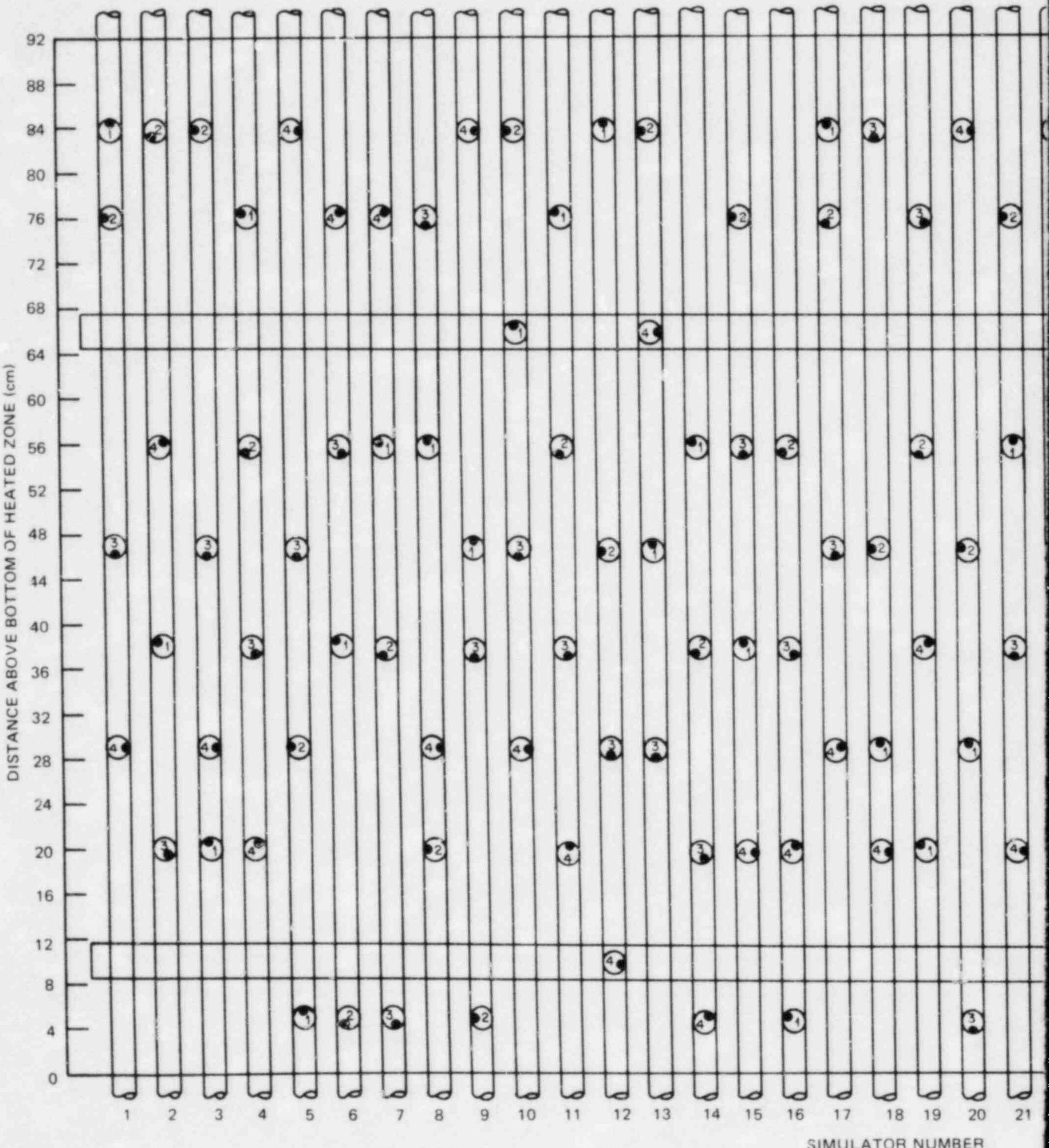


**Fig. 4. As-built thermocouple locations in B-4**

ORNL–DWG 82–6517 ETD

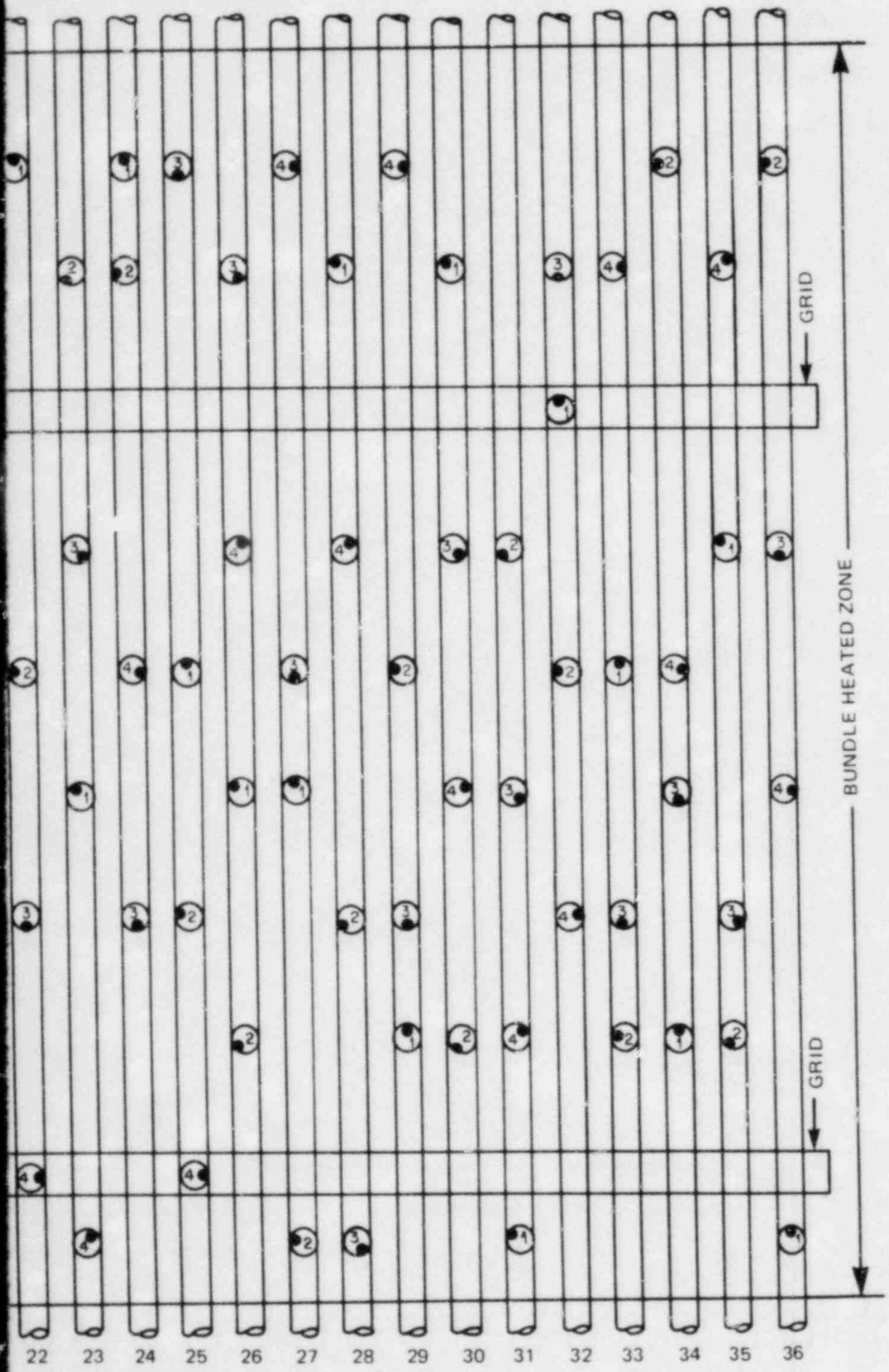


test (elevation).

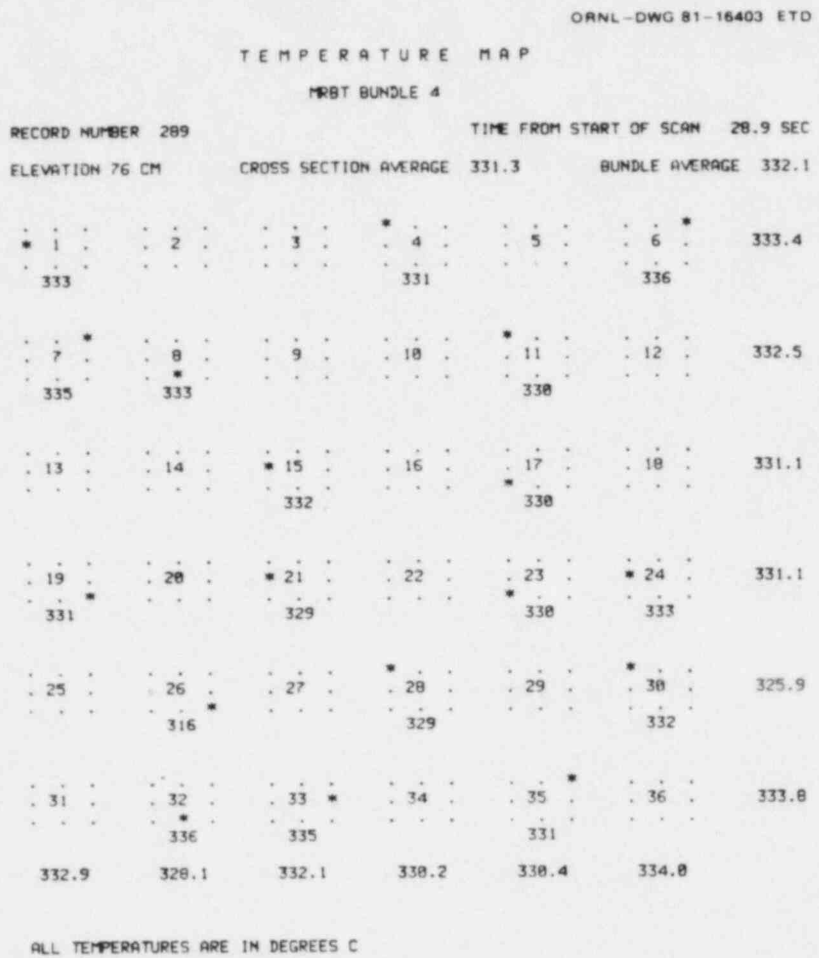


Fig. 7. Temperatures measured at 76-cm elevation 1 s before power-on.

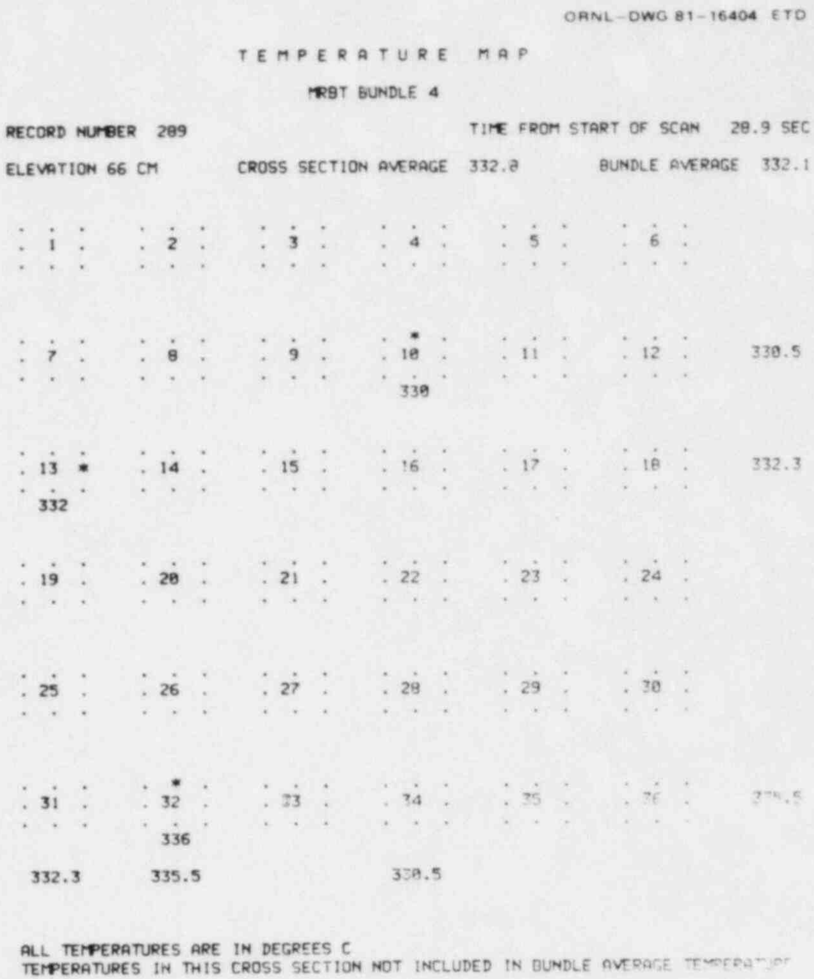


Fig. 8. Temperatures measured at 66-cm (upper grid) elevation 1 s before power-on.

ORNL-DWG 81-16405 ETD

TEMPERATURE MAP

MRBT BUNDLE 4

RECORD NUMBER 289 TIME FROM START OF SCAN 28.9 SEC

ELEVATION 56 CM CROSS SECTION AVERAGE 333.1 BUNDLE AVERAGE 332.1

| | | | | | | |
|---|---|---|---|---|---|---|
| 1 | 2 336 | 3 | 4 332 | 5 | 6 336 | 334.5 |
| 7 336 | 8 335 | 9 | 10 | 11 332 | 12 | 334.2 |
| 13 | 14 332 | 15 335 | 16 (331) | 17 | 18 | 333.2 |
| 19 332 | 20 | 21 332 | 22 | 23 332 | 24 | 332.1 |
| 25 | 26 333 | 27 | 28 331 | 29 | 30 332 | 332.2 |
| 31 333 | 32 | 33 | 34 | 35 332 | 36 333 | 332.6 |
| 333.5 | 333.8 | 333.2 | 331.8 | 332.0 | 333.7 | |

ALL TEMPERATURES ARE IN DEGREES C
VALUES IN PARENTHESES ARE NOT USED IN DETERMINING AVERAGES

**Fig. 9. Temperatures measured at 56-cm elevation 1 s before power-on.**

ORNL-DWG 81-16406 ETD

TEMPERATURE MAP

MRBT BUNDLE 4

RECORD NUMBER 289 TIME FROM START OF SCAN 28.9 SEC

ELEVATION 47 CM CROSS SECTION AVERAGE 332.4 BUNDLE AVERAGE 332.1

| | | | | | | |
|---|---|---|---|---|---|---|
| 1 331 | 2 | 3 331 | 4 | 5 334 | 6 | 332.3 |
| 7 | 8 | 9 335 | 10 331 | 11 | 12 331 | 332.5 |
| 13 331 | 14 | 15 | 16 | 17 332 | 18 332 | 331.9 |
| 19 | 20 335 | 21 | 22 332 | 23 | 24 332 | 332.9 |
| 25 335 | 26 | 27 329 | 28 | 29 332 | 30 | 332.1 |
| 31 | 32 334 | 33 333 | 34 331 | 35 | 36 | 332.5 |
| 332.5 | 334.1 | 332.0 | 331.6 | 332.0 | 331.9 | |

ALL TEMPERATURES ARE IN DEGREES C

**Fig. 10. Temperatures measured at 47-cm elevation 1 s before power-on.**

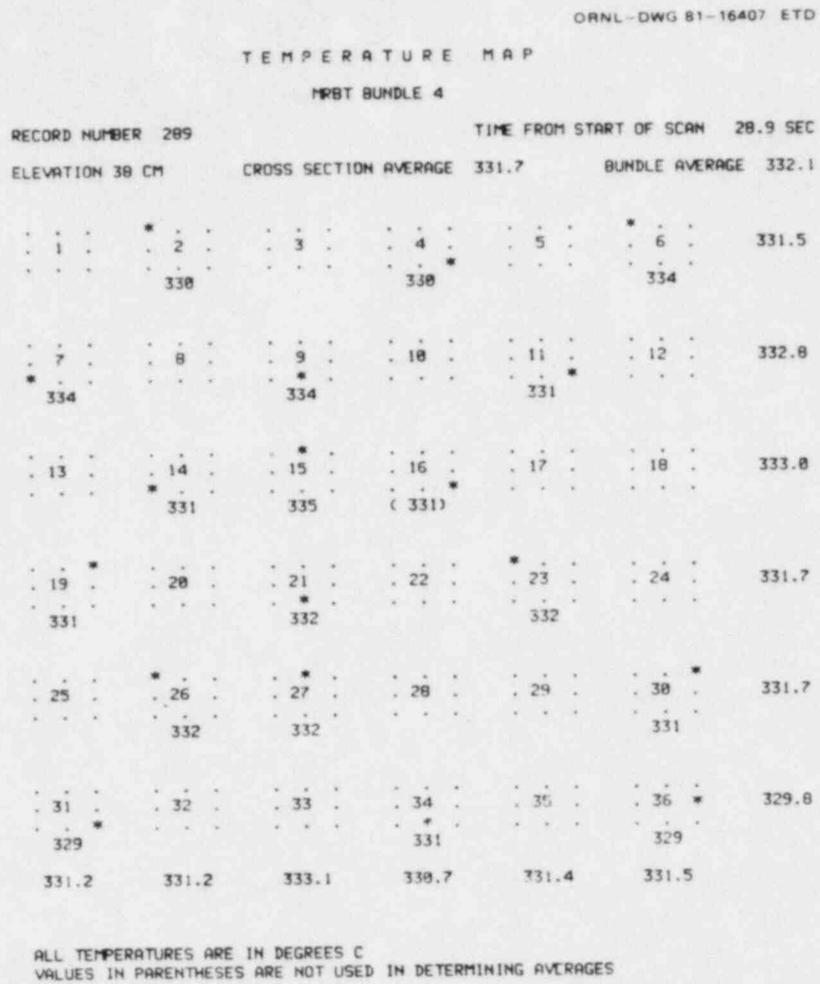


Fig. 11. Temperatures measured at 38-cm elevation 1 s before power-on.

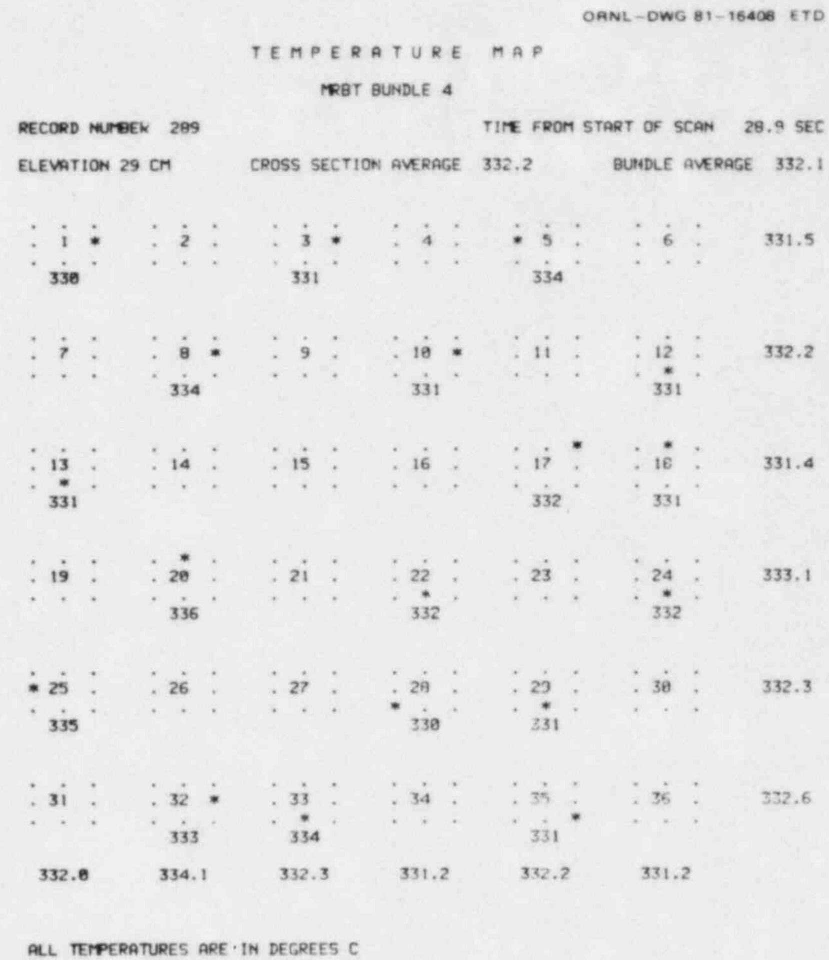


Fig. 12. Temperatures measured at 29-cm elevation 1 s before power-on.

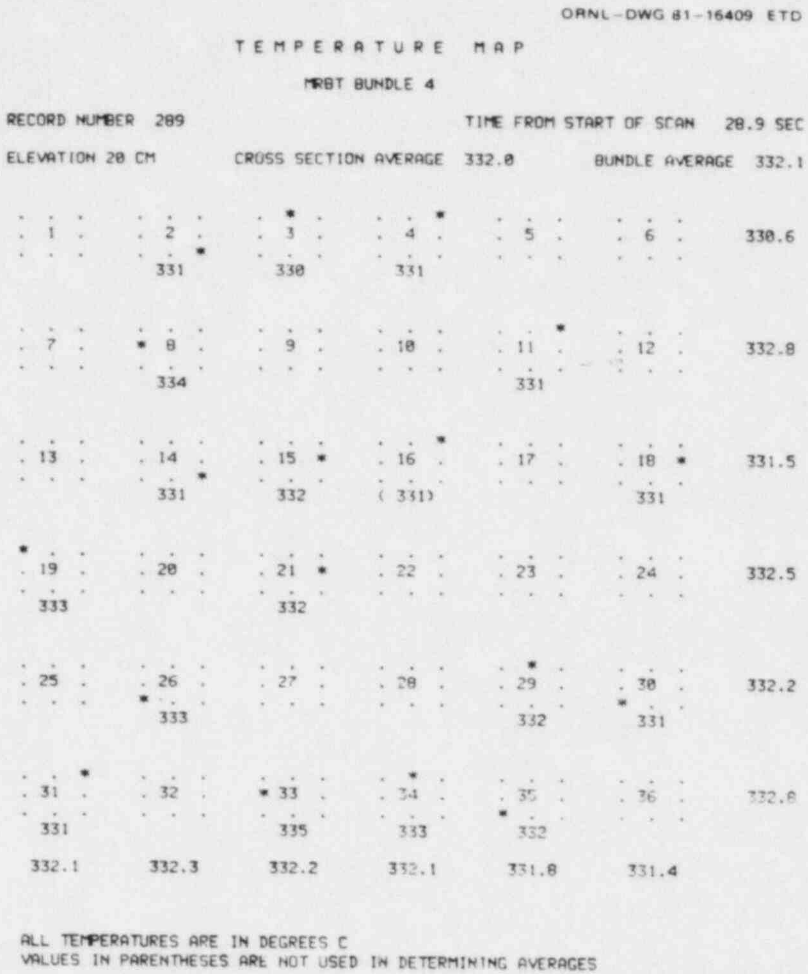


Fig. 13. Temperatures measured at 20-cm elevation 1 s before power-on.

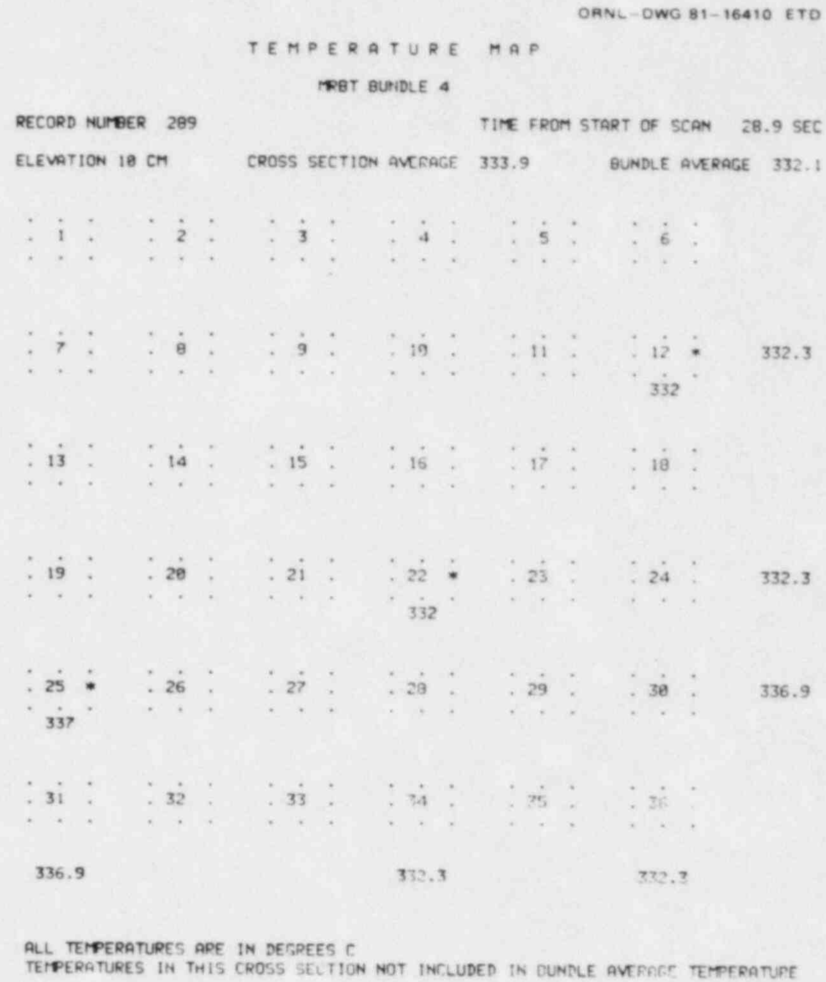


Fig. 14. Temperatures measured at 10-cm (lower grid) elevation 1 s before power-on.

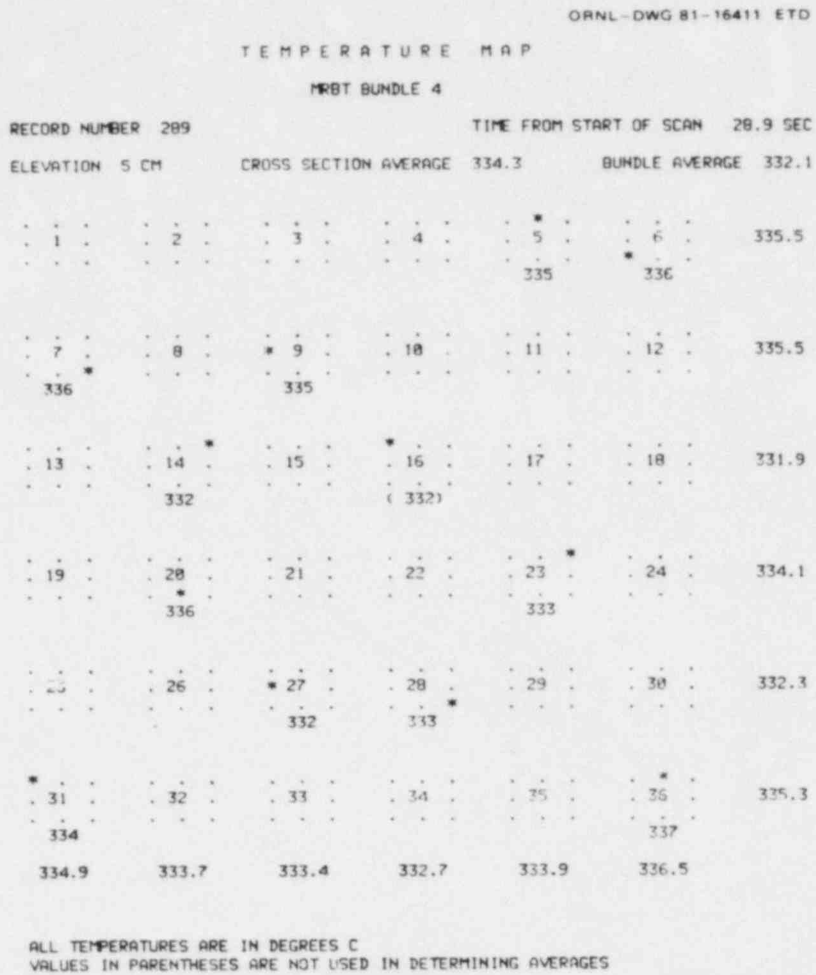


Fig. 15. Temperatures measured at 5-cm elevation 1 s before power-on.

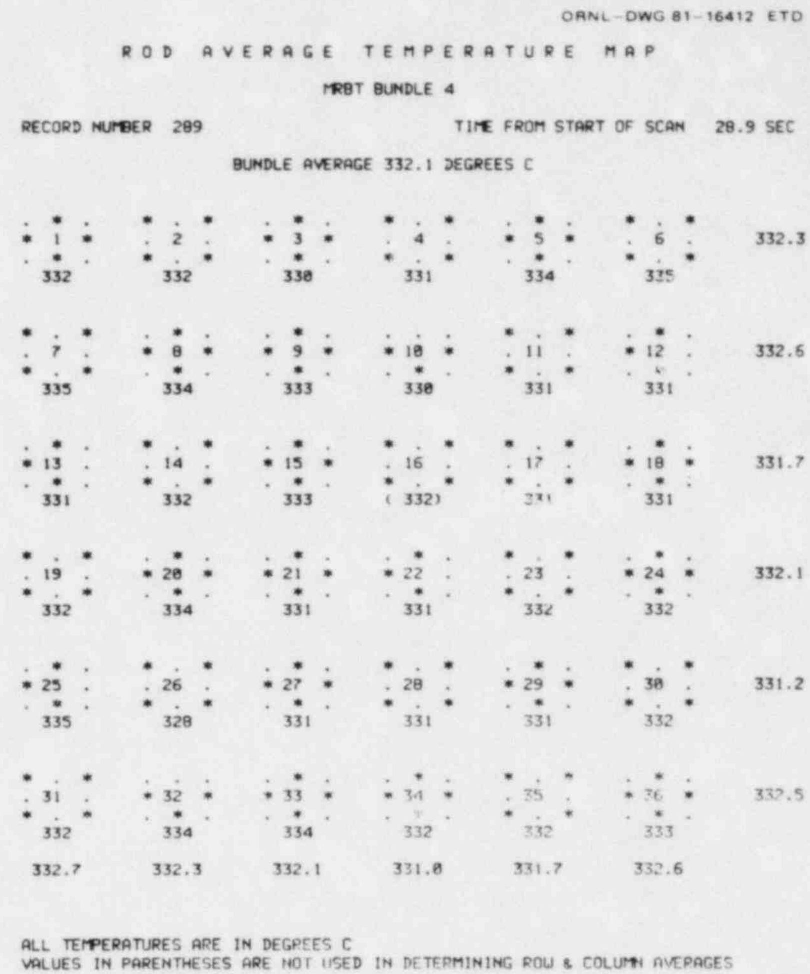


Fig. 16. Average simulator temperatures measured 1 s before power-on.

ORNL-DWG 81-16413 ETD

PRESSURE MAP

MRBT BUNDLE 4

RECORD NUMBER 289 TIME FROM START OF SCAN 28.9 SEC

AVERAGE PRESSURE 9091 KPA (DIFFERENTIAL)
STEAM PRESSURE 206 KPA (GAGE)

| | | | | | | |
|---|---|---|---|---|---|---|
| 1 | 2 | 3 | 4 | 5 | 6 | 9090 |
| 9101 | 9078 | 9093 | 9091 | 9099 | 9079 | |
| 7 | 8 | 9 | 10 | 11 | 12 | 9081 |
| 9105 | 9089 | 9080 | 9082 | 9064 | 9067 | |
| 13 | 14 | 15 | 16 | 17 | 18 | 9083 |
| 9092 | 9096 | 9095 | ( 559) | 9069 | 9063 | |
| 19 | 20 | 21 | 22 | 23 | 24 | 9093 |
| 9111 | 9120 | 9103 | 9096 | 9066 | 9059 | |
| 25 | 26 | 27 | 28 | 29 | 30 | 9100 |
| 9111 | 9110 | 9100 | 9107 | 9103 | 9070 | |
| 31 | 32 | 33 | 34 | 35 | 36 | 9101 |
| 9094 | 9084 | 9105 | 9113 | 9116 | 9093 | |
| 9102 | 9096 | 9096 | 9098 | 9086 | 9072 | |

ALL SIMULATOR PRESSURES ARE DIFFERENTIAL AND ARE IN KPA
VALUES IN PARENTHESES ARE NOT USED IN DETERMINING AVERAGES

**Fig. 17. Simulator pressures measured 1 s before power-on.**

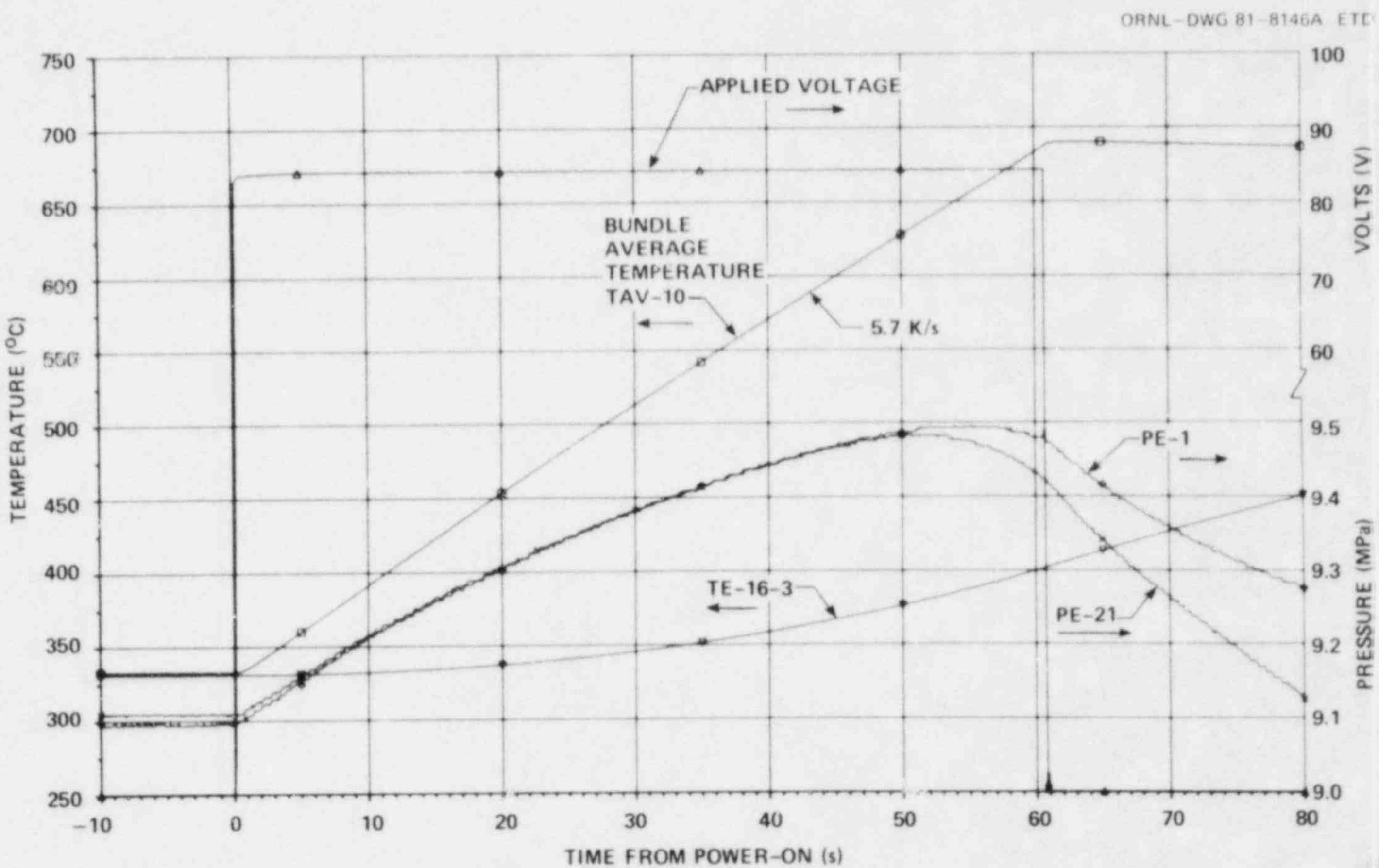


Fig. 18. Characteristic temperatures and pressures during powered portion of B-4 transient.

ORNL-DWG 81-16414 ETD

PRESSURE MAP

MRBT BUNDLE 4

RECORD NUMBER 903 TIME FROM START OF SCAN 90.3 SEC

AVERAGE PRESSURE 9437 KPA (DIFFERENTIAL)
STEAM PRESSURE 207 KPA (GAGE)

| | | | | | | |
|---|---|---|---|---|---|---|
| 1 | 2 | 3 | 4 | 5 | 6 | 9453 |
| 9472 | 9446 | 9452 | 9483 | 9436 | 9420 | |
| 7 | 8 | 9 | 10 | 11 | 12 | 9424 |
| 9424 | 9440 | 9390 | 9432 | 9421 | 9427 | |
| 13 | 14 | 15 | 16 | 17 | 18 | 9434 |
| 9433 | 9453 | 9430 | ( 551) | 9434 | 9419 | |
| 19 | 20 | 21 | 22 | 23 | 24 | 9432 |
| 9447 | 9467 | 9423 | 9433 | 9402 | 9417 | |
| 25 | 26 | 27 | 28 | 29 | 30 | 9441 |
| 9446 | 9456 | 9432 | 9470 | 9437 | 9406 | |
| 31 | 32 | 33 | 34 | 35 | 36 | 9440 |
| 9444 | 9431 | 9443 | 9440 | 9443 | 9435 | |
| 9445 | 9450 | 9428 | 9452 | 9429 | 9422 | |

ALL SIMULATOR PRESSURES ARE DIFFERENTIAL AND ARE IN KPA
VALUES IN PARENTHESES ARE NOT USED IN DETERMINING AVERAGES

Fig. 19. Simulator pressures measured 0.2 s before power-off.

ORNL-DWG 81-16415 ETD

TEMPERATURE MAP

MRBT BUNDLE 4

RECORD NUMBER 903 TIME FROM START OF SCAN 90.3 SEC

ELEVATION 84 CM CROSS SECTION AVERAGE 666.9 BUNDLE AVERAGE 670.7

| | | | | | | |
|---|---|---|---|---|---|---|
| 1 | 2 | 3 | 4 | 5 | 6 | 669.5 |
| 669 | 671 | 668 | | 670 | | |
| 7 | 8 | 9 | 10 | 11 | 12 | 667.1 |
| | | 671 | 666 | | 664 | |
| 13 | 14 | 15 | 16 | 17 | 18 | 662.3 |
| 664 | | | | 659 | 664 | |
| 19 | 20 | 21 | 22 | 23 | 24 | 669.7 |
| | 680 | | 665 | | 664 | |
| 25 | 26 | 27 | 28 | 29 | 30 | 670.2 |
| 669 | | 670 | | 672 | | |
| 31 | 32 | 33 | 34 | 35 | 36 | 659.2 |
| | | | 662 | | 657 | |
| 667.2 | 675.5 | 669.7 | 664.2 | 666.8 | 66[illegible].3 | |

ALL TEMPERATURES ARE IN DEGREES C

Fig. 20. Temperatures measured at 84-cm elevation 0.2 s before power-off.

ORNL-DWG 81-16416 ETD

T E M P E R A T U R E   M A P

MRBT BUNDLE 4

RECORD NUMBER 903 — TIME FROM START OF SCAN 90.3 SEC

ELEVATION 76 CM — CROSS SECTION AVERAGE 670.4 — BUNDLE AVERAGE 670.7

| | | | | | | |
|---|---|---|---|---|---|---|
| 1<br>669 | 2 | 3 | 4<br>663 | 5 | 6<br>677 | 669.4 |
| 7<br>683 | 8<br>684 | 9 | 10 | 11<br>679 | 12 | 681.8 |
| 13 | 14 | 15<br>677 | 16 | 17<br>662 | 18 | 669.6 |
| 19<br>668 | 20 | 21<br>679 | 22 | 23<br>679 | 24<br>674 | 675.0 |
| 25 | 26<br>647 | 27 | 28<br>673 | 29 | 30<br>679 | 666.3 |
| 31 | 32<br>646 | 33<br>663 | 34 | 35<br>666 | 36 | 658.4 |
| 673.0 | 658.9 | 672.9 | 660.2 | 671.8 | 676.3 | |

ALL TEMPERATURES ARE IN DEGREES C

**Fig. 21. Temperatures measured at 76-cm elevation 0.2 s before power-off.**

ORNL-DWG 81-16417 ETD

T E M P E R A T U R E   M A P

MRBT BUNDLE 4

RECORD NUMBER 903 — TIME FROM START OF SCAN 90.3 SEC

ELEVATION 66 CM — CROSS SECTION AVERAGE 649.8 — BUNDLE AVERAGE 670.7

| | | | | | | |
|---|---|---|---|---|---|---|
| 1 | 2 | 3 | 4 | 5 | 6 | |
| 7 | 8 | 9 | 10<br>648 | 11 | 12 | 648.2 |
| 13<br>649 | 14 | 15 | 16 | 17 | 18 | 649.2 |
| 19 | 20 | 21 | 22 | 23 | 24 | |
| 25 | 26 | 27 | 28 | 29 | 30 | |
| 31 | 32<br>652 | 33 | 34 | 35 | 36 | 652.1 |
| 649.2 | 652.1 | | 648.2 | | | |

ALL TEMPERATURES ARE IN DEGREES C
TEMPERATURES IN THIS CROSS SECTION NOT INCLUDED IN BUNDLE AVERAGE TEMPERATURE

**Fig. 22. Temperatures measured at 66-cm (upper grid) elevation 0.2 s before power-off.**

ORNL-DWG 81-16418 ETD

TEMPERATURE MAP

MRBT BUNDLE 4

RECORD NUMBER 903 — TIME FROM START OF SCAN 90.3 SEC

ELEVATION 56 CM — CROSS SECTION AVERAGE 673.5 — BUNDLE AVERAGE 670.7

| | | | | | | |
|---|---|---|---|---|---|---|
| 1 | 2<br>678 | 3 | 4<br>665 | 5 | 6<br>671 | 671.5 |
| 7<br>679 | 8<br>686 | 9 | 10 | 11<br>674 | 12 | 679.5 |
| 13 | 14<br>683 | 15<br>675 | 16<br>( 409) | 17 | 18 | 679.1 |
| 19<br>672 | 20 | 21<br>679 | 22 | 23<br>675 | 24 | 675.4 |
| 25 | 26<br>684 | 27 | 28<br>677 | 29 | 30<br>663 | 674.6 |
| 31<br>661 | 32 | 33 | 34 | 35<br>664 | 36<br>663 | 662.7 |
| 670.6 | 683.0 | 677.1 | 671.0 | 670.9 | 665.6 | |

ALL TEMPERATURES ARE IN DEGREES C
VALUES IN PARENTHESES ARE NOT USED IN DETERMINING AVERAGES

Fig. 23. Temperatures measured at 56-cm elevation 0.2 s before power-off.

ORNL-DWG 81-16419 ETD

TEMPERATURE MAP

MRBT BUNDLE 4

RECORD NUMBER 903 — TIME FROM START OF SCAN 90.3 SEC

ELEVATION 47 CM — CROSS SECTION AVERAGE 673.1 — BUNDLE AVERAGE 670.7

| | | | | | | |
|---|---|---|---|---|---|---|
| 1<br>662 | 2 | 3<br>668 | 4 | 5<br>675 | 6 | 668.2 |
| 7 | 8 | 9<br>682 | 10<br>670 | 11 | 12<br>681 | 677.6 |
| 13<br>669 | 14 | 15 | 16 | 17<br>667 | 18<br>669 | 668.5 |
| 19 | 20<br>682 | 21 | 22<br>674 | 23 | 24<br>672 | 675.7 |
| 25<br>672 | 26 | 27<br>675 | 28 | 29<br>679 | 30 | 675.3 |
| 31 | 32<br>677 | 33<br>670 | 34<br>674 | 35 | 36 | 673.5 |
| 667.9 | 679.2 | 673.6 | 672.6 | 673.6 | 673.7 | |

ALL TEMPERATURES ARE IN DEGREES C

Fig. 24. Temperatures measured at 47-cm elevation 0.2 s before power-off.

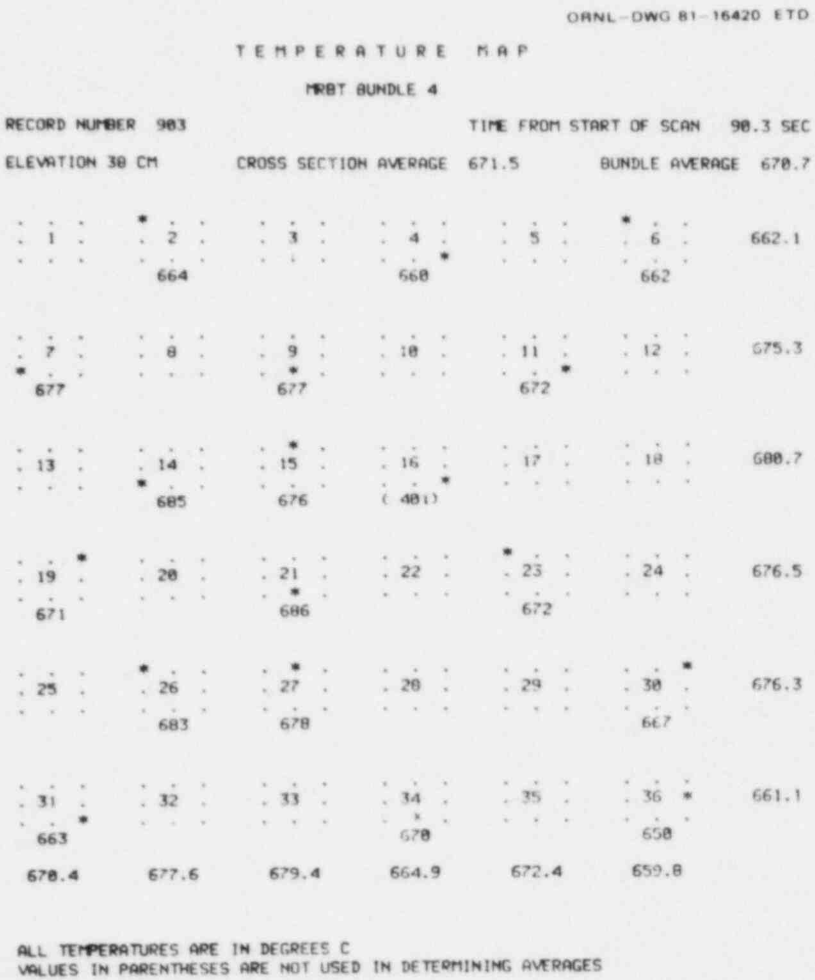


**Fig. 25. Temperatures measured at 38-cm elevation 0.2 s before power-off.**

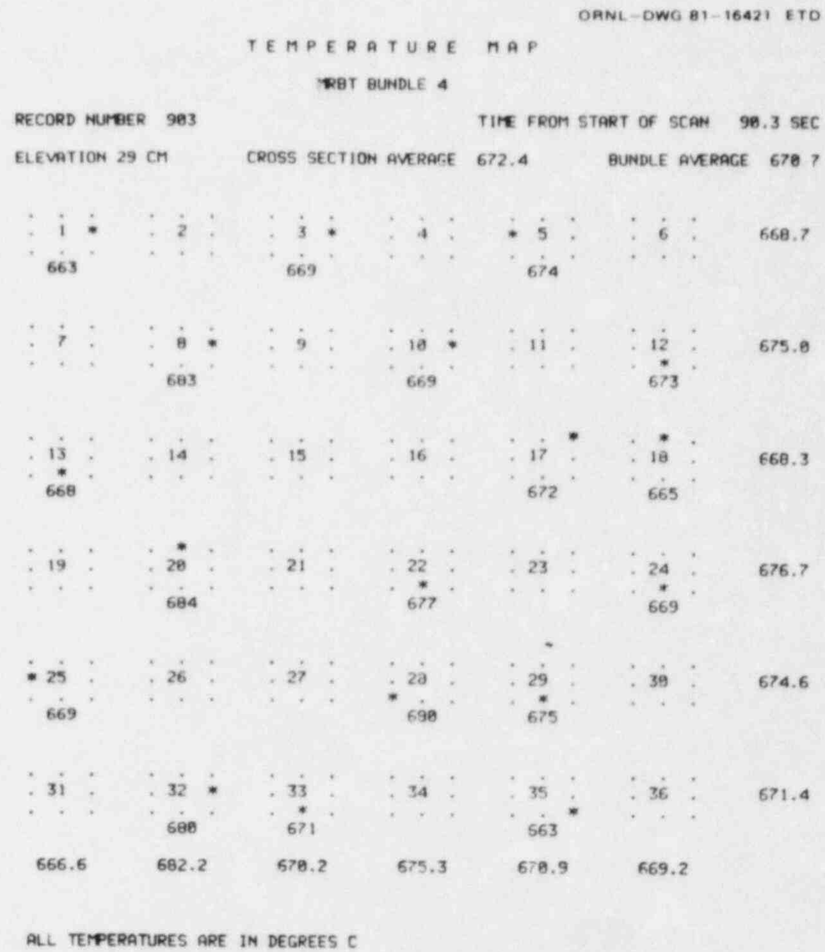


**Fig. 26. Temperatures measured at 29-cm elevation 0.2 s before power-off.**

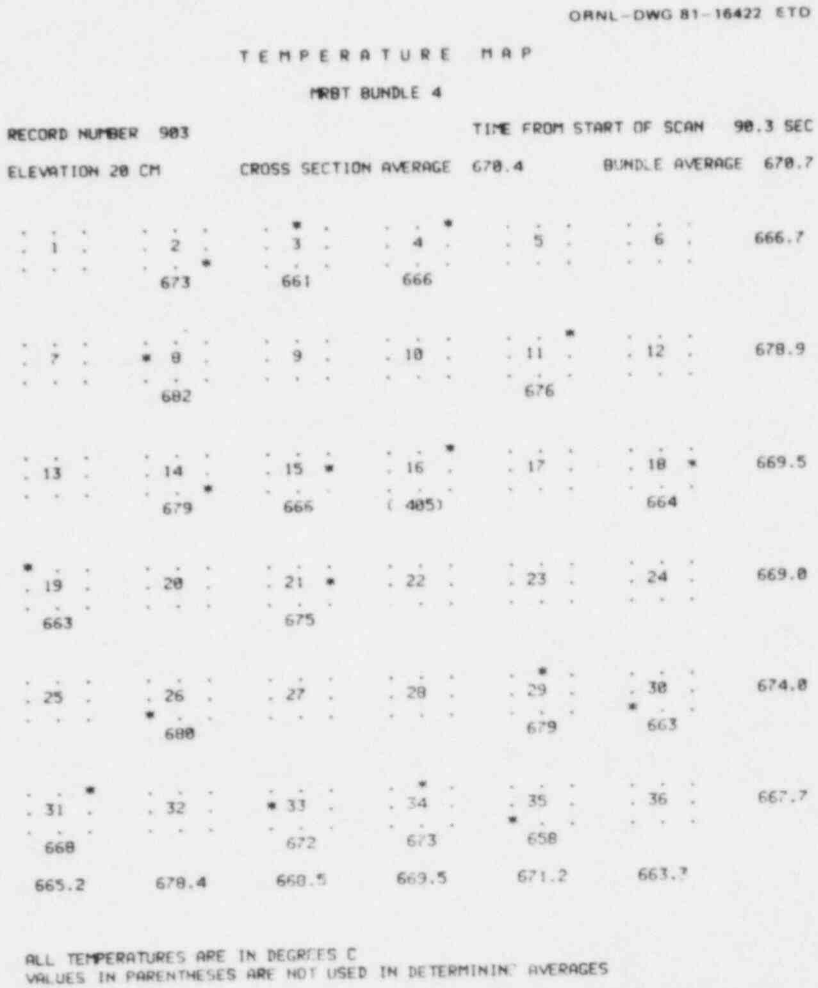


Fig. 27. Temperatures measured at 20-cm elevation 0.2 s before power-off.

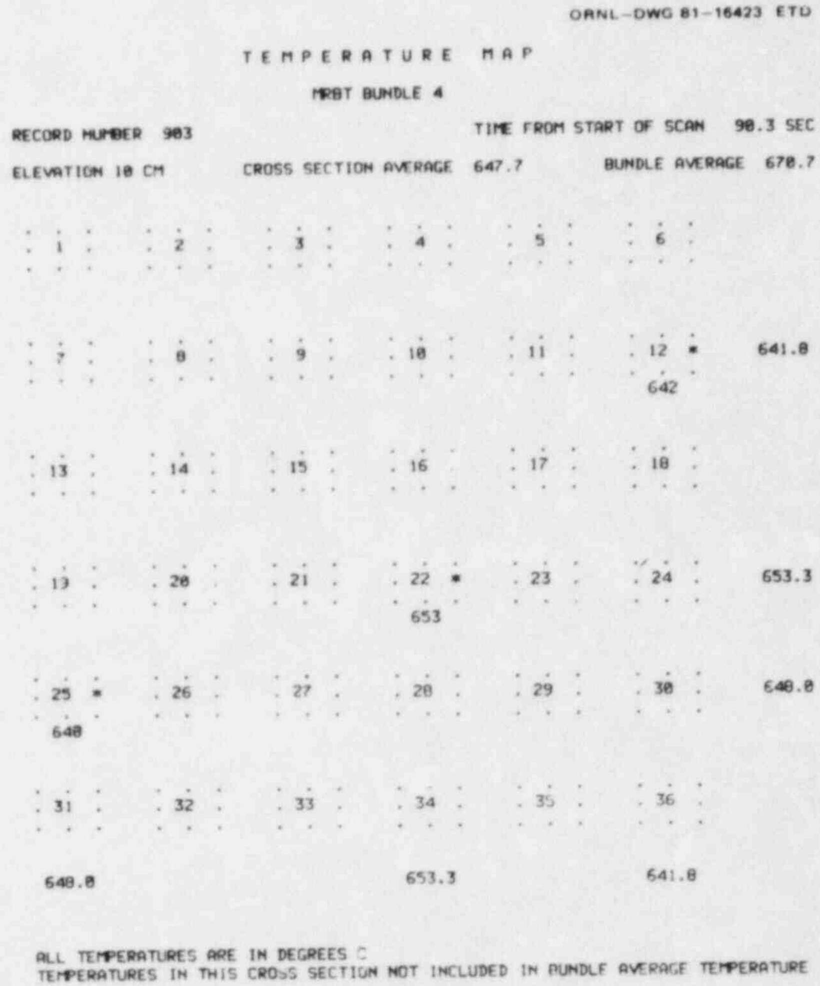


Fig. 28. Temperatures measured at 10-cm (lower grid) elevation 0.2 s before power-off.

ORNL-DWG 81-16424 ETD

TEMPERATURE MAP

MRBT BUNDLE 4

RECORD NUMBER 903 TIME FROM START OF SCAN 90.3 SEC

ELEVATION 5 CM CROSS SECTION AVERAGE 665.4 BUNDLE AVERAGE 670.7

| | | | | | | |
|---|---|---|---|---|---|---|
| 1 | 2 | 3 | 4 | 5<br>663 | 6<br>667 | 665.3 |
| 7<br>674 | 8 | 9<br>674 | 10 | 11 | 12 | 674.1 |
| 13 | 14<br>669 | 15 | 16<br>( 398) | 17 | 18 | 669.5 |
| 19 | 20<br>675 | 21 | 22 | 23<br>663 | 24 | 669.0 |
| 25 | 26 | 27<br>666 | 28<br>663 | 29 | 30 | 664.4 |
| 31<br>652 | 32 | 33 | 34 | 35 | 36<br>653 | 652.3 |
| 662.9 | 672.4 | 670.2 | 662.8 | 663.0 | 660.0 | |

ALL TEMPERATURES ARE IN DEGREES C
VALUES IN PARENTHESES ARE NOT USED IN DETERMINING AVERAGES

Fig. 29. Temperatures measured at 5-cm elevation 0.2 s before power-off.

ORNL-DWG 81-16425 ETD

ROD AVERAGE TEMPERATURE MAP

MRBT BUNDLE 4

RECORD NUMBER 903 TIME FROM START OF SCAN 90.3 SEC

BUNDLE AVERAGE 670.7 DEGREES C

| | | | | | | |
|---|---|---|---|---|---|---|
| 1<br>666 | 2<br>672 | 3<br>667 | 4<br>663 | 5<br>670 | 6<br>669 | 667.9 |
| 7<br>670 | 8<br>683 | 9<br>676 | 10<br>668 | 11<br>675 | 12<br>673 | 676.1 |
| 13<br>667 | 14<br>679 | 15<br>673 | 16<br>( 403) | 17<br>665 | 18<br>665 | 670.2 |
| 19<br>668 | 20<br>680 | 21<br>680 | 22<br>672 | 23<br>672 | 24<br>678 | 673.8 |
| 25<br>670 | 26<br>674 | 27<br>672 | 28<br>673 | 29<br>676 | 30<br>668 | 672.3 |
| 31<br>661 | 32<br>668 | 33<br>669 | 34<br>670 | 35<br>663 | 36<br>655 | 664.1 |
| 668.3 | 676.3 | 672.9 | 669.2 | 670.4 | 666.5 | |

ALL TEMPERATURES ARE IN DEGREES C
VALUES IN PARENTHESES ARE NOT USED IN DETERMINING ROW & COLUMN AVERAGES

Fig. 30. Average simulator temperatures measured 0.2 s before power-off.

ORNL-DWG 81-8143A ETD

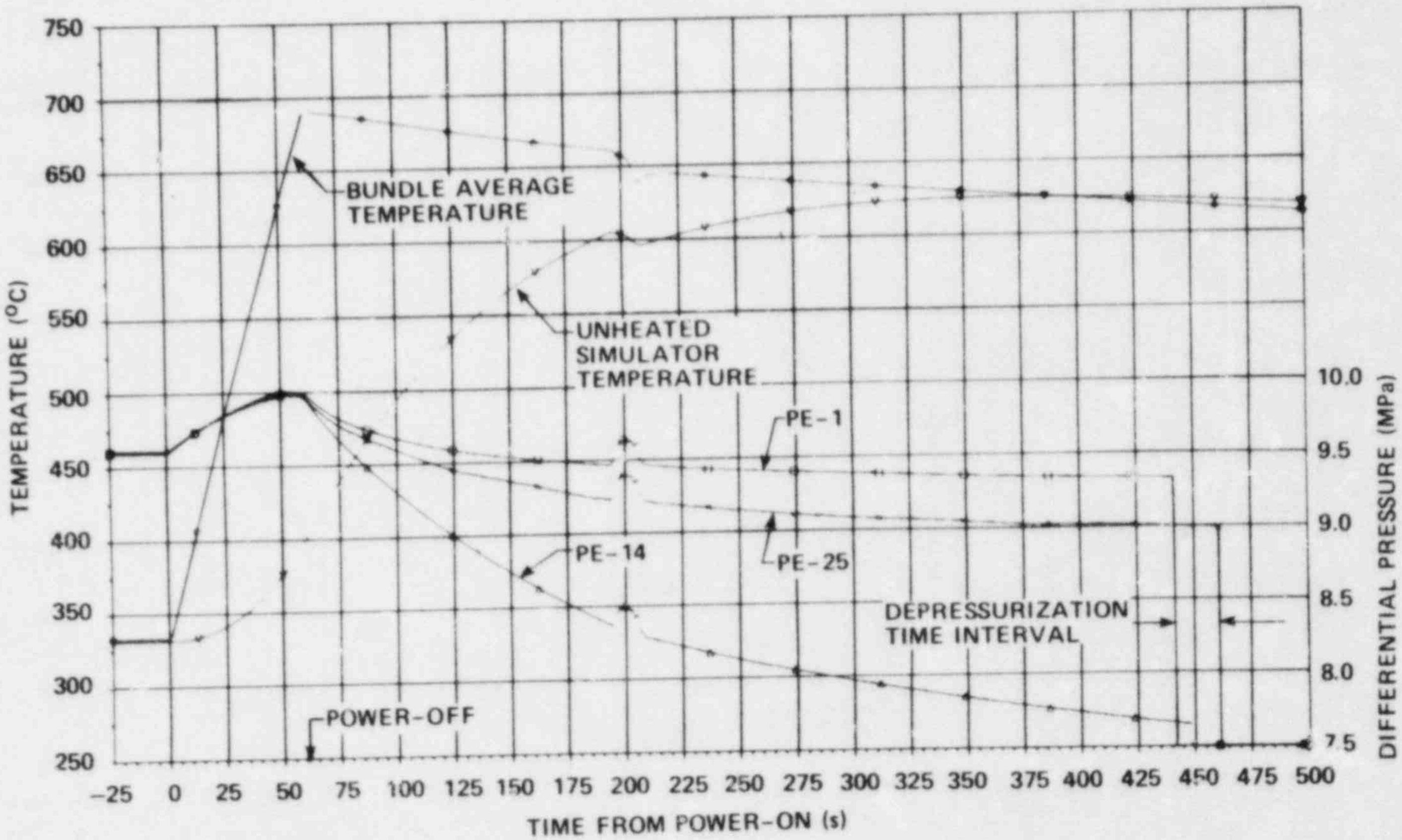


Fig. 31. Characteristic B-4 temperatures and pressures during transient.

ORNL-DWG 81-16426 ETD

PRESSURE MAP

MRBT BUNDLE 4

RECORD NUMBER 4710 TIME FROM START OF SCAN 471.0 SEC

AVERAGE PRESSURE 8266 KPA (DIFFERENTIAL)
STEAM PRESSURE 201 KPA (GAGE)

| | | | | | | |
|---|---|---|---|---|---|---|
| 1 | 2 | 3 | 4 | 5 | 6 | 8642 |
| 8825 | 8515 | 8520 | 8581 | 8611 | 8799 | |
| 7 | 8 | 9 | 10 | 11 | 12 | 8149 |
| 8311 | 7769 | 7823 | 8283 | 8197 | 8513 | |
| 13 | 14 | 15 | 16 | 17 | 18 | 8064 |
| 8325 | 7164 | 8014 | ( 400) | 8402 | 8515 | |
| 19 | 20 | 21 | 22 | 23 | 24 | 8016 |
| 8383 | 7743 | 7457 | 7976 | 8007 | 8531 | |
| 25 | 26 | 27 | 28 | 29 | 30 | 8059 |
| 8583 | 7738 | 7646 | 7882 | 7963 | 8622 | |
| 31 | 32 | 33 | 34 | 35 | 36 | 8645 |
| 8821 | 8536 | 8484 | 8470 | 8634 | 8927 | |
| 8528 | 7911 | 7991 | 8239 | 8382 | 8651 | |

ALL SIMULATOR PRESSURES ARE DIFFERENTIAL AND ARE IN KPA
VALUES IN PARENTHESES ARE NOT USED IN DETERMINING AVERAGES

Fig. 32. Simulator pressures measured 0.7 s before depressurization.

ORNL-DWG 81-16427 ETD

TEMPERATURE MAP

MRBT BUNDLE 4

RECORD NUMBER 4710 TIME FROM START OF SCAN 471.0 SEC

ELEVATION 84 CM CROSS SECTION AVERAGE 515.5 BUNDLE AVERAGE 503.5

| | | | | | | |
|---|---|---|---|---|---|---|
| * 1 | * 2 | * 3 | 4 | 5 * | 6 | 511.4 |
| 508 | 514 | 514 | | 509 | | |
| 7 | 8 | 9 * | * 10 | 11 | * 12 | 513.3 |
| | | 520 | 513 | | 507 | |
| * 13 | 14 | 15 | 16 | * 17 | 18 * | 516.1 |
| 524 | | | | 512 | 512 | |
| 19 | 20 * | 21 | * 22 | 23 | * 24 | 521.1 |
| | 527 | | 521 | | 515 | |
| 25 * | 26 | 27 * | 28 | 29 * | 30 | 520.9 |
| 520 | | 526 | | 517 | | |
| 31 | 32 | 33 | * 34 | 35 | * 36 | 509.4 |
| | | | 517 | | 502 | |
| 517.4 | 520.7 | 520.0 | 516.9 | 512.0 | 50[illegible].0 | |

ALL TEMPERATURES ARE IN DEGREES C

Fig. 33. Temperatures measured at 84-cm elevation 0.7 s before depressurization.

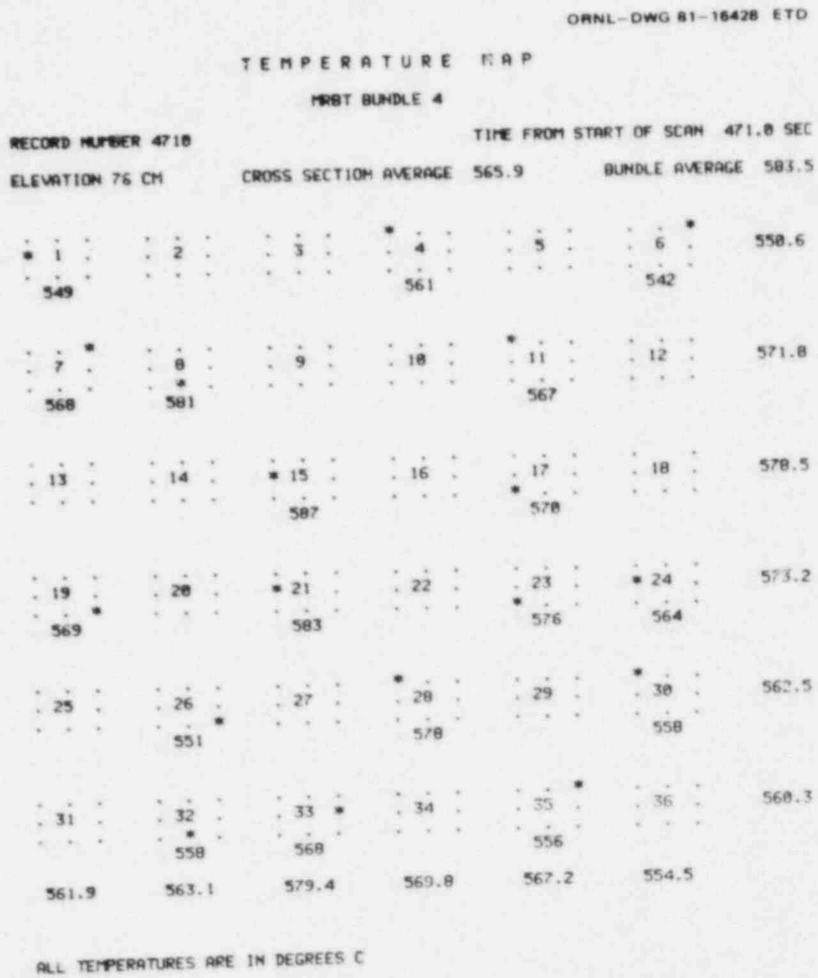


Fig. 34. Temperatures measured at 76-cm elevation 0.7 s before depressurization.

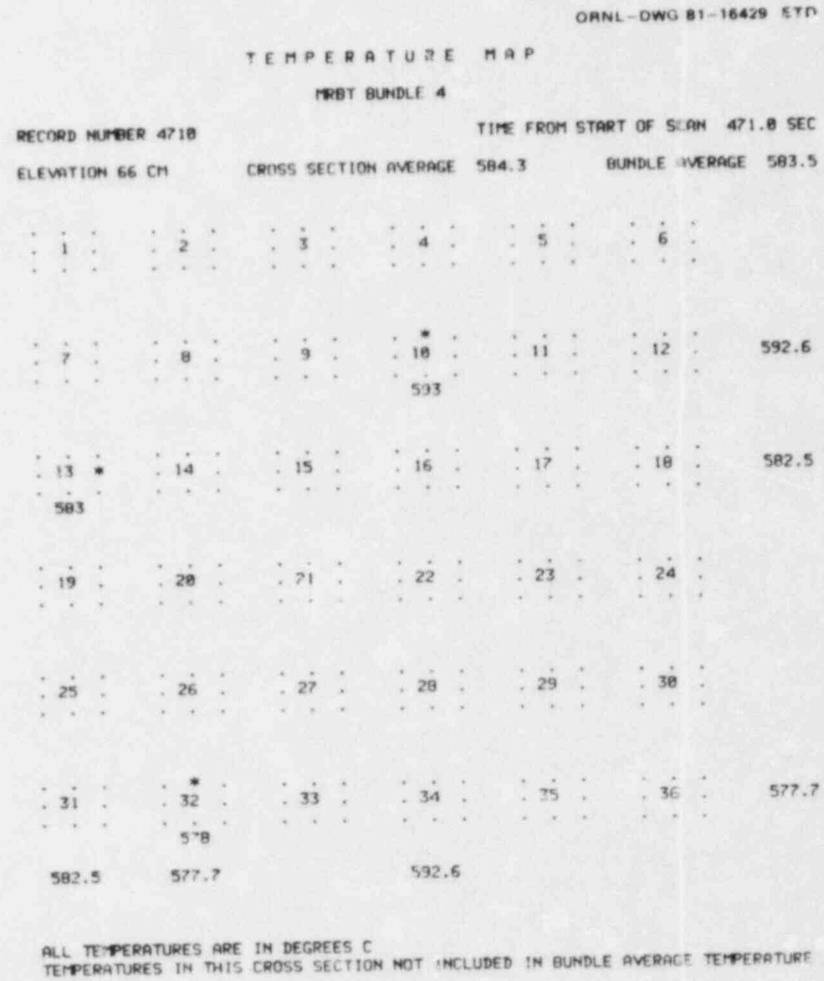


Fig. 35. Temperatures measured at 66-cm (upper grid) elevation 0.7 s before depressurization.

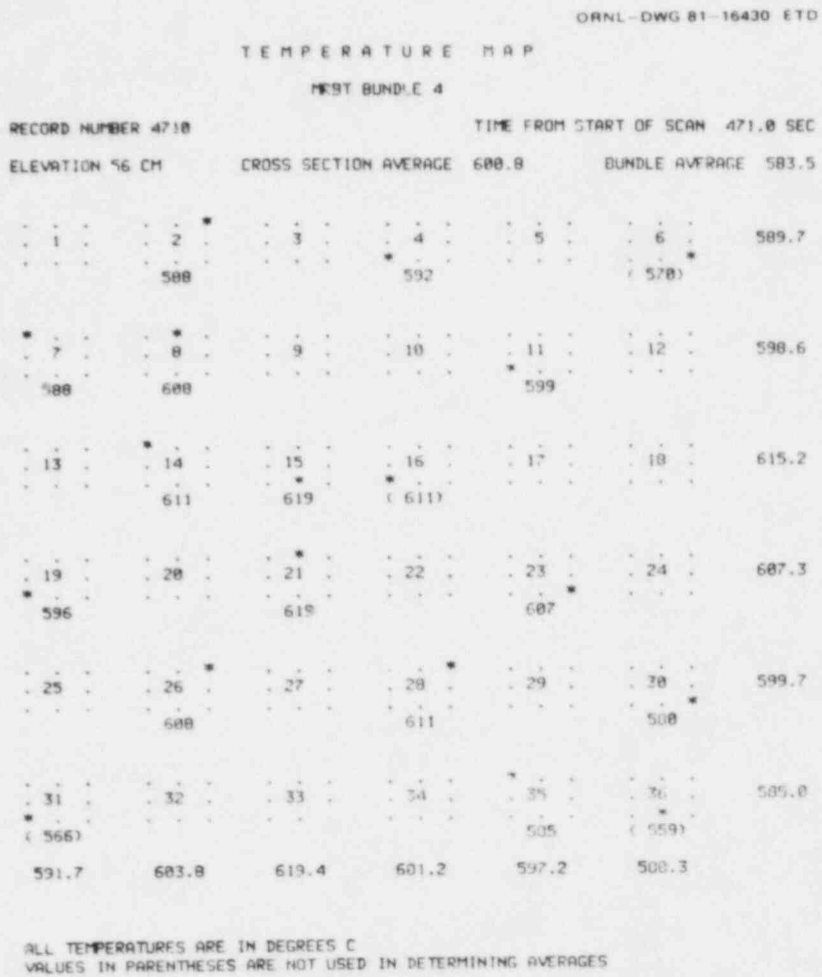


Fig. 36. Temperatures measured at 56-cm elevation 0.7 s before depressurization.

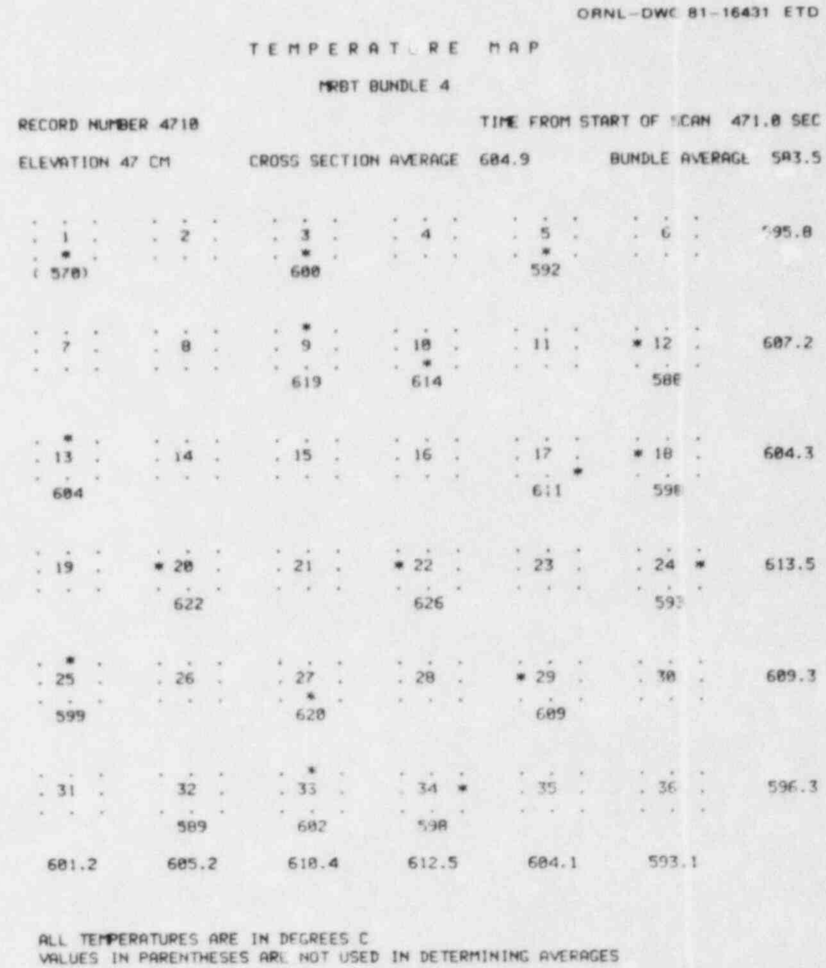


Fig. 37. Temperatures measured at 47-cm elevation 0.7 s before depressurization.

ORNL-DWG 81-16432 ETD

TEMPERATURE MAP

MRBT BUNDLE 4

RECORD NUMBER 4710 TIME FROM START OF SCAN 471.0 SEC

ELEVATION 38 CM CROSS SECTION AVERAGE 611.5 BUNDLE AVERAGE 583.5

| | | | | | | |
|---|---|---|---|---|---|---|
| 1 | 2: 591 | 3 | 4: 597 | 5 | 6: (577) | 593.6 |
| 7: 598 | 8 | 9: 623 | 10 | 11: 606 | 12 | 609.3 |
| 13 | 14: 626 | 15: 632 | 16: (623) | 17 | 18 | 629.0 |
| 19: 606 | 20 | 21: 633 | 22 | 23: 619 | 24 | 619.1 |
| 25 | 26: 611 | 27: 626 | 28 | 29 | 30: 509 | 600.8 |
| 31: (572) | 32 | 33 | 34: 604 | 35 | 36: (561) | 603.6 |
| 602.0 | 609.2 | 628.4 | 600.2 | 612.7 | 509.4 | |

ALL TEMPERATURES ARE IN DEGREES C
VALUES IN PARENTHESES ARE NOT USED IN DETERMINING AVERAGES

Fig. 38. Temperatures measured at 38-cm elevation 0.7 s before depressurization.

ORNL-DWG 81-16433 ETD

TEMPERATURE MAP

MRBT BUNDLE 4

RECORD NUMBER 4710 TIME FROM START OF SCAN 471.0 SEC

ELEVATION 29 CM CROSS SECTION AVERAGE 600.2 BUNDLE AVERAGE 583.5

| | | | | | | |
|---|---|---|---|---|---|---|
| 1: (573) | 2 | 3: 600 | 4 | 5: 594 | 6 | 596.[illegible] |
| 7 | 8: 620 | 9 | 10: 618 | 11 | 12: 593 | 610.6 |
| 13: 607 | 14 | 15 | 16 | 17: 616 | 18: 5[illegible]8 | 607.1 |
| 19 | 20: 630 | 21 | 22: 630 | 23 | 24: 5[illegible]9 | 620.1 |
| 25: 596 | 26 | 27 | 28: 624 | 29: 612 | 33 | 610.7 |
| 31 | 32: 600 | 33: 608 | 34 | 35: 593 | 3[illegible] | 600.3 |
| 601.7 | 616.8 | 604.3 | 624.4 | 603.4 | 597.0 | |

ALL TEMPERATURES ARE IN DEGREES C
VALUES IN PARENTHESES ARE NOT USED IN DETERMINING AVERAGES

Fig. 39. Temperatures measured at 29-cm elevation 0.7 s before depressurization.

ORNL-DWG 81-16434 ETD

TEMPERATURE MAP

MRBT BUNDLE 4

RECORD NUMBER 4710 — TIME FROM START OF SCAN 471.0 SEC

ELEVATION 20 CM — CROSS SECTION AVERAGE 603.9 — BUNDLE AVERAGE 583.5

| | | | | | | |
|---|---|---|---|---|---|---|
| 1 | 2 *<br>595 | * 3<br>596 | 4 *<br>598 | 5 | 6 | 596.3 |
| 7 | * 8<br>615 | 9 | 10 | 11 *<br>610 | 12 | 614.1 |
| 13 | 14 *<br>627 | 15 *<br>( 631) | 16 *<br>( 625) | 17 | 18 *<br>594 | 610.4 |
| * 19<br>602 | 20 | 21 *<br>( 633) | 22 | 23 | 24 | 602.0 |
| 25 | 26 *<br>611 | 27 | 28 | * 29<br>614 | 30 *<br>598 | 604.6 |
| 31 *<br>( 577) | 32 | * 33<br>606 | * 34<br>605 | 35 *<br>591 | 36 | 600.5 |
| 602.0 | 612.9 | 600.6 | 601.8 | 604.8 | 59[illegible] | |

ALL TEMPERATURES ARE IN DEGREES C
VALUES IN PARENTHESES ARE NOT USED IN DETERMINING AVERAGES

Fig. 40. Temperatures measured at 20-cm elevation 0.7 s before depressurization.

ORNL-DWG 81-16435 ETD

TEMPERATURE MAP

MRBT BUNDLE 4

RECORD NUMBER 4710 — TIME FROM START OF SCAN 471.0 SEC

ELEVATION 10 CM — CROSS SECTION AVERAGE 594.1 — BUNDLE AVERAGE 583.5

| | | | | | | |
|---|---|---|---|---|---|---|
| 1 | 2 | 3 | 4 | 5 | 6 | |
| 7 | 8 | 9 | 10 | 11 | 12 *<br>578 | 577.5 |
| 13 | 14 | 15 | 16 | 17 | 18 | |
| 19 | 20 | 21 | 22 *<br>614 | 23 | 24 | 614.2 |
| 25 *<br>591 | 26 | 27 | 28 | 29 | 30 | 590.5 |
| 31 | 32 | 33 | 34 | 35 | 36 | |
| 590.5 | | | 614.2 | | 577.5 | |

ALL TEMPERATURES ARE IN DEGREES C
TEMPERATURES IN THIS CROSS SECTION NOT INCLUDED IN BUNDLE AVERAGE TEMPERATURE

Fig. 41. Temperatures measured at 10-cm (lower grid) elevation 0.7 s before depressurization.

ORNL-DWG 81-16436 ETD

T E M P E R A T U R E   M A P

MRBT BUNDLE 4

RECORD NUMBER 4710 — TIME FROM START OF SCAN 471.0 SEC

ELEVATION 5 CM — CROSS SECTION AVERAGE 565.5 — BUNDLE AVERAGE 583.5

| | | | | | | |
|---|---|---|---|---|---|---|
| 1 | 2 | 3 | 4 | 5<br>548 | 6<br>545 | 546.6 |
| 7<br>551 | 8 | 9<br>586 | 10 | 11 | 12 | 568.6 |
| 13 | 14<br>571 | 15 | 16<br>( 575) | 17 | 18 | 570.6 |
| 19 | 20<br>577 | 21 | 22 | 23<br>570 | 24 | 573.4 |
| 25 | 26 | 27<br>571 | 28<br>570 | 29 | 30 | 570.8 |
| 31<br>( 535) | 32 | 33 | 34 | 35 | 36<br>( 528) | |
| 551.2 | 573.7 | 578.6 | 570.4 | 558.9 | 545.2 | |

ALL TEMPERATURES ARE IN DEGREES C
VALUES IN PARENTHESES ARE NOT USED IN DETERMINING AVERAGES

Fig. 42. Temperatures measured at 5-cm elevation 0.7 s before depressurization.

ORNL-DWG 81-16437 ETD

R O D   A V E R A G E   T E M P E R A T U R E   M A P

MRBT BUNDLE 4

RECORD NUMBER 4710 — TIME FROM START OF SCAN 471.0 SEC

BUNDLE AVERAGE 583.5 DEGREES C

| | | | | | | |
|---|---|---|---|---|---|---|
| 1<br>550 | 2<br>572 | 3<br>577 | 4<br>587 | 5<br>561 | 6<br>558 | 567.6 |
| 7<br>576 | 8<br>607 | 9<br>587 | 10<br>582 | 11<br>596 | 12<br>563 | 586.3 |
| 13<br>570 | 14<br>609 | 15<br>617 | 16<br>( 609) | 17<br>577 | 18<br>576 | 592.1 |
| 19<br>593 | 20<br>589 | 21<br>617 | 22<br>592 | 23<br>593 | 24<br>568 | 592.1 |
| 25<br>571 | 26<br>595 | 27<br>586 | 28<br>596 | 29<br>588 | 30<br>579 | 586.6 |
| 31<br>562 | 32<br>582 | 33<br>596 | 34<br>591 | 35<br>581 | 36<br>537 | 572.9 |
| 571.7 | 592.8 | 596.8 | 587.7 | 582.6 | 563.6 | |

ALL TEMPERATURES ARE IN DEGREES C
VALUES IN PARENTHESES ARE NOT USED IN DETERMINING ROW & COLUMN AVERAGES

Fig. 43. Average simulator temperatures measured 0.7 s before depressurization.

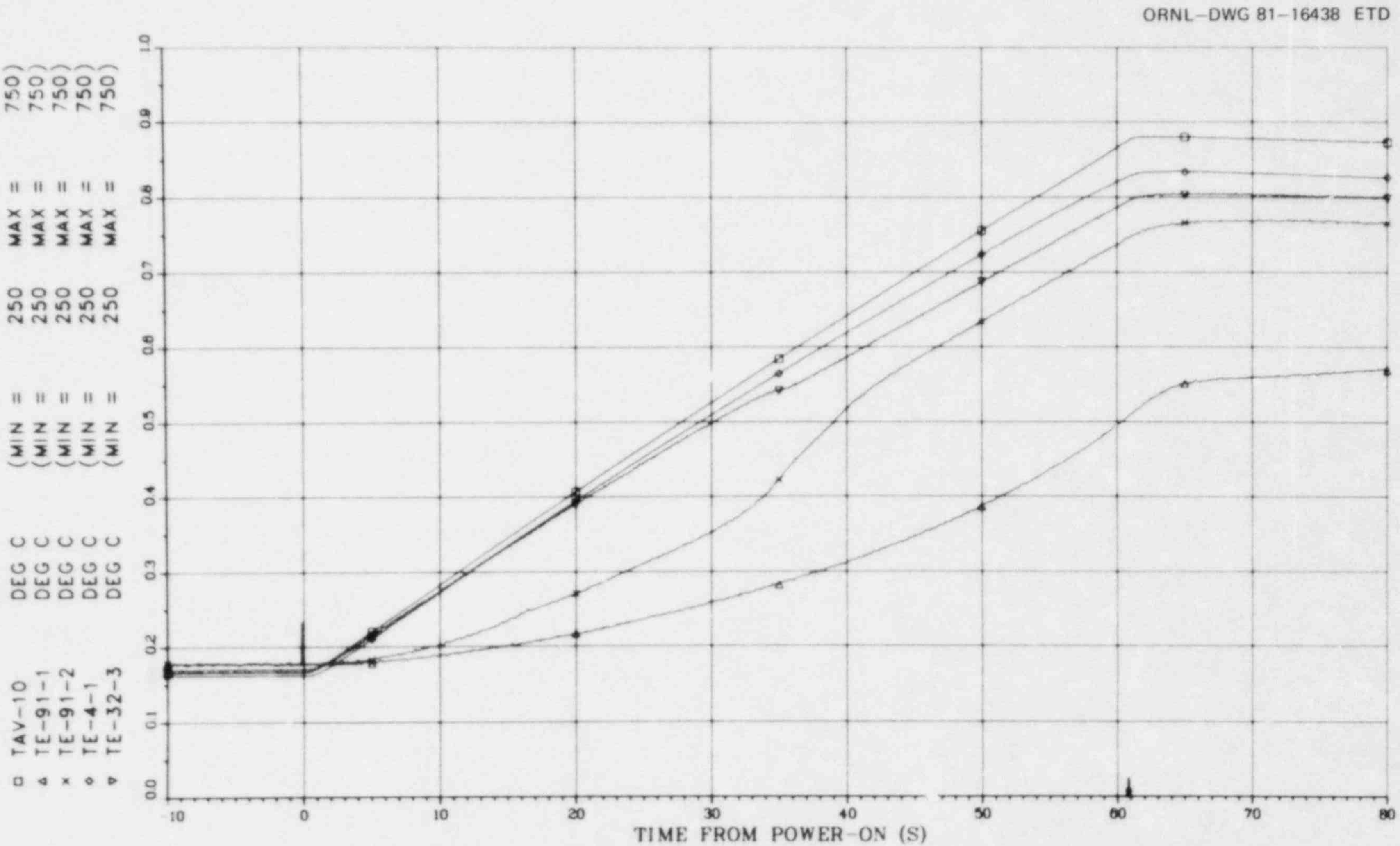


Fig. 44. B-4 shroud and simulator temperatures measured at 76-cm elevation during powered portion of transient.

ORNL-DWG 81-16439 ETD

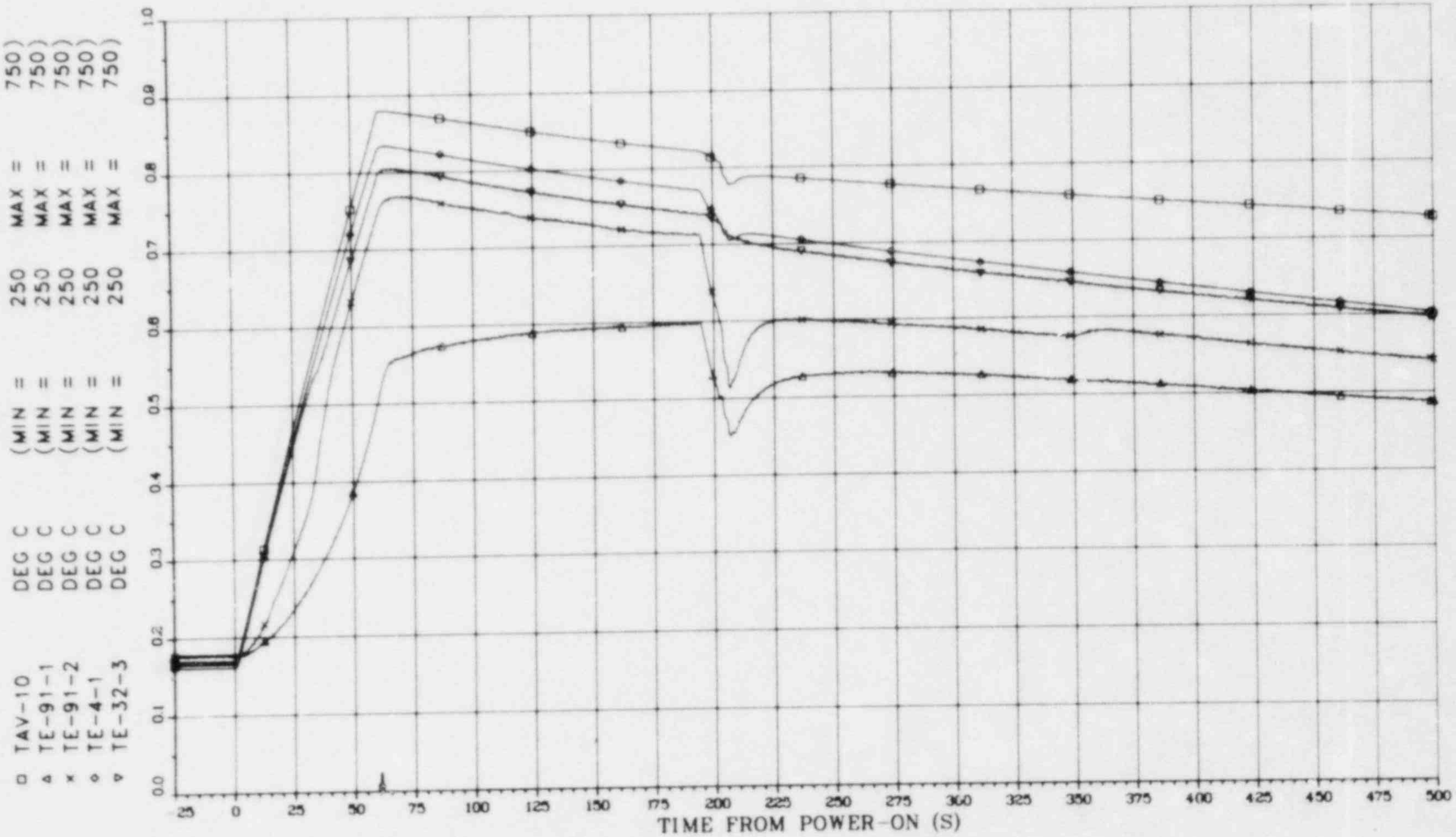


Fig. 45. B-4 shroud and simulator temperatures measured at 76-cm elevation during transient.

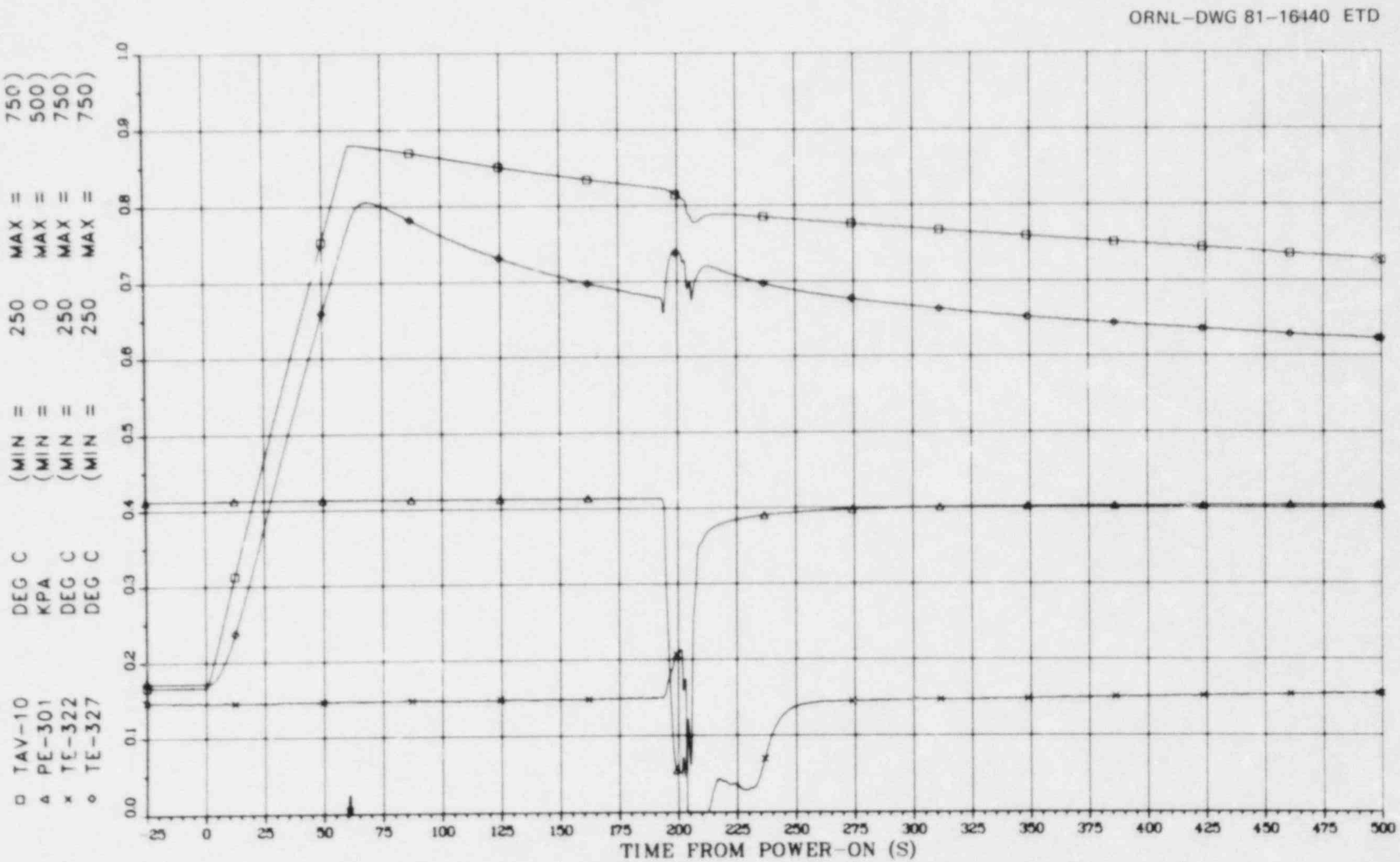


Fig. 46. B-4 steam pressure and characteristic temperatures measured during transient.

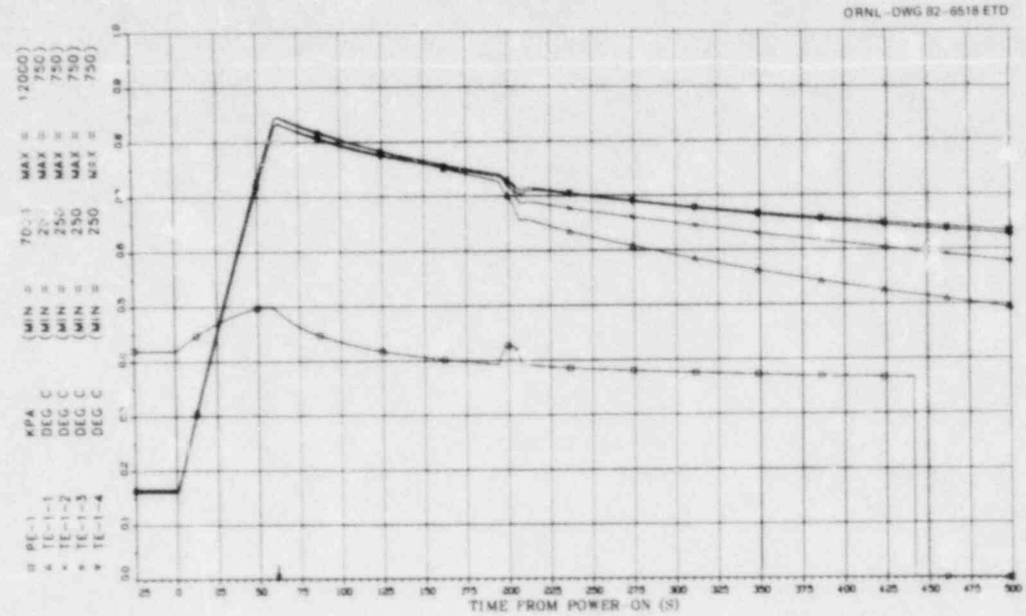


Fig. 47. Temperature and pressure transients for B-4 rod No. 1.

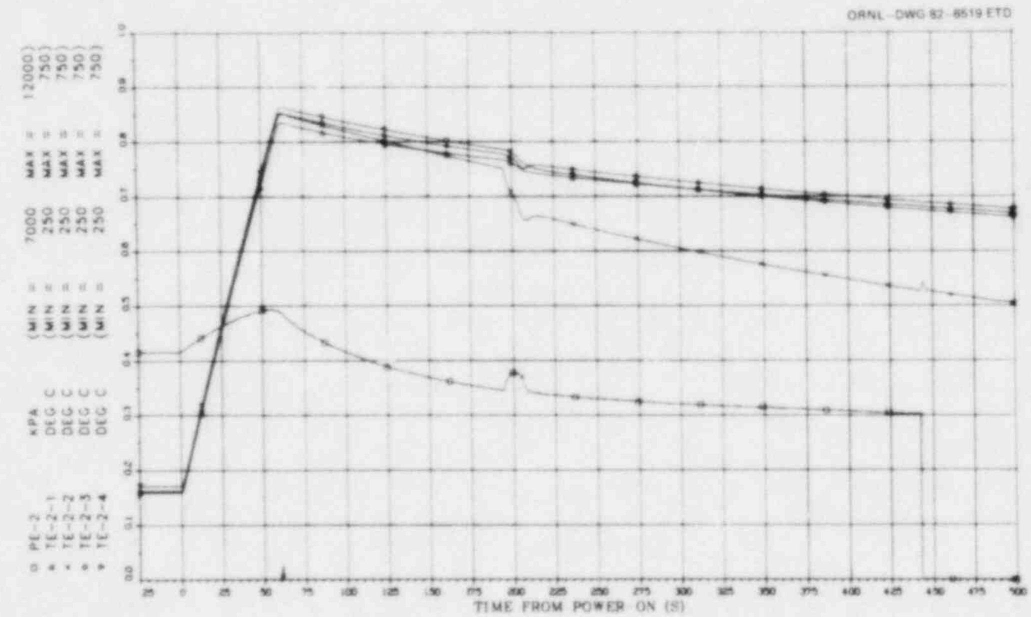


Fig. 48. Temperature and pressure transients for B-4 rod No. 2.

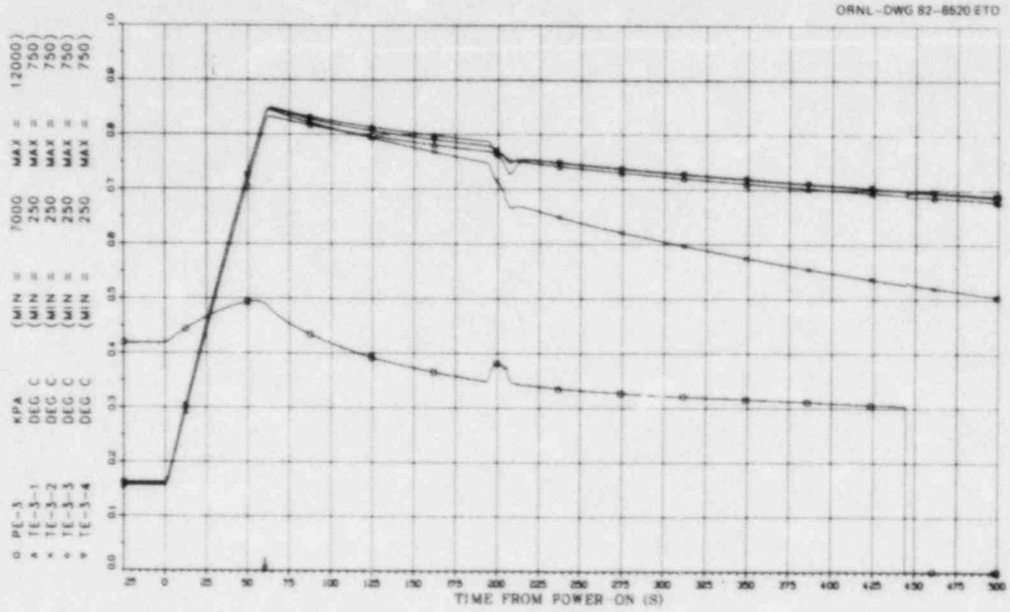


Fig. 49. Temperature and pressure transients for B-4 rod No. 3.

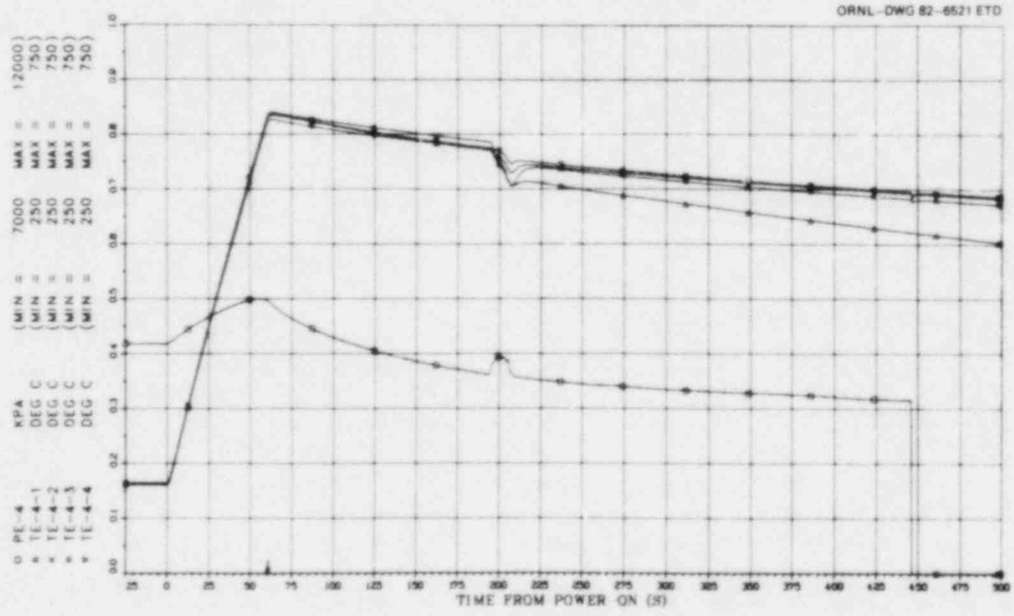


Fig. 50. Temperature and pressure transients for B-4 rod No. 4.

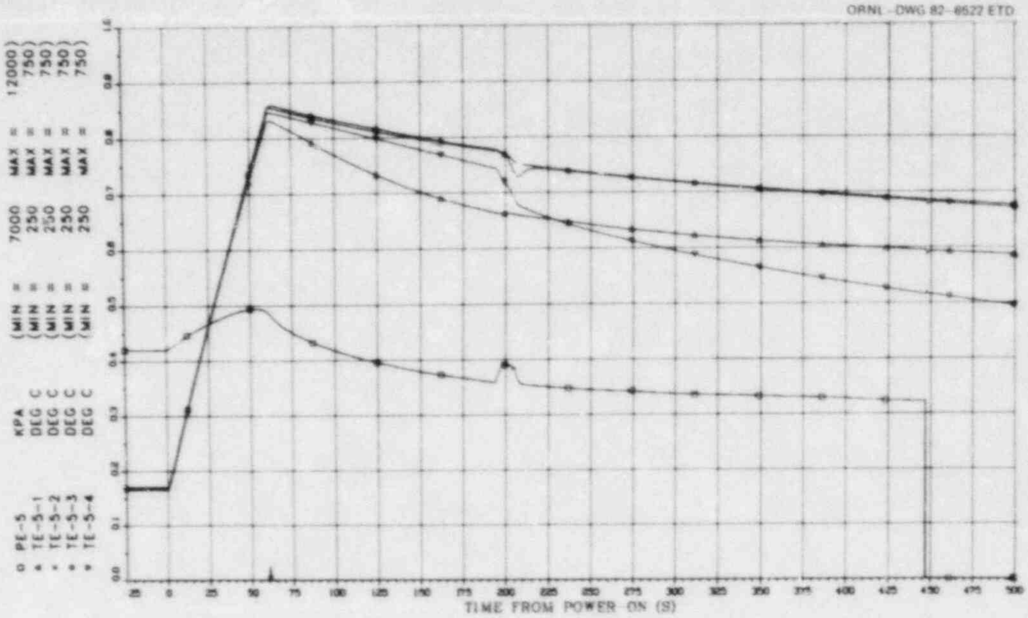


Fig. 51. Temperature and pressure transients for B-4 rod No. 5.

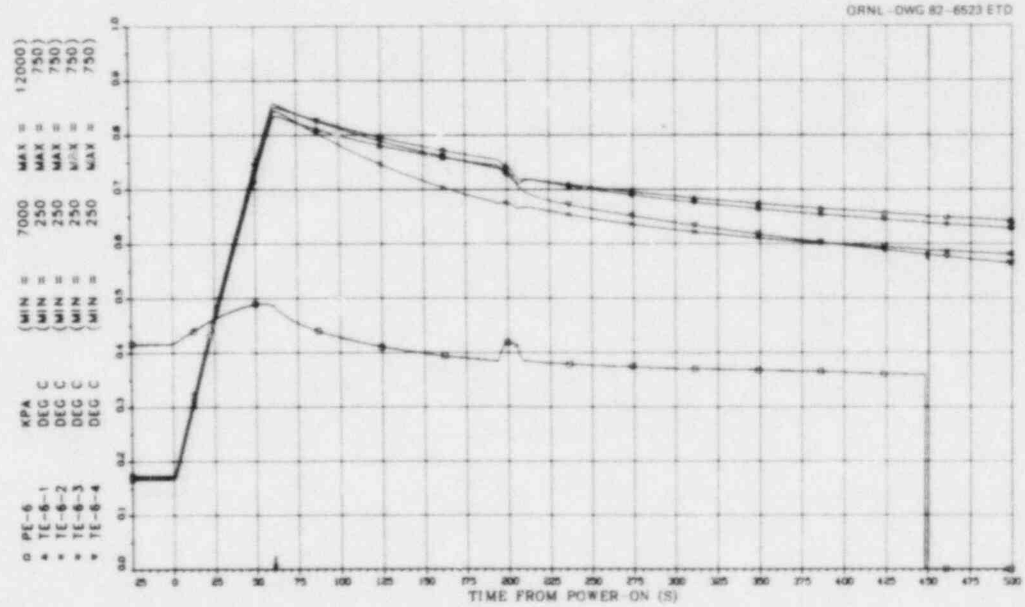


Fig. 52. Temperature and pressure transients for B-4 rod No. 6.

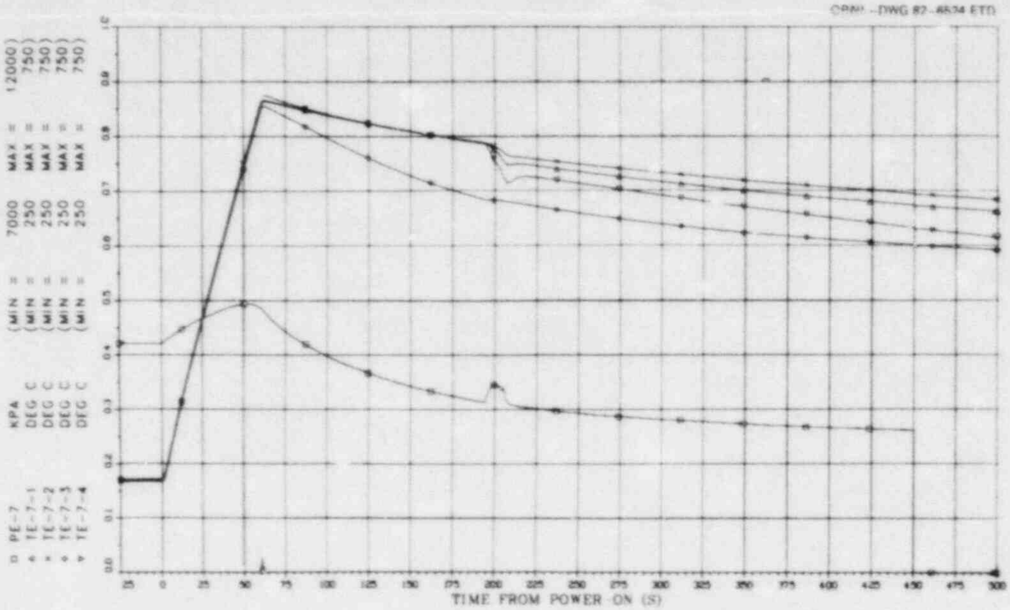


Fig. 53. Temperature and pressure transients for B-4 rod No. 7.

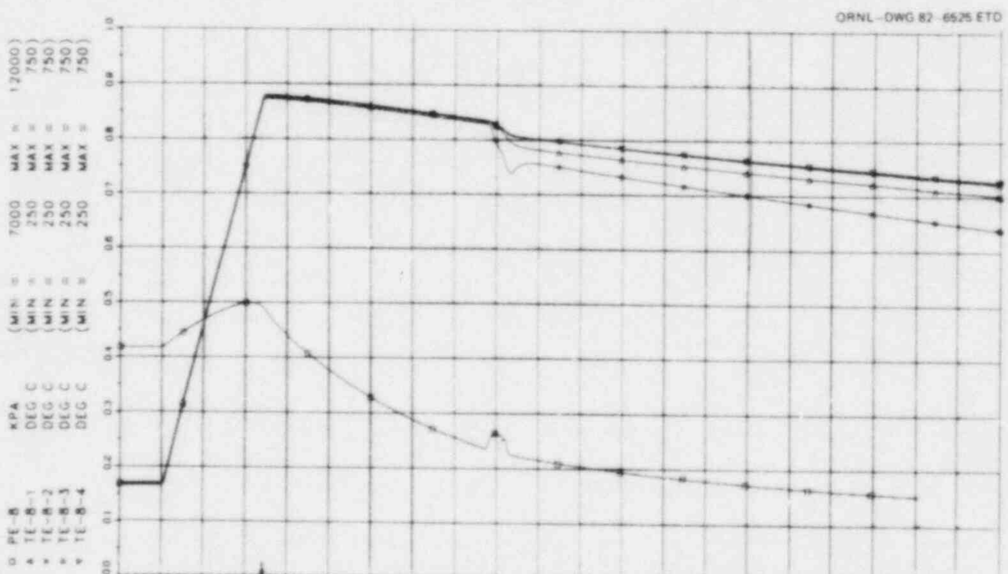


Fig. 54. Temperature and pressure transients for B-4 rod No. 8.

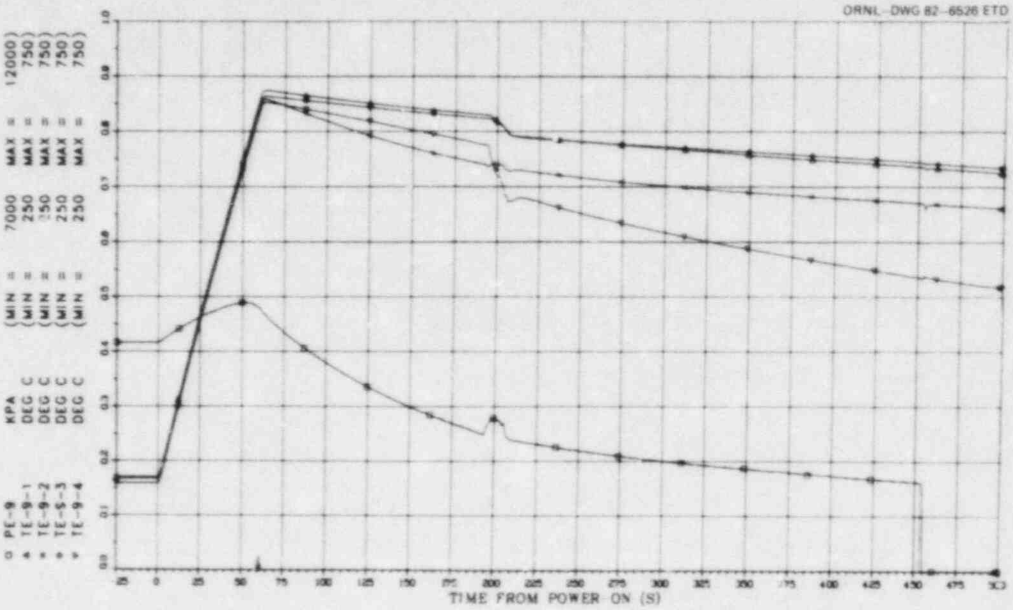


Fig. 55. Temperature and pressure transients for B-4 rod No. 9.

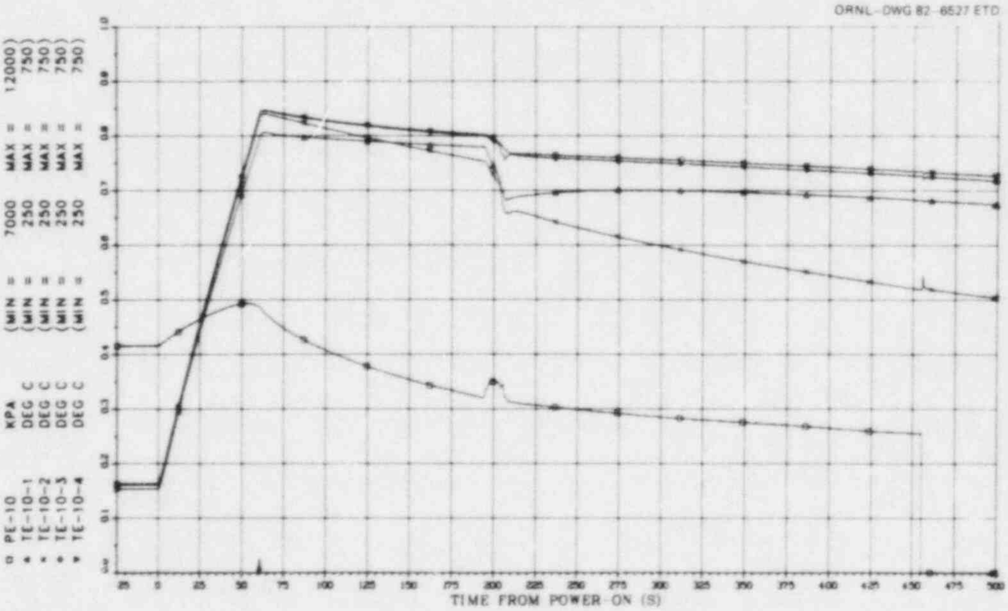


Fig. 56. Temperature and pressure transients for B-4 rod No. 10.

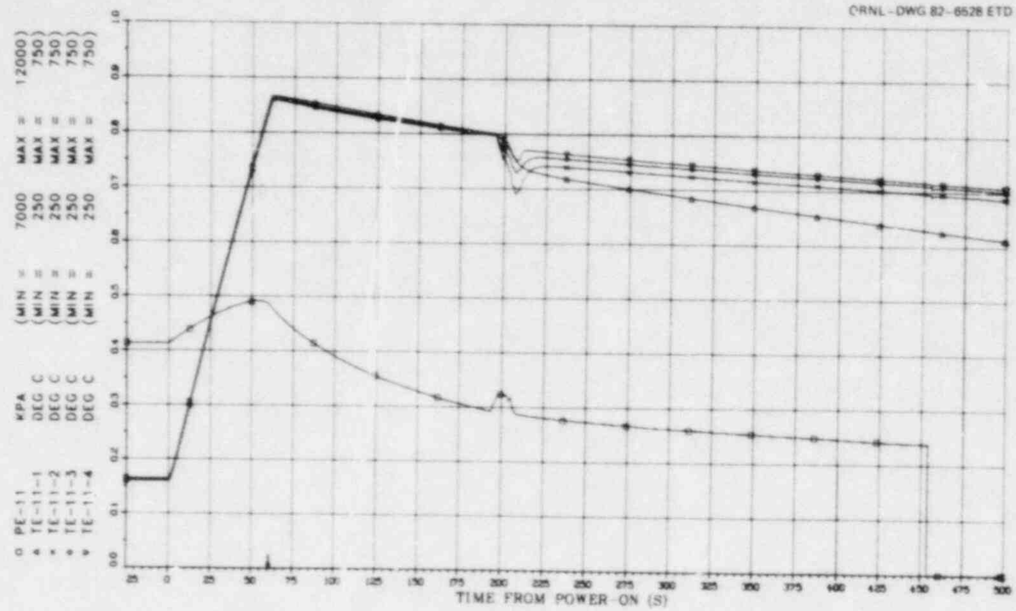


Fig. 57. Temperature and pressure transients for B-4 rod No. 11.

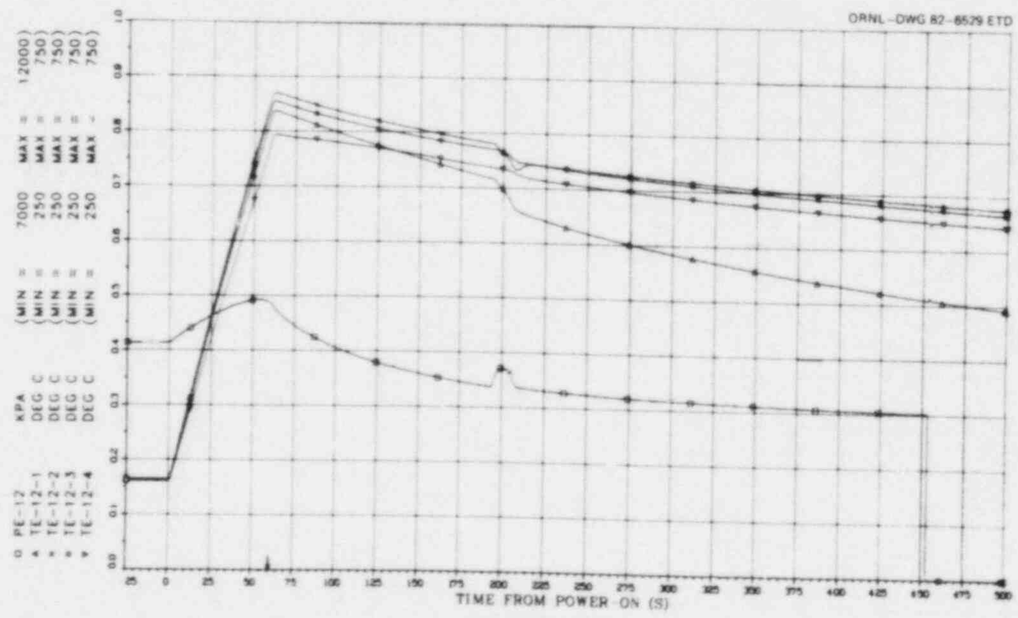


Fig. 58. Temperature and pressure transients for B-4 rod No. 12.

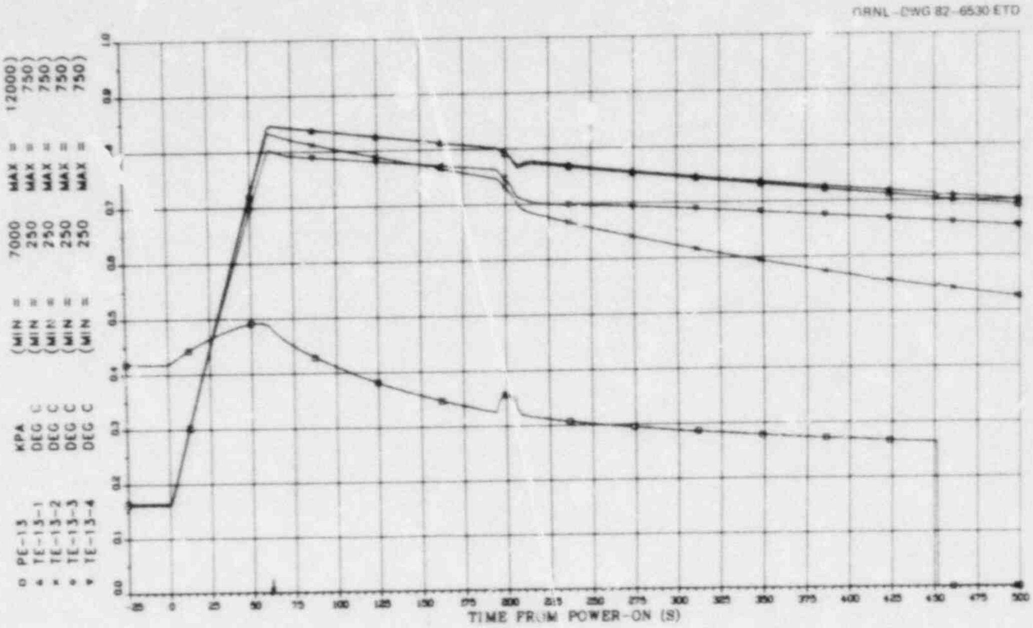


Fig. 59. Temperature and pressure transients for B-4 rod No. 13.

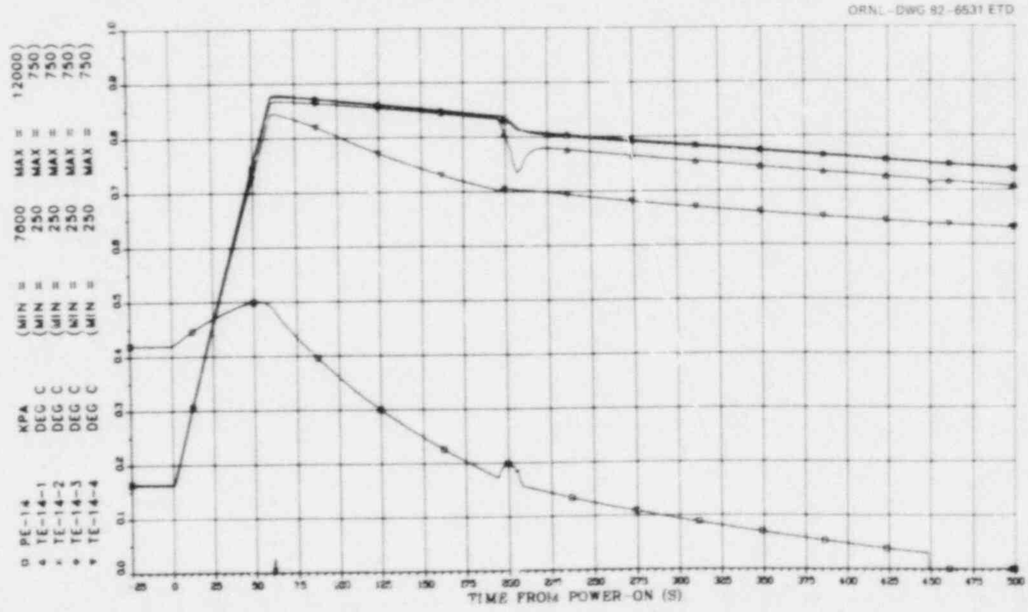


Fig. 60. Temperature and pressure transients for B-4 rod No. 14.

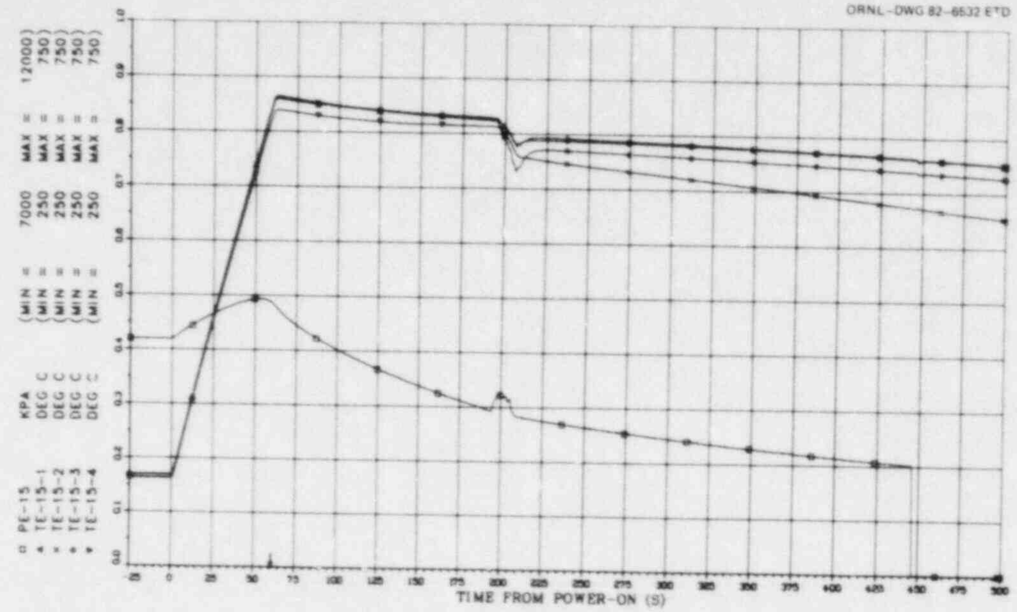


Fig. 61. Temperature and pressure transients for B-4 rod No. 15.

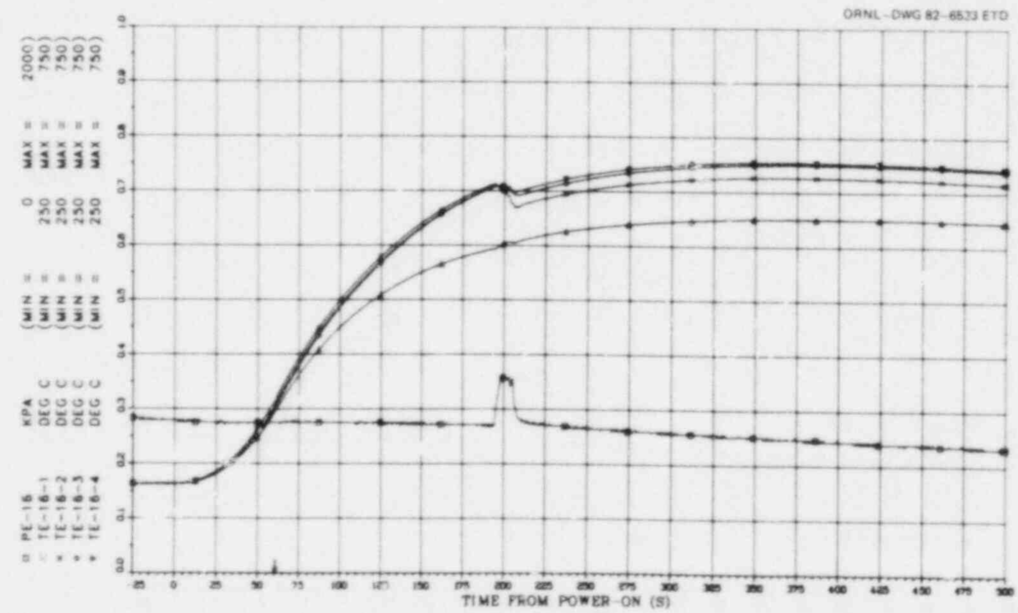


Fig. 62. Temperature and pressure transients for B-4 rod No. 16.

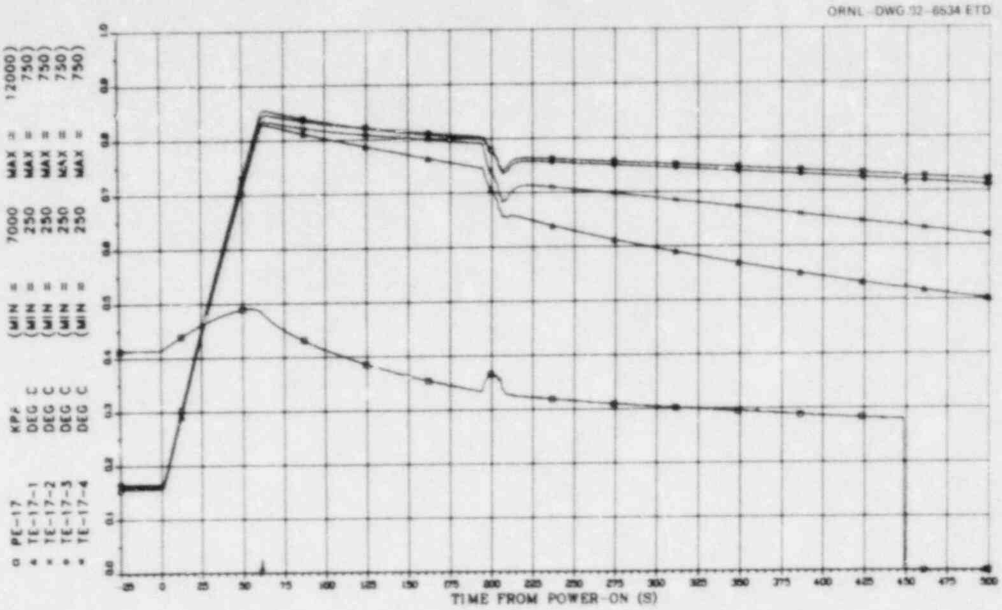


Fig. 63. Temperature and pressure transients for B-4 rod No. 17.

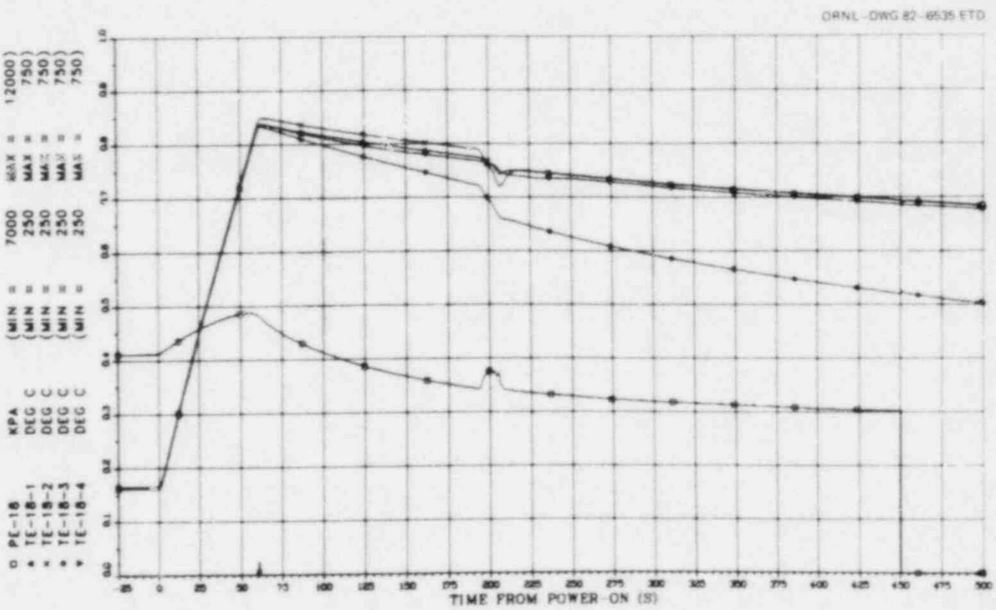


Fig. 64. Temperature and pressure transients for B-4 rod No. 18.

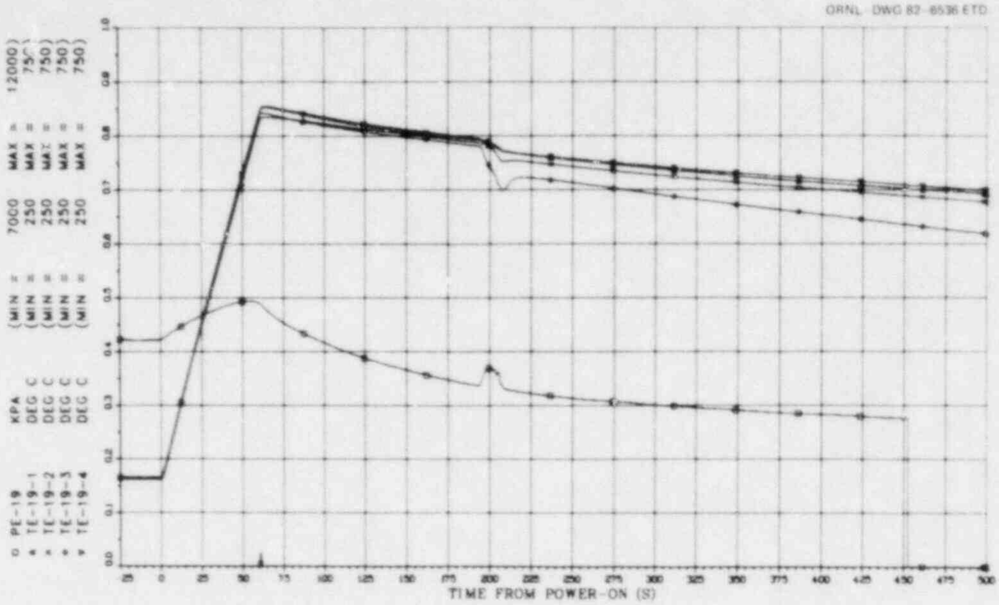


Fig. 65. Temperature and pressure transients for B-4 rod No. 19.

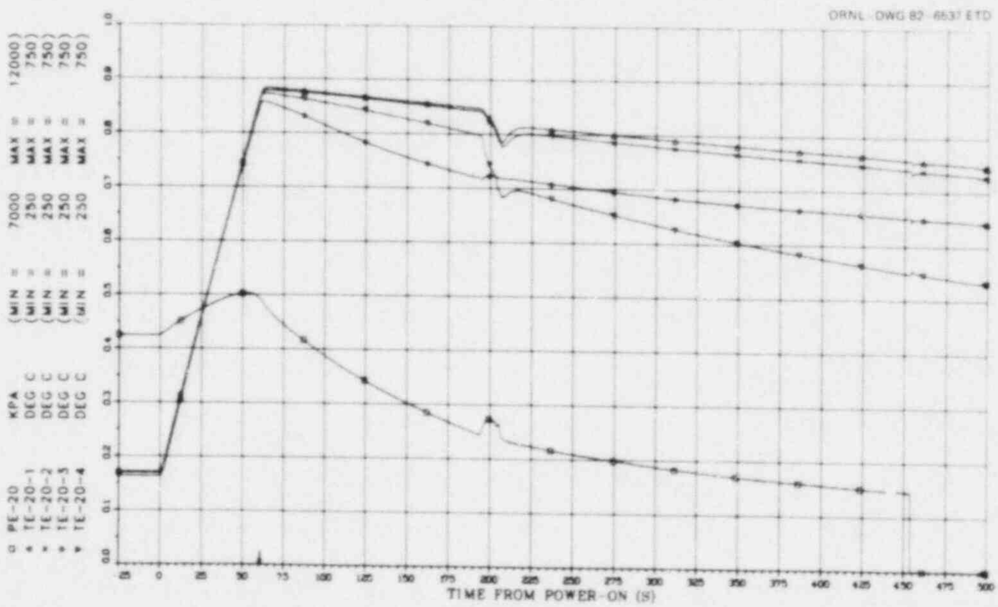


Fig. 66. Temperature and pressure transients for B-4 rod No. 20.

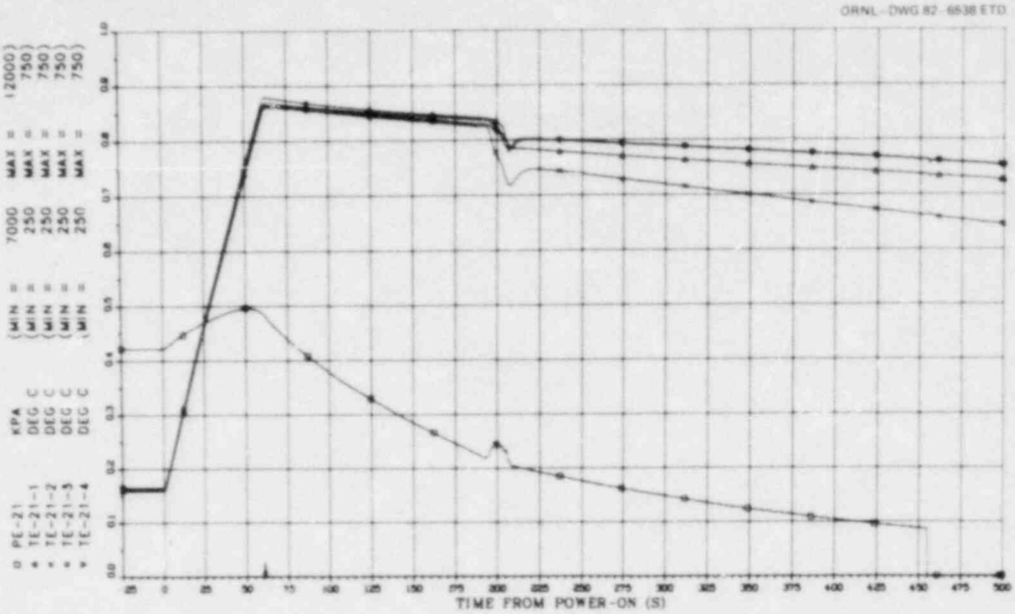


Fig. 67. Temperature and pressure transients for B-4 rod No. 21.

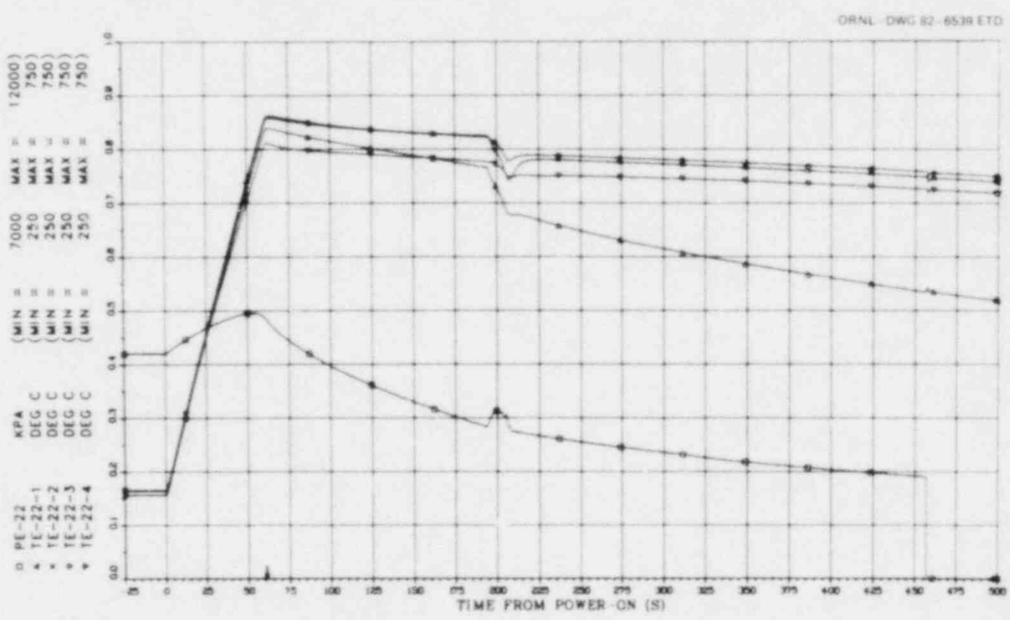


Fig. 68. Temperature and pressure transients for B-4 rod No. 22.

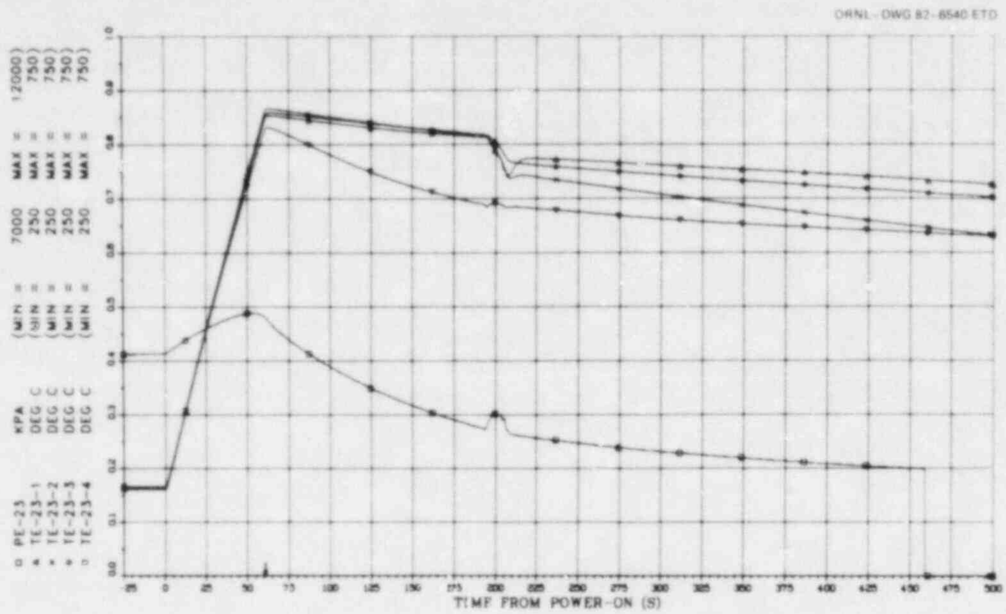


Fig. 69. Temperature and pressure transients for B-4 rod No. 23.

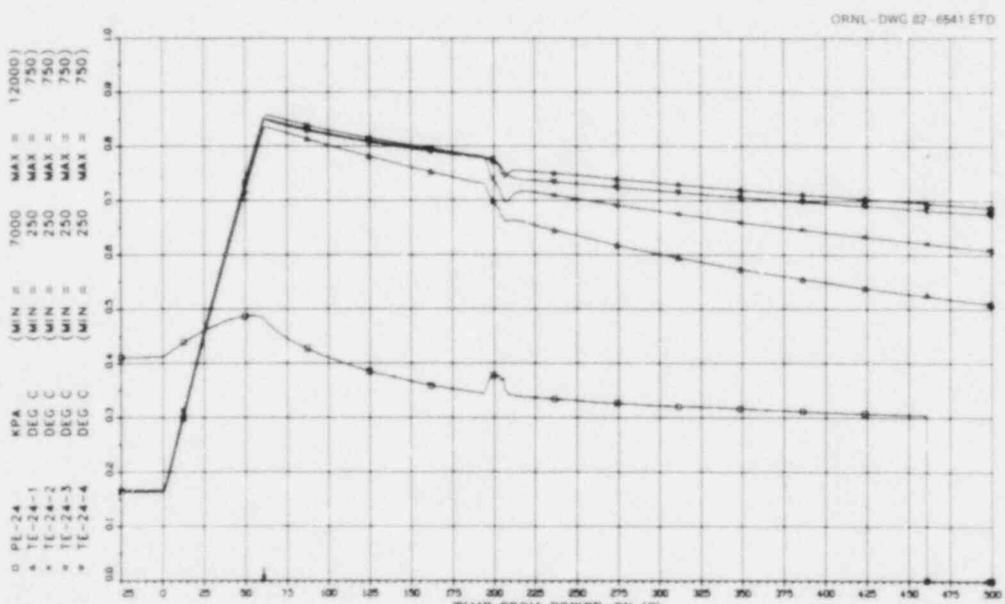


Fig. 70. Temperature and pressure transients for B-4 rod No. 24.

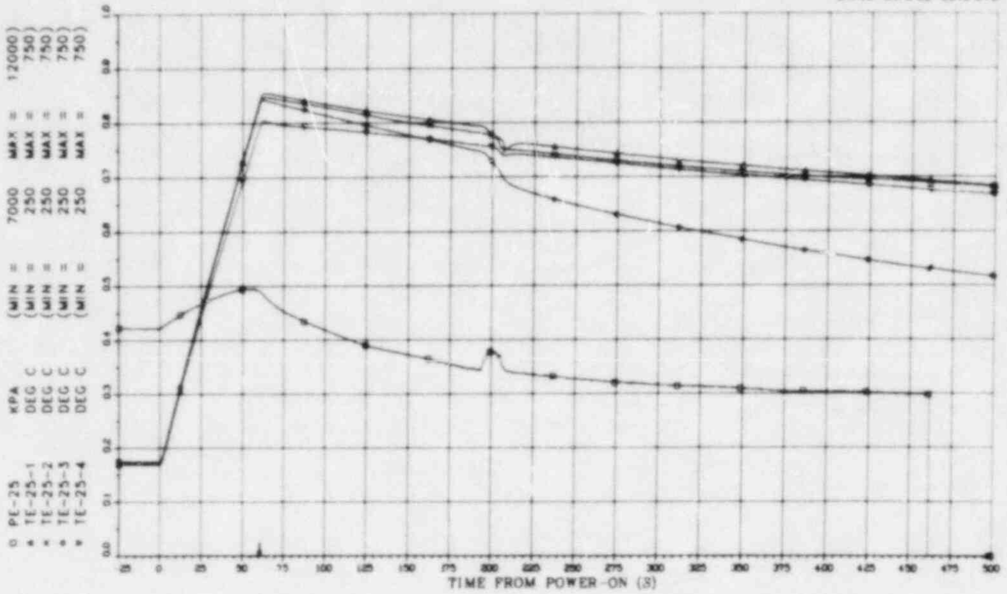


Fig. 71. Temperature and pressure transients for B-4 rod No. 25.

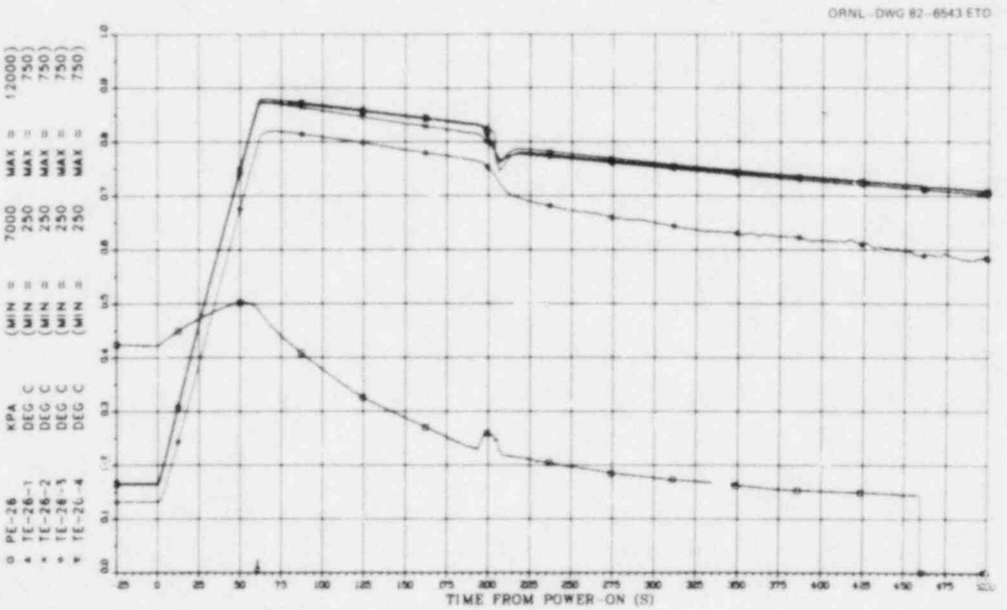


Fig. 72. Temperature and pressure transients for B-4 rod No. 26.

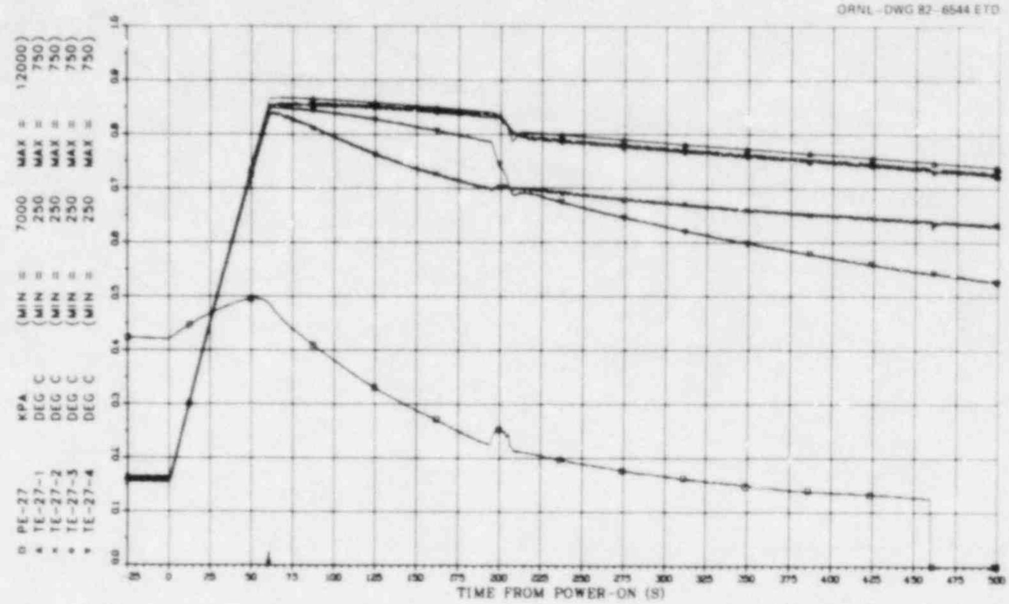


Fig. 73. Temperature and pressure transients for B-4 rod No. 27.

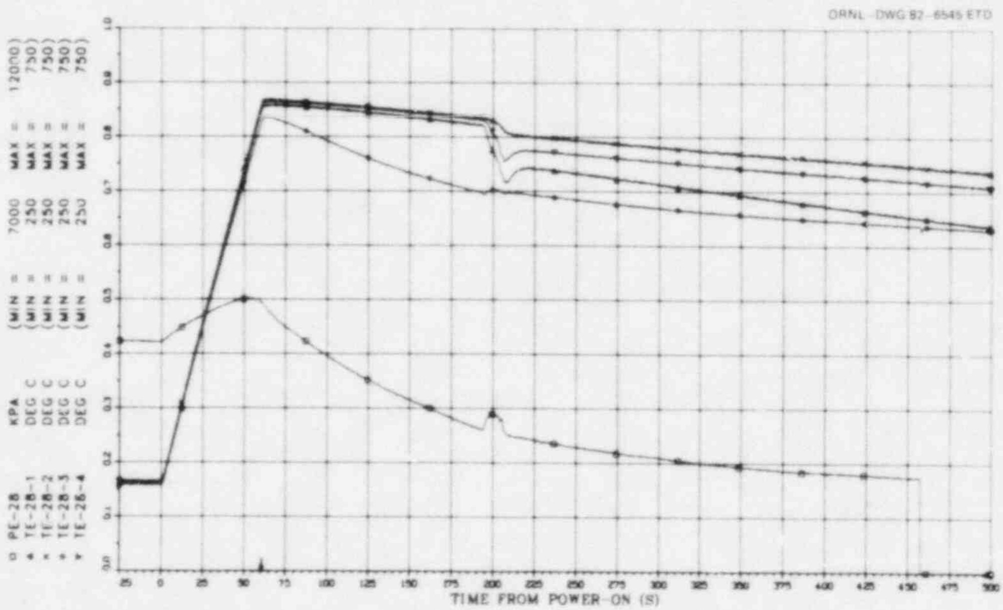


Fig. 74. Temperature and pressure transients for B-4 rod No. 28.

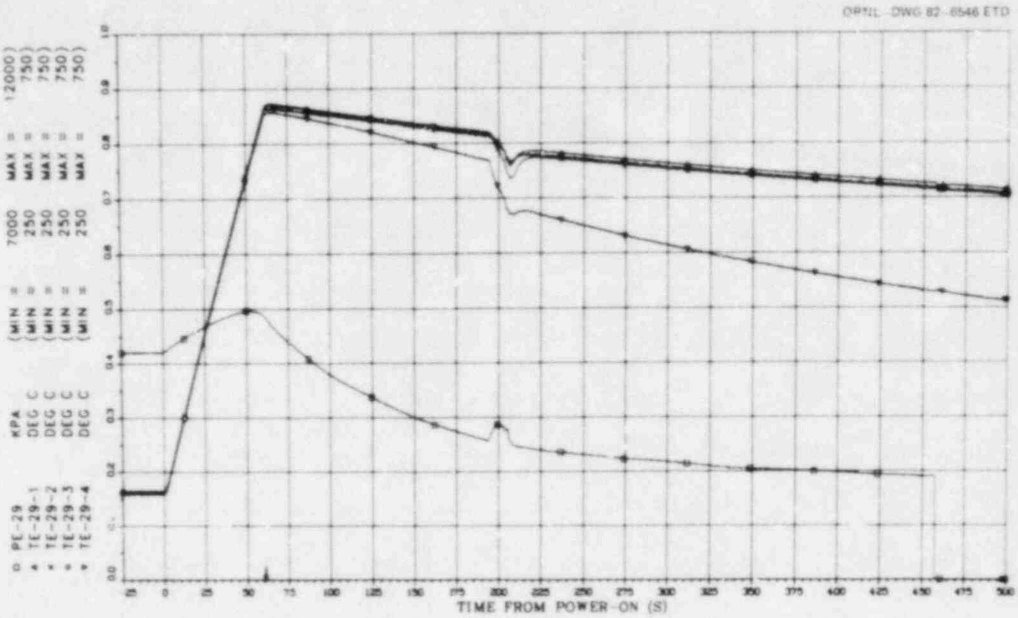


Fig. 75. Temperature and pressure transients for B-4 rod No. 29.

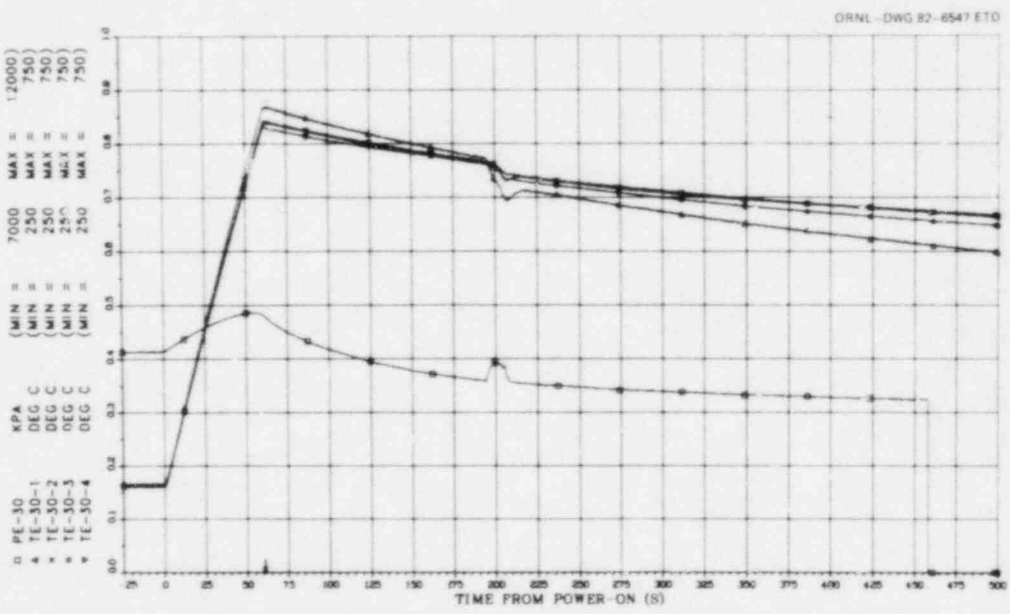


Fig. 76. Temperature and pressure transients for B-4 rod No. 30.

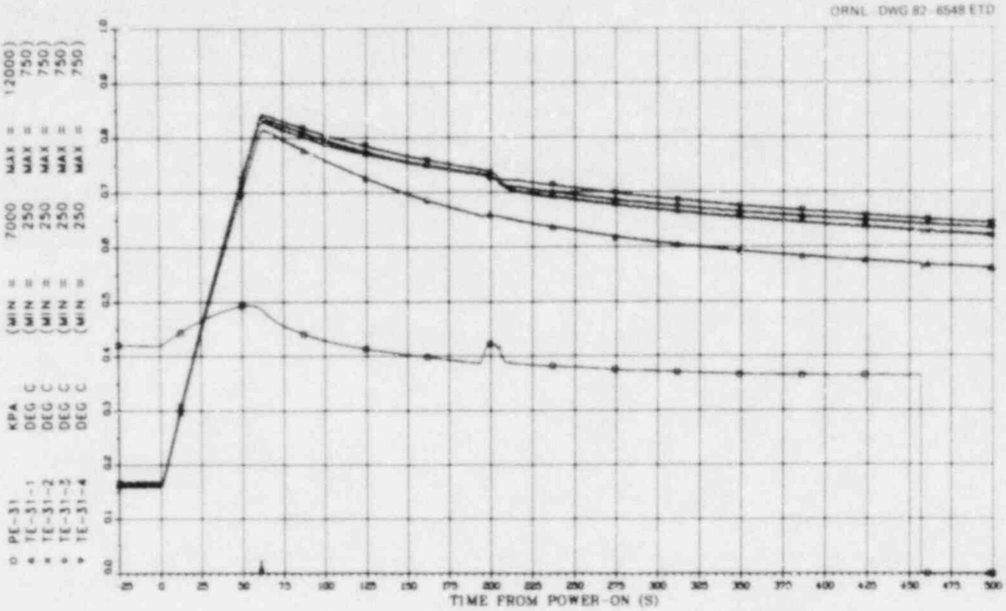


Fig. 77. Temperature and pressure transients for B-4 rod No. 31.

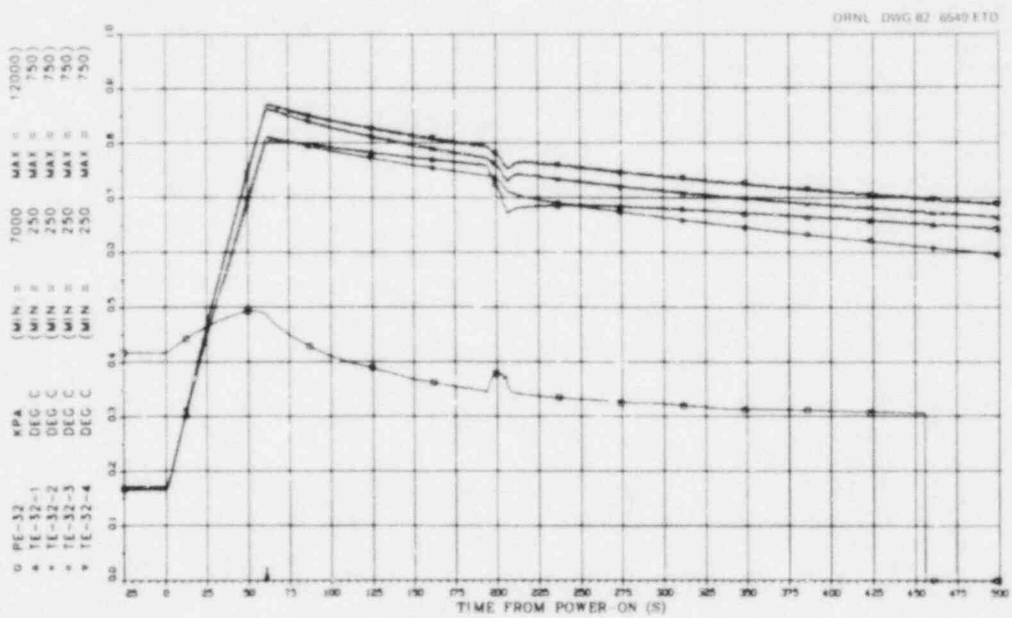


Fig. 78. Temperature and pressure transients for B-4 rod No. 32.

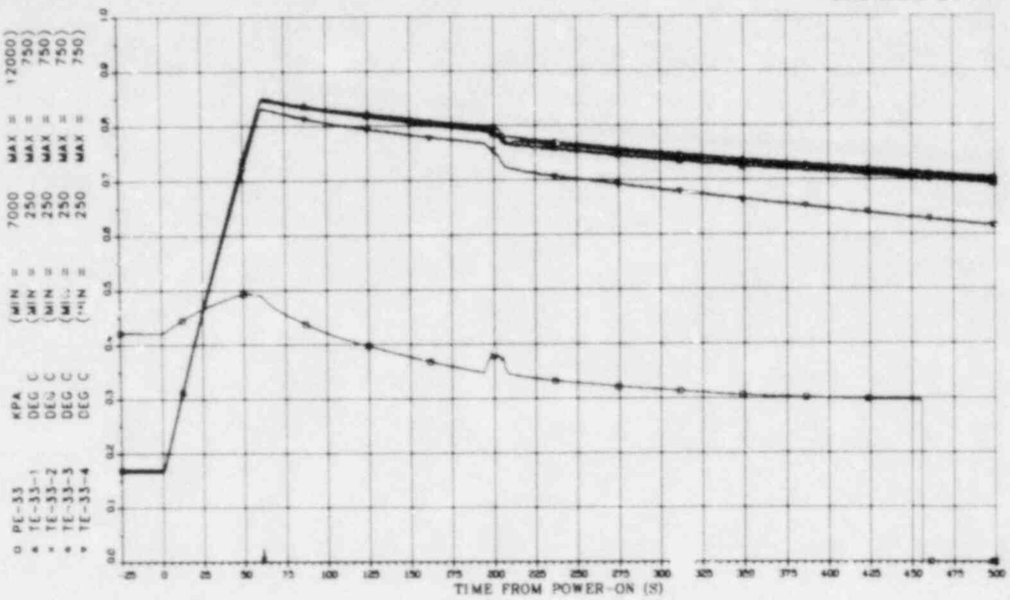


Fig. 79. Temperature and pressure transients for B-4 rod No. 33.

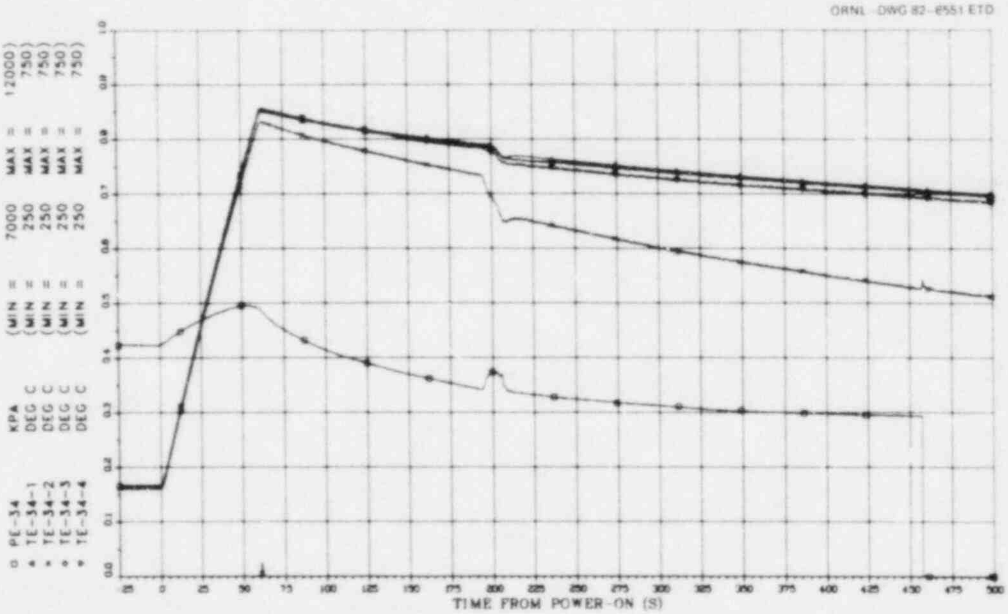


Fig. 80. Temperature and pressure transients for B-4 rod No. 34.

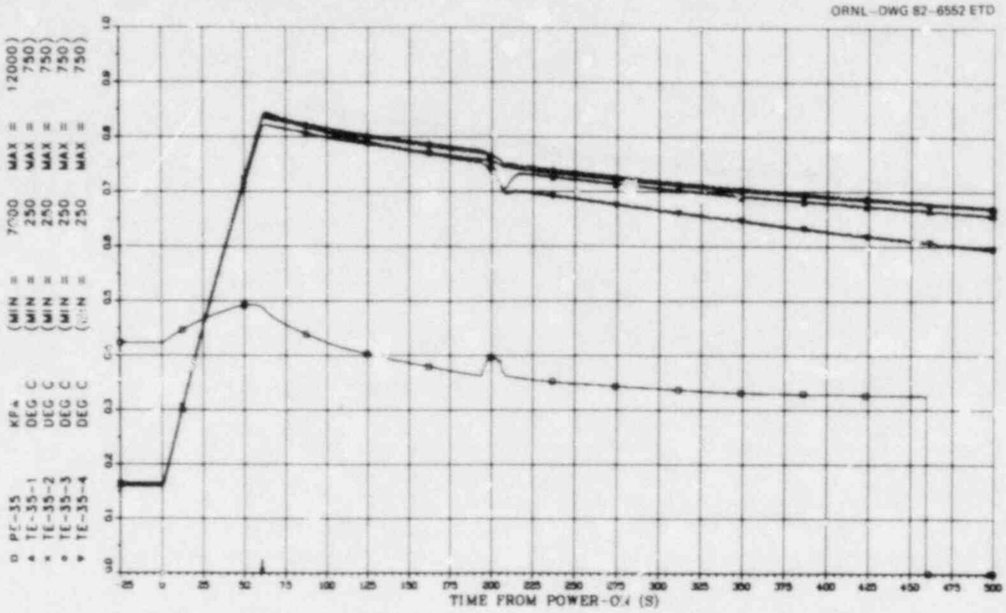


Fig. 81. Temperature and pressure transients for B-4 rod No. 35.

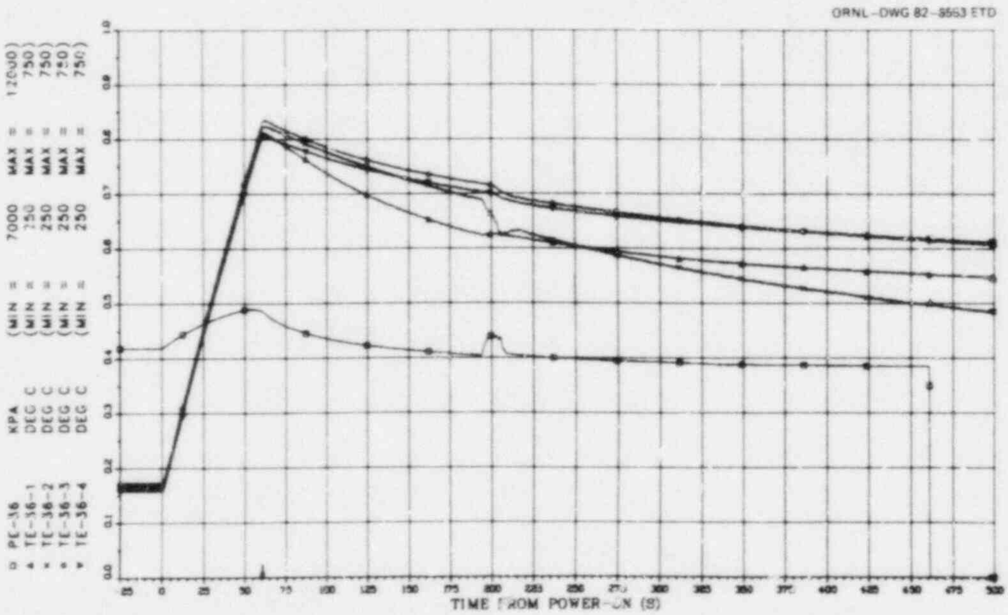


Fig. 82. Temperature and pressure transients for B-4 rod No. 36.

ORNL PHOTO 7469-80A

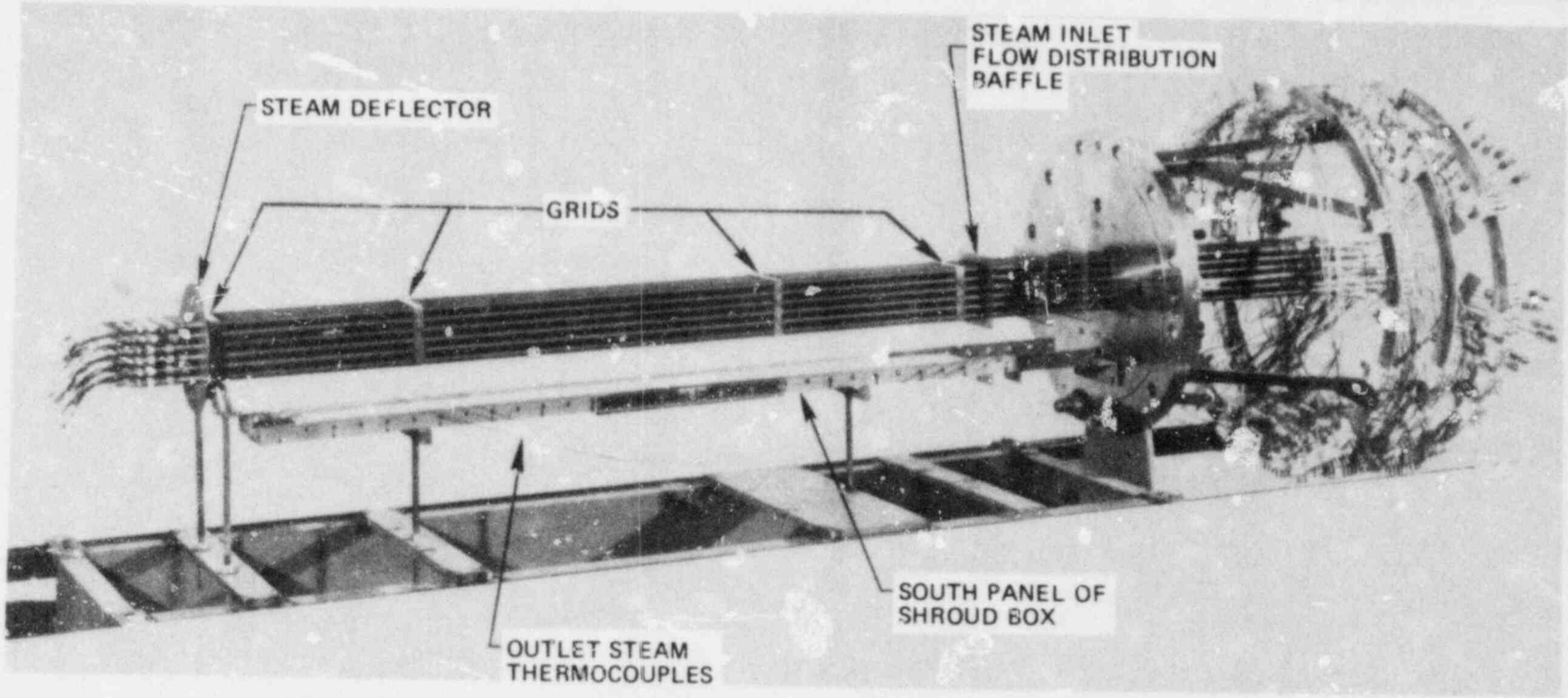


Fig. 83 Partially assembled B-4 bundle.

ORNL PHOTO 7082-81A

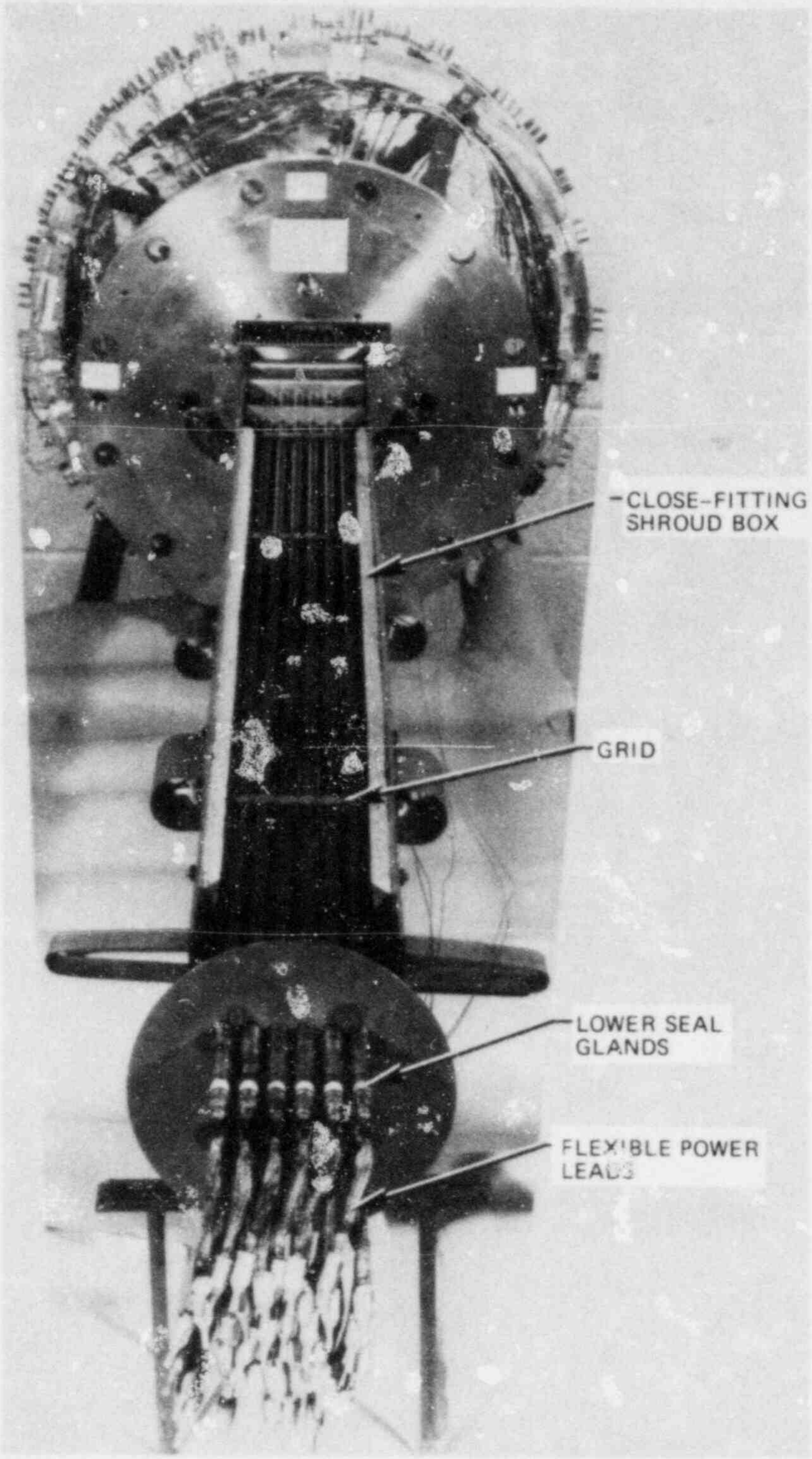


Fig. 84. Bundle B-4 before installation of north panel of shroud box.

ORNL PHOTO 7467–80A

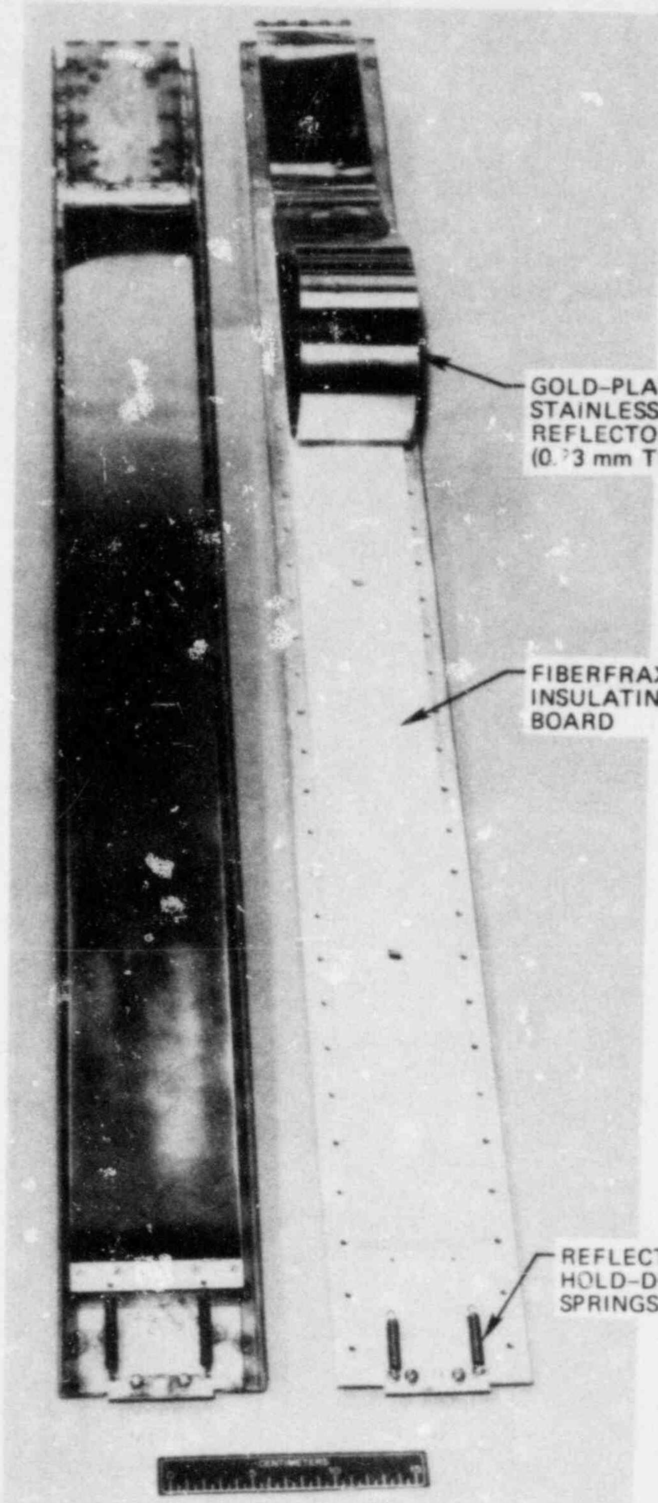


Fig. 85. Bundle B-4 shroud panels with reflector strip folded back on west panel to show insulating material.

ORNL PHOTO 7490–80A

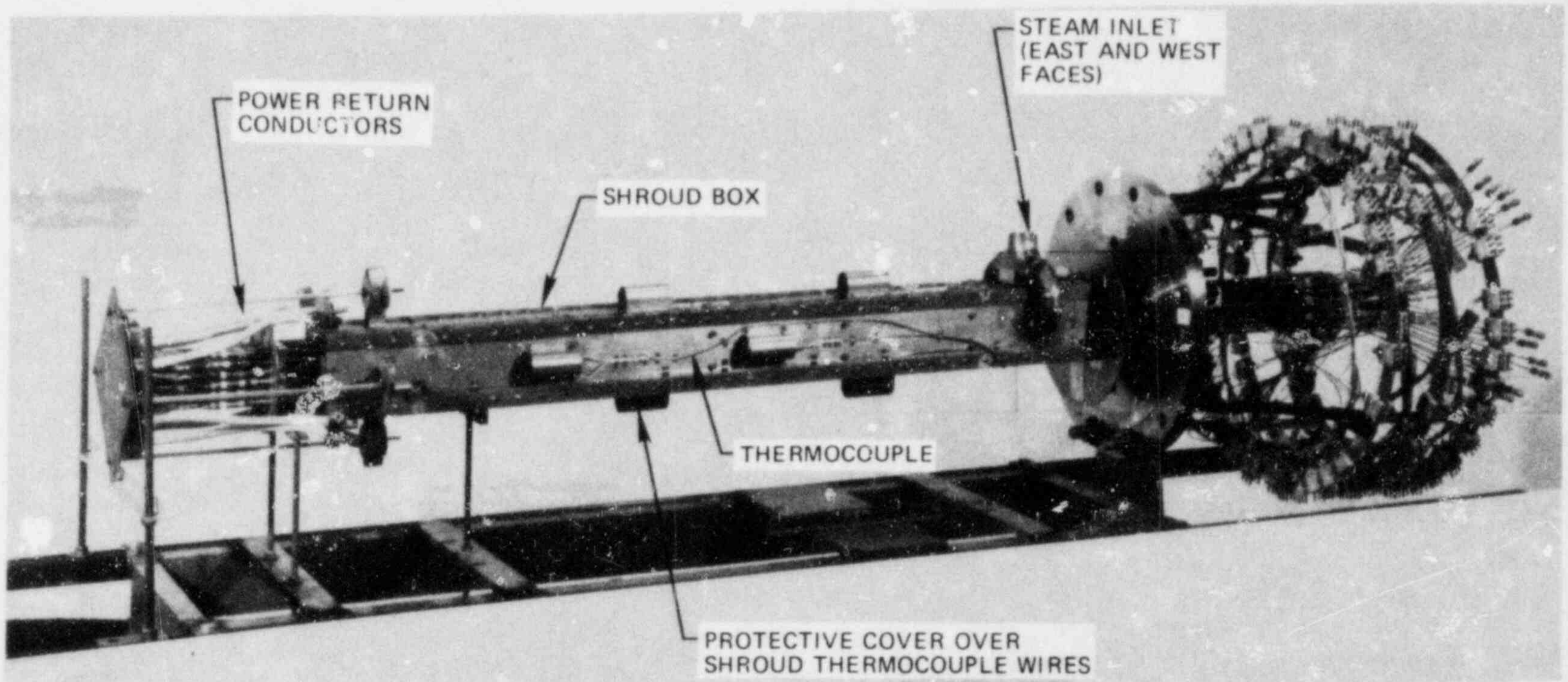


**Fig. 86. Completely assembled B-4 bundle.**

ORNL PHOTO 7463–80A

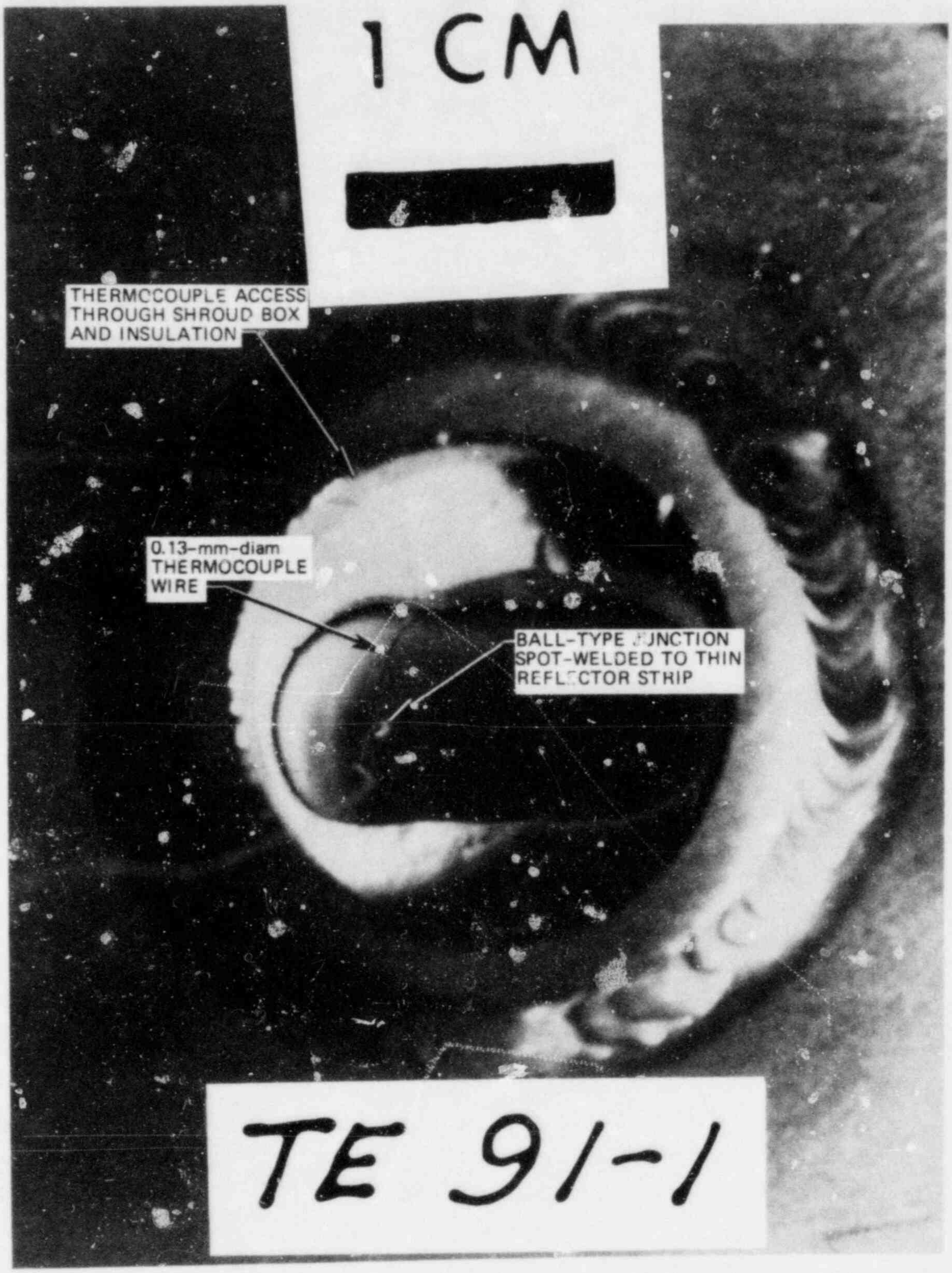


Fig. 87. Shroud thermocouple attachment in B-4 test.

ORNL PHOTO 7493–80A

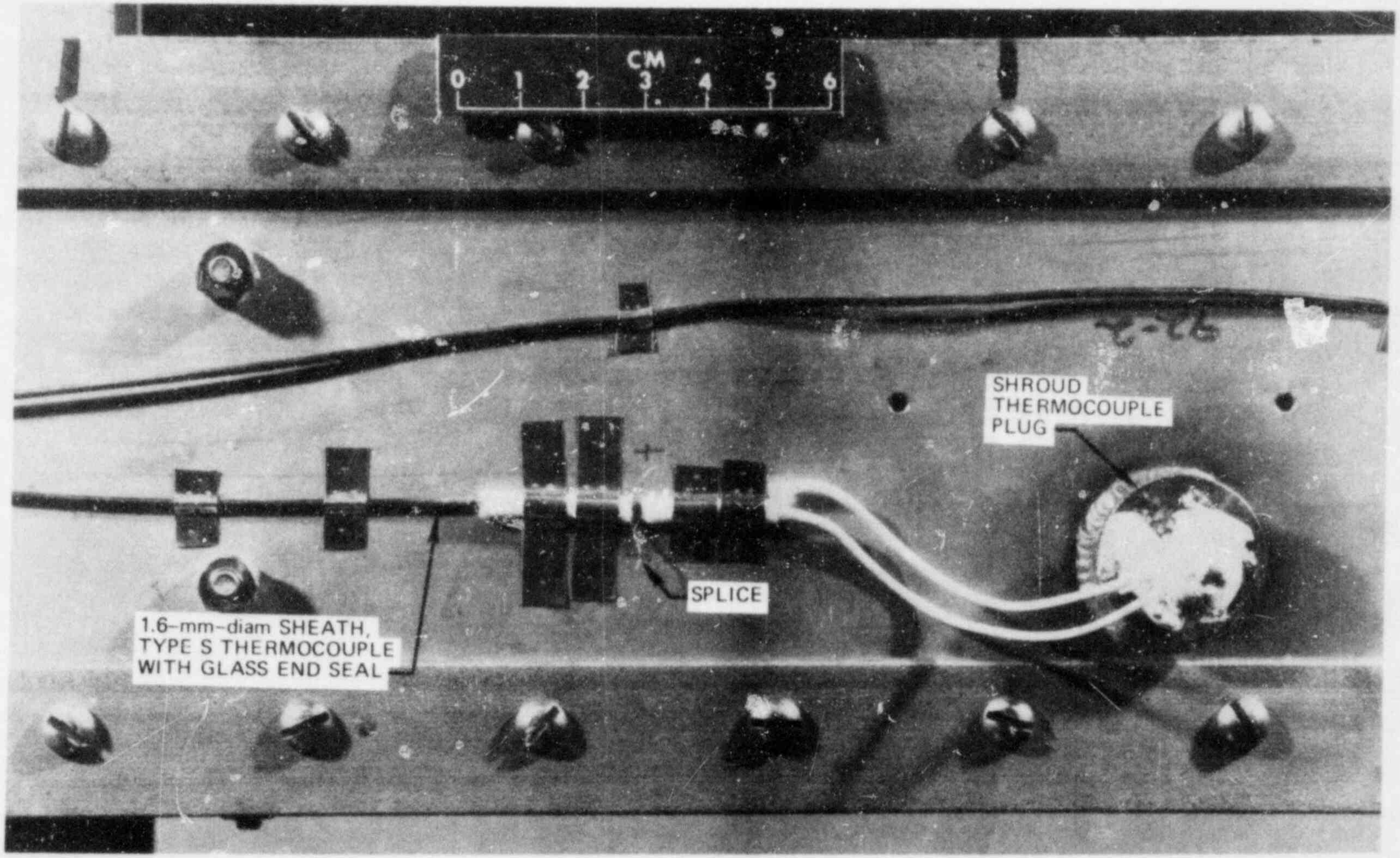


Fig. 88. Detail of shroud thermocouple installation on east face of B-4 shroud.

ORNL PHOTO 7465-80A

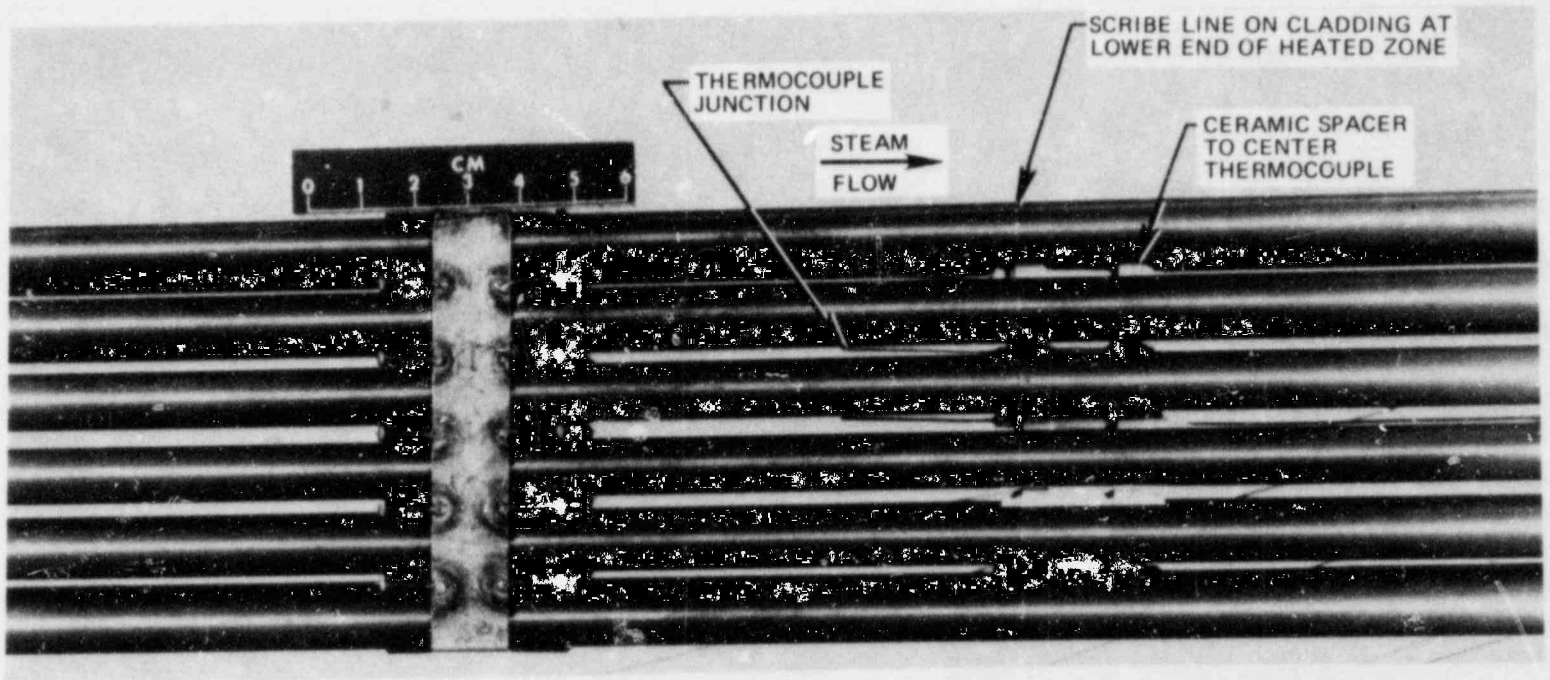


Fig. 89. Detail of outlet steam thermocouple installation in B-4 test.

ORNL PHOTO 7169–81

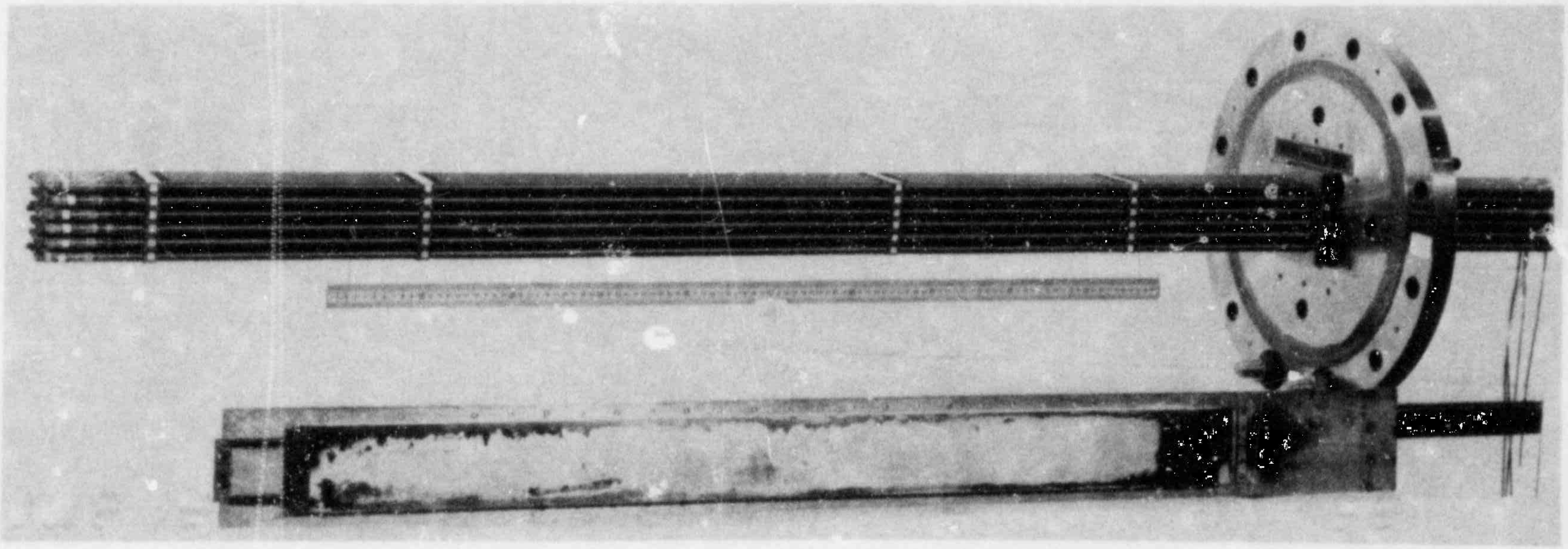

Fig. 90. Posttest view of west face of bundle B-4 and shroud.

ORNL PHOTO 2409–81A

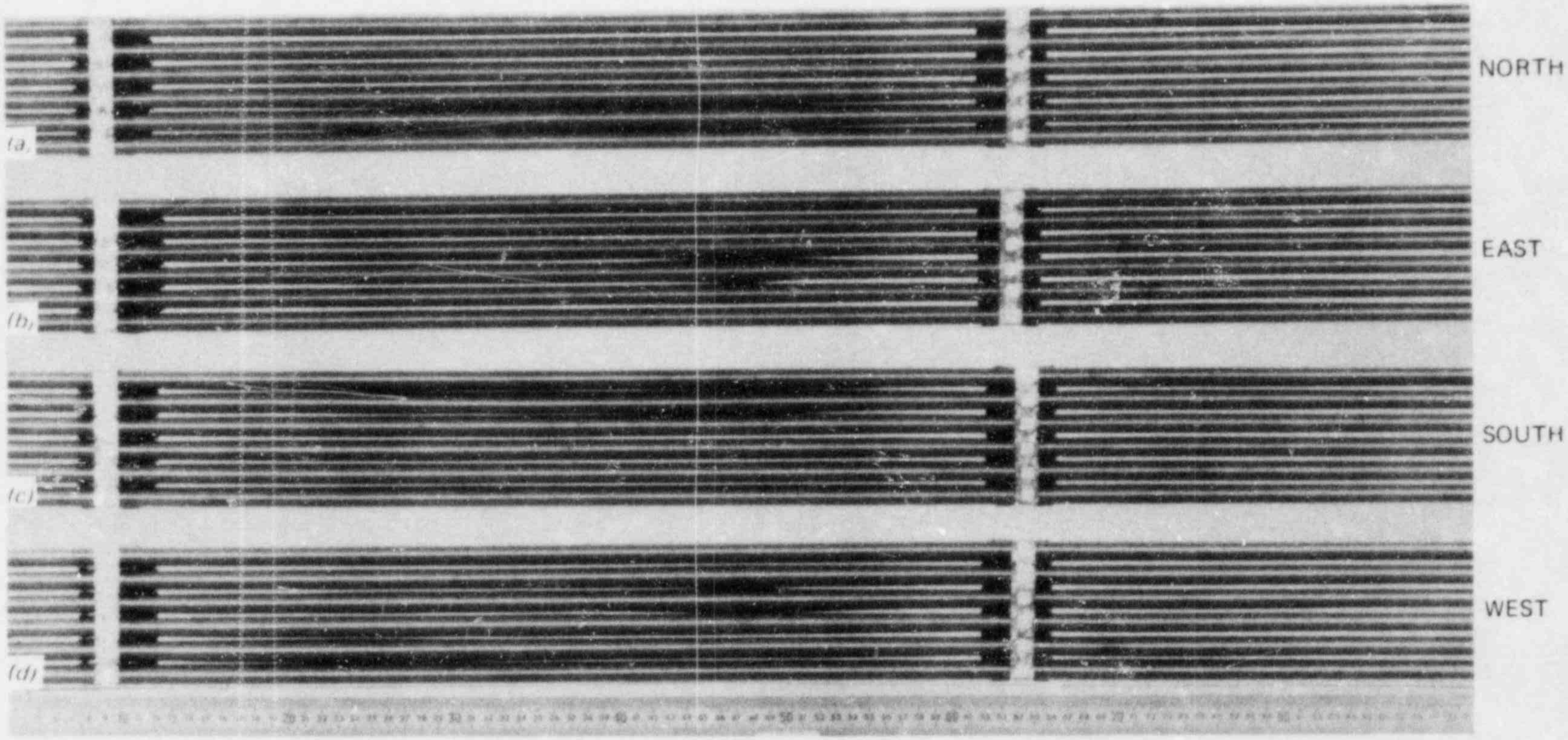


Fig. 91. 91 Posttest views of (*a*) north, (*b*) east, (*c*) south, and (*d*) west faces of bundle B-4.

ORNL PHOTO 6029-81

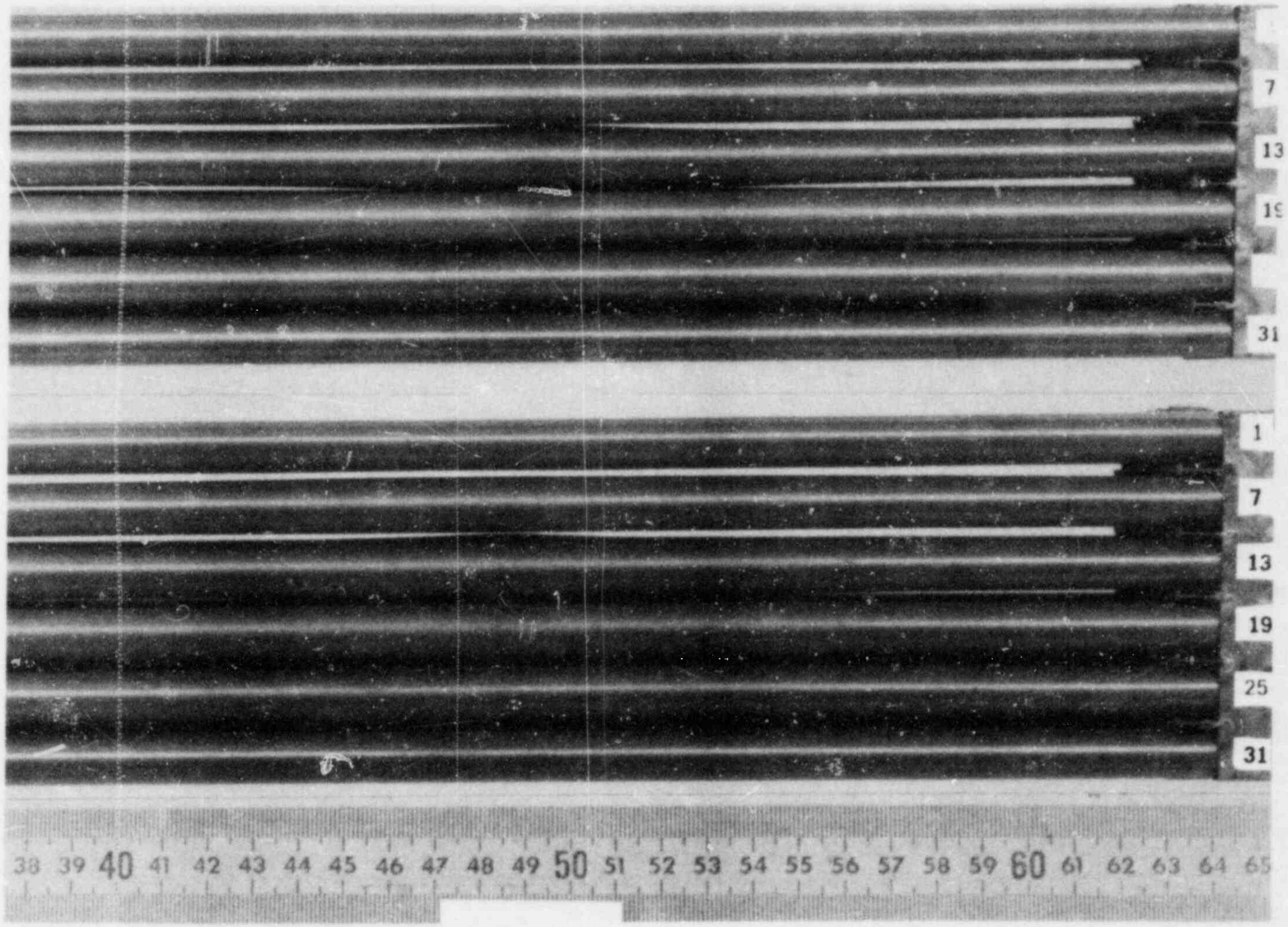


WEST

Fig. 92. Close-up views of west face of bundle B-4 showing ballooned zone of No. 14 simulator.

ORNL PHOTO 6016–81

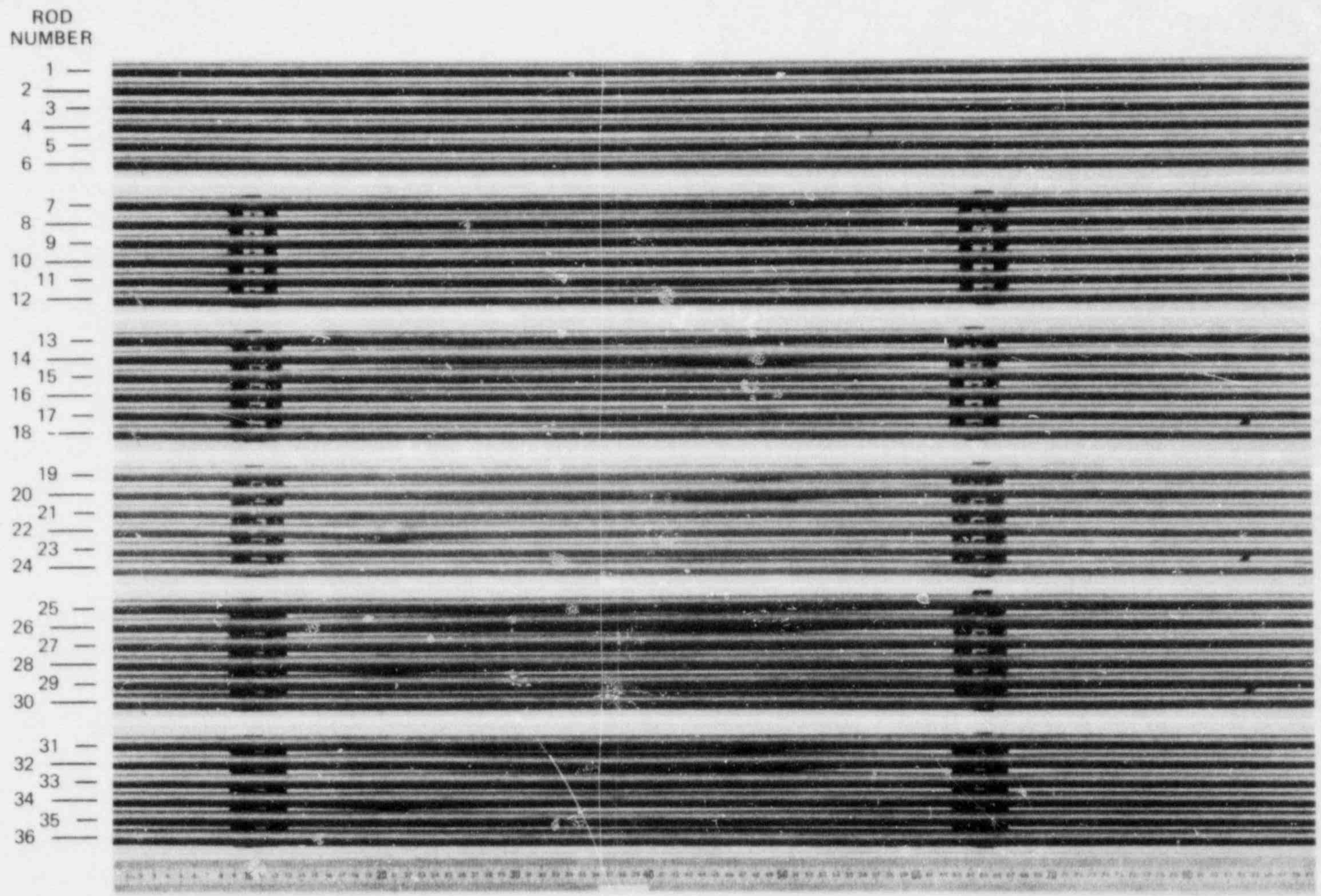


Fig. 93. B-4 bundle viewed from south side as successive layers of rods were removed from undle starting at bottom of photograph and progressing to top. Rod 16 was unpressurized and unheated (electrically) during test.

ORNL PHOTO 7247–81B

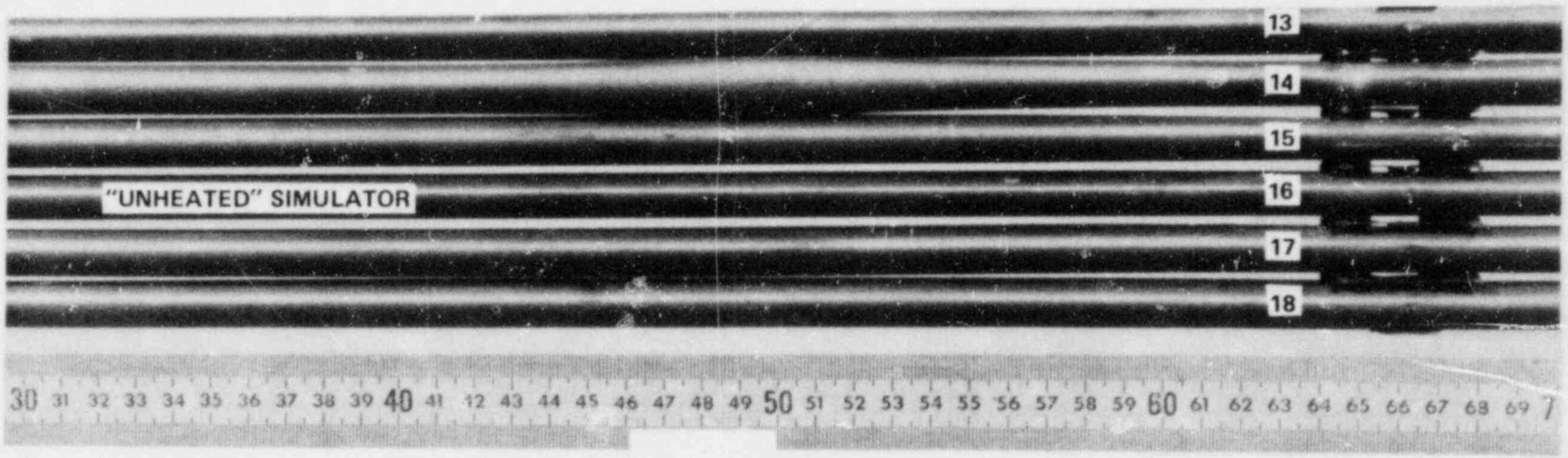


SOUTH

Fig. 94. Ballooned region in B-4 tube No. 14.

ORNL-DWG 81-16442 ETD

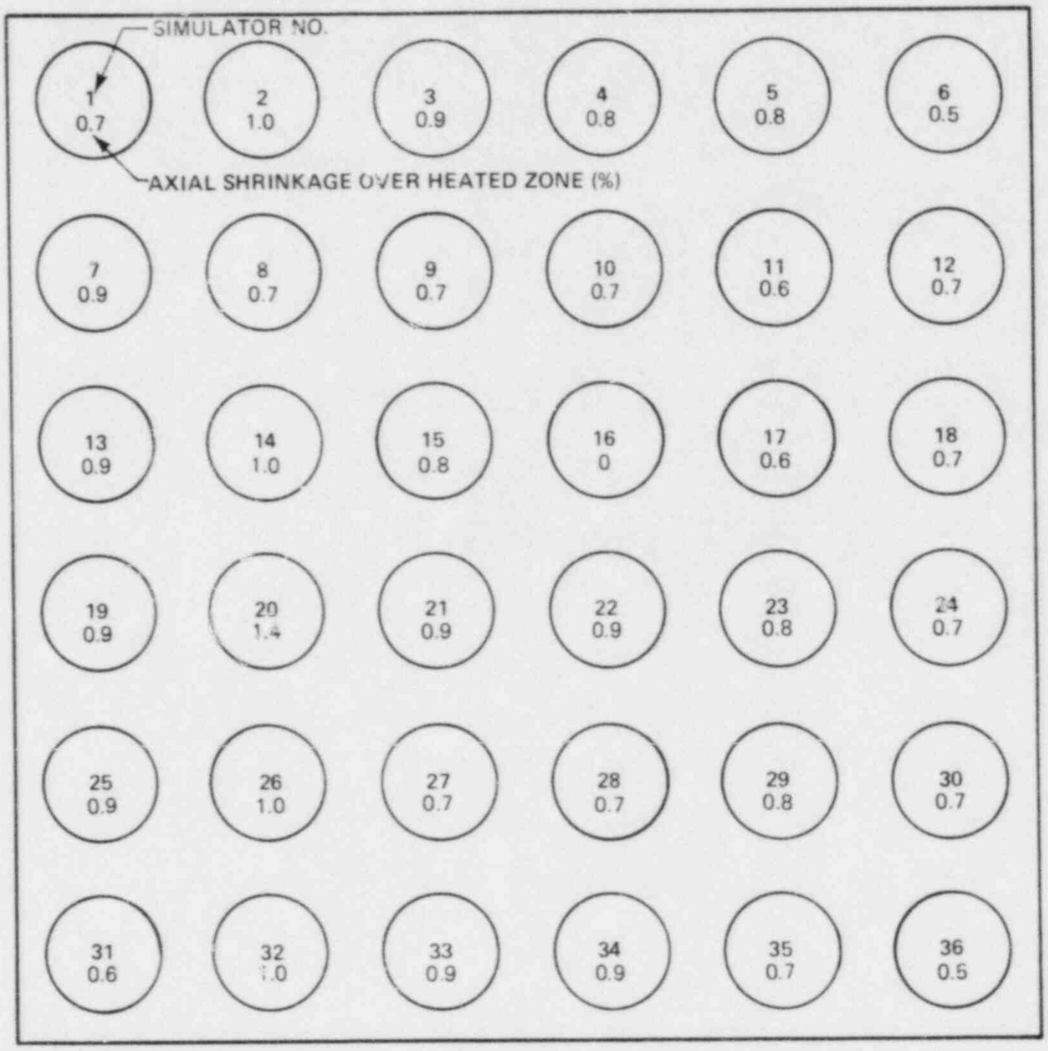


Fig. 95. Simulator axial shrinkage in B-4 test.

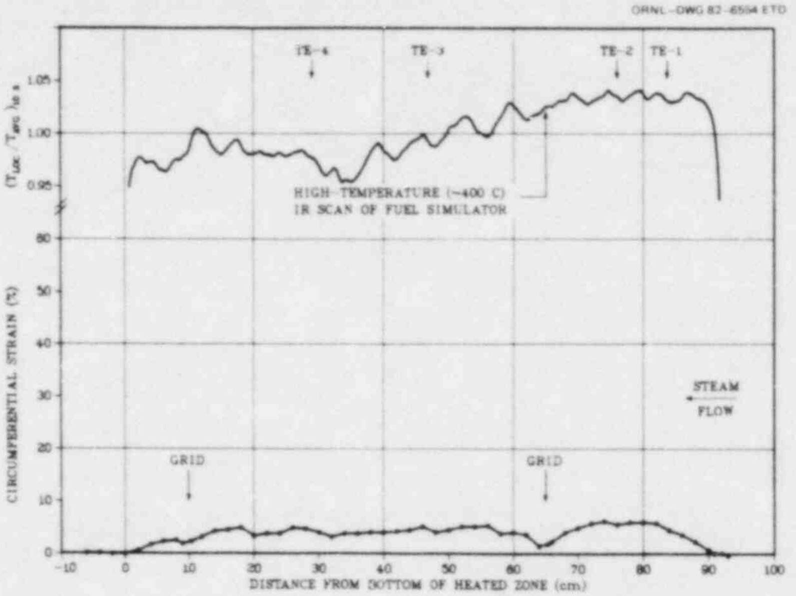


Fig. 96. Deformation profile of tube 1 in B-4 test.

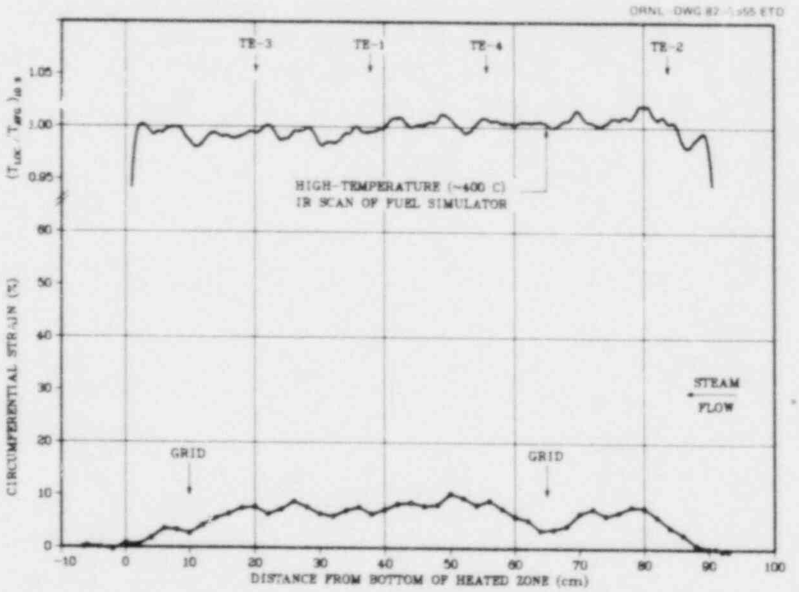


Fig. 97. Deformation profile of tube 2 in B-4 test.

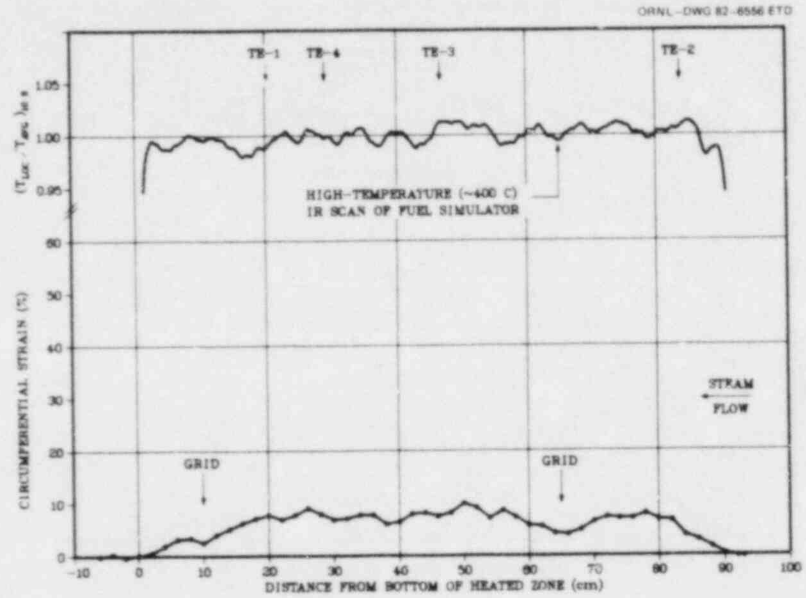


Fig. 98. Deformation profile of tube 3 in B-4 test.

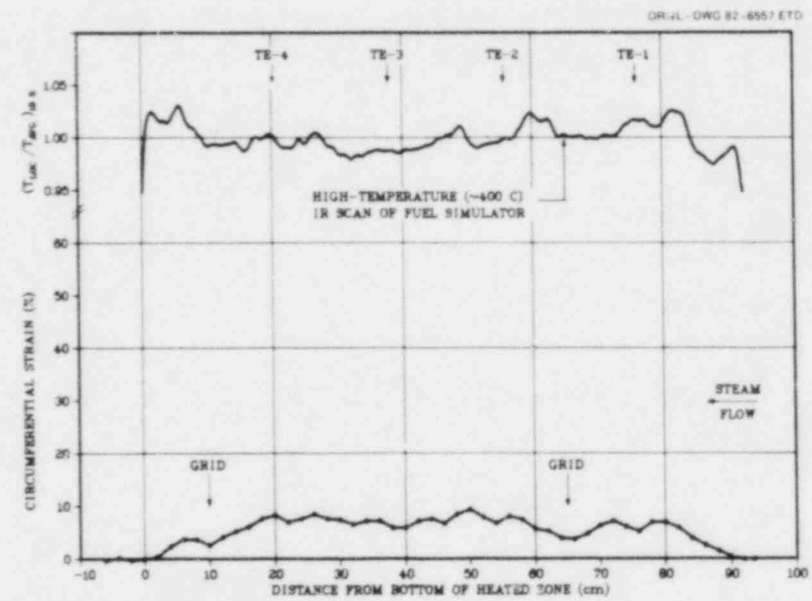


Fig. 99. Deformation profile of tube 4 in B-4 test.

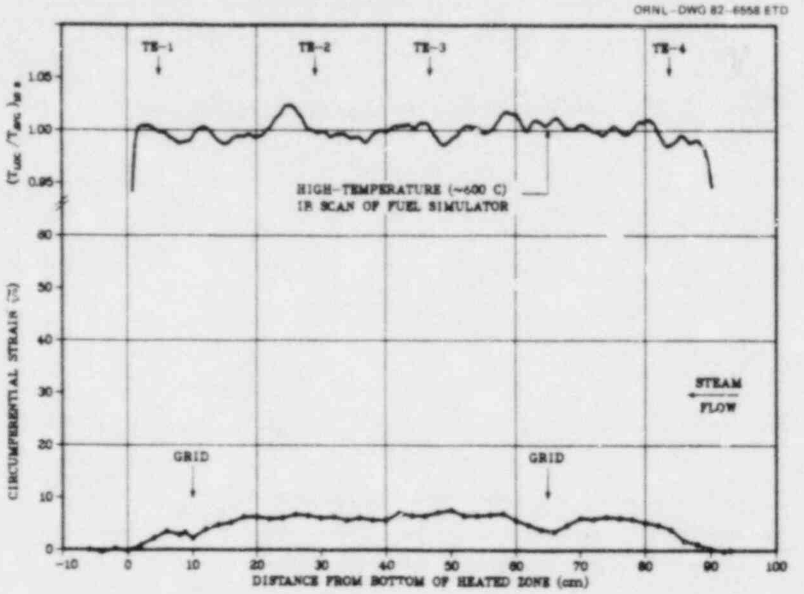


Fig. 100. Deformation profile of tube 5 in B-4 test.

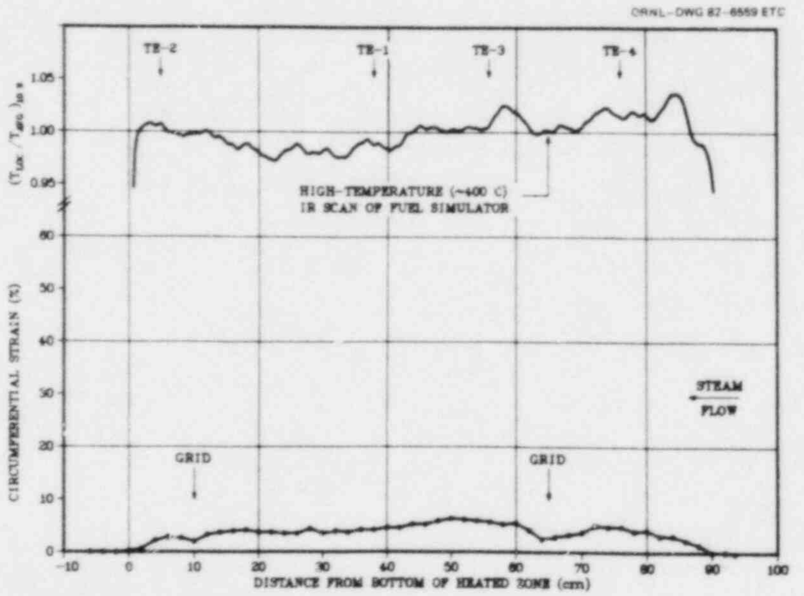


Fig. 101. Deformation profile of tube 6 in B-4 test.

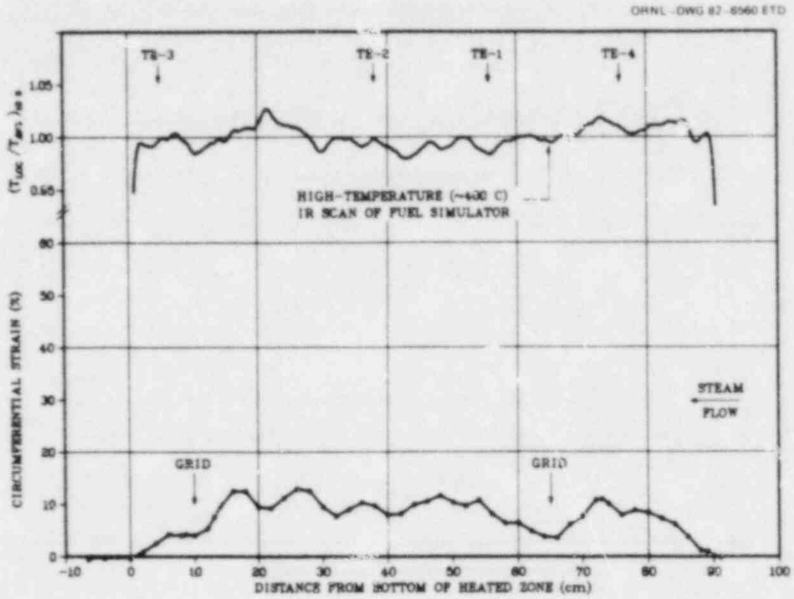


Fig. 102. Deformation profile of tube 7 in B-4 test.

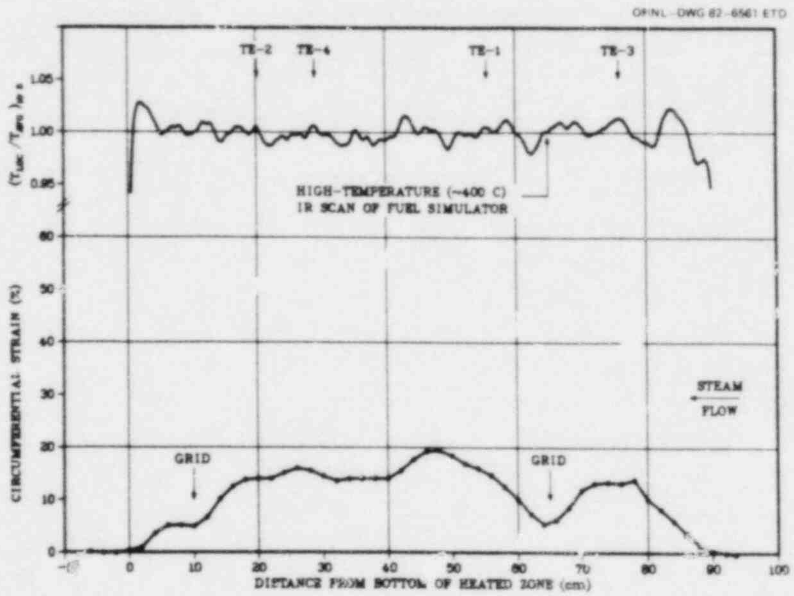


Fig. 103. Deformation profile of tube 8 in B-4 test.

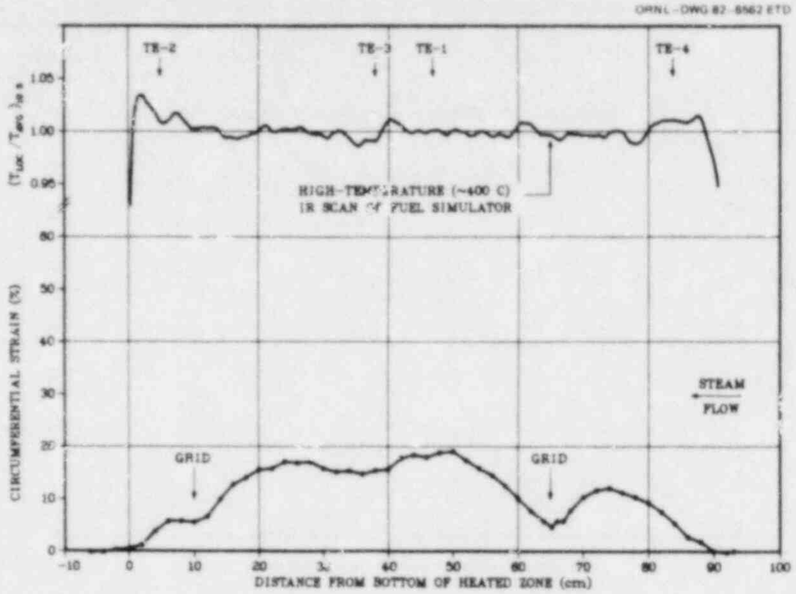


Fig. 104. Deformation profile of tube 9 in B-4 test.

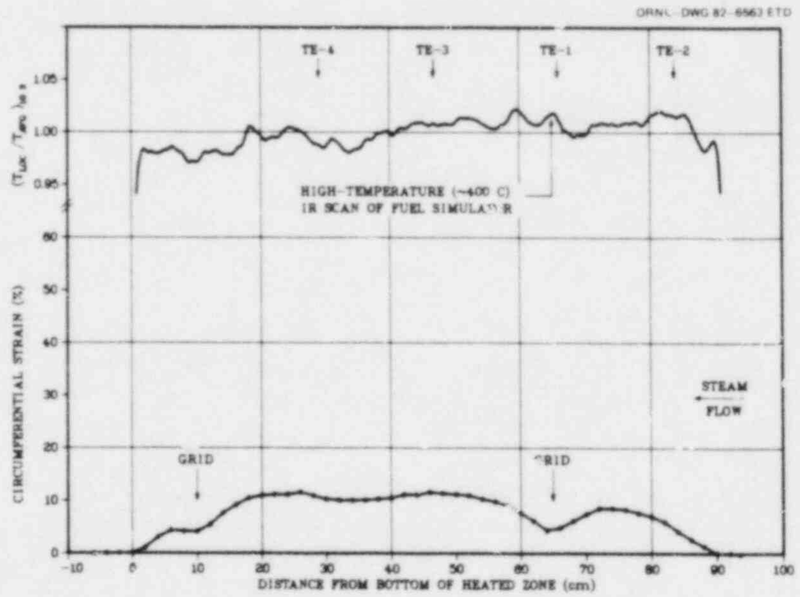


Fig. 105. Deformation profile of tube 10 in B-4 test.

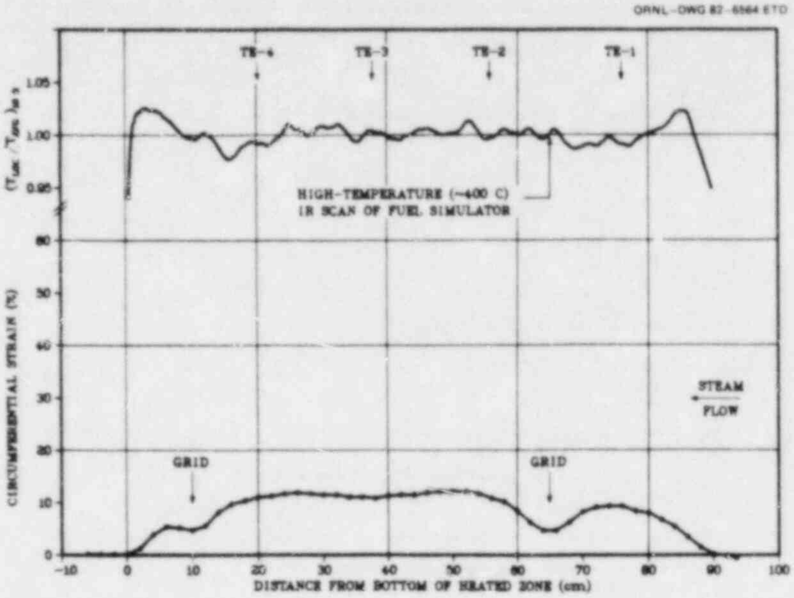


Fig. 106. Deformation profile of tube 11 in B-4 test.

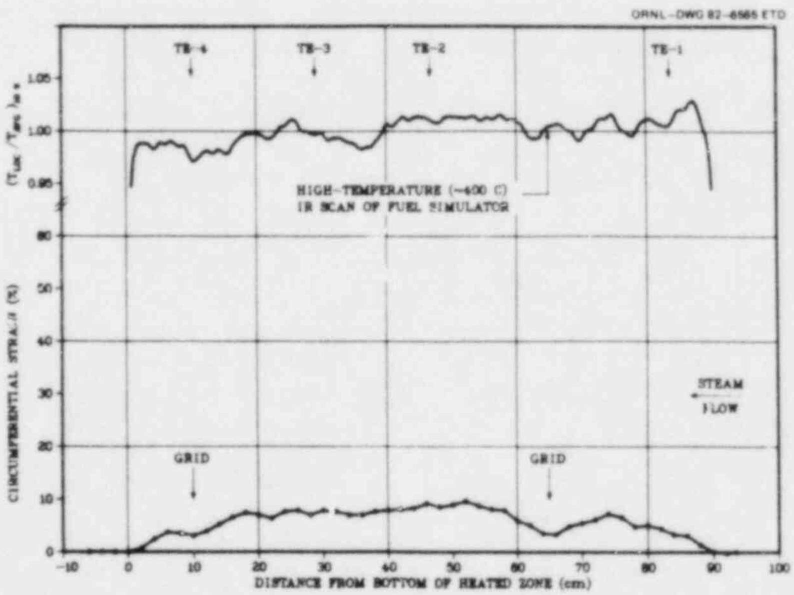


Fig. 107. Deformation profile of tube 12 in B-4 test.

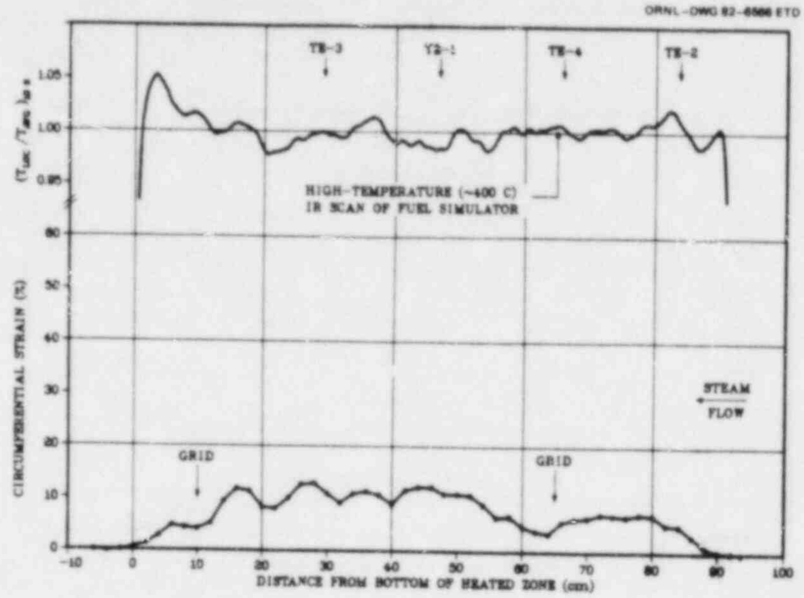


Fig. 108. Deformation profile of tube 13 in B-4 test.

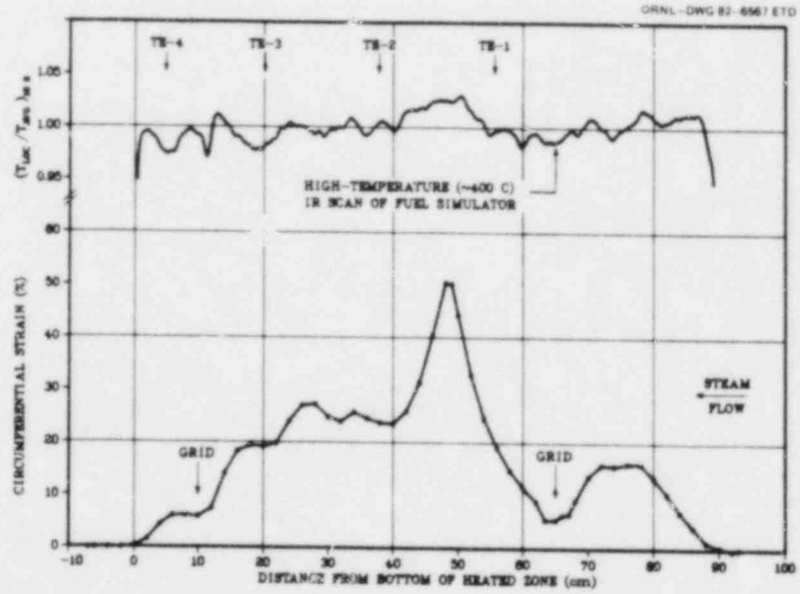


Fig. 109. Deformation profile of tube 14 in B-4 test.

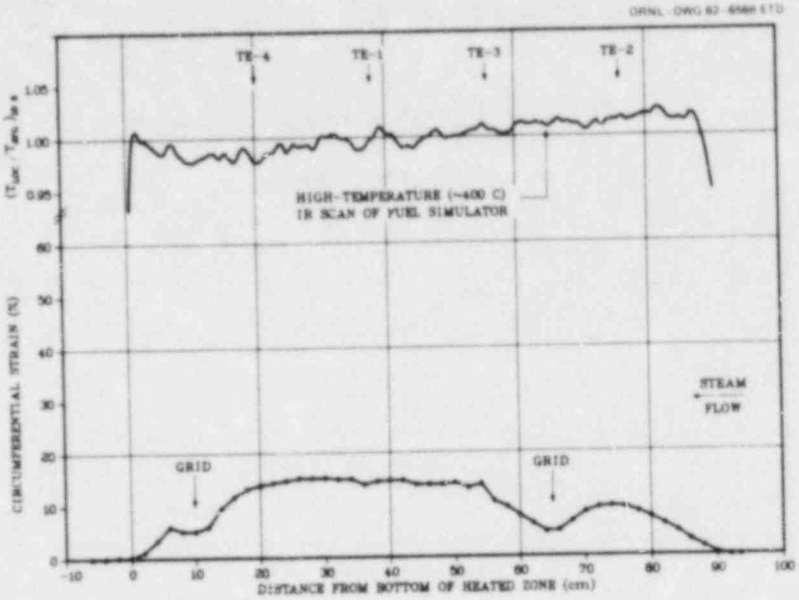


Fig. 110. Deformation profile of tube 15 in B-4 test.

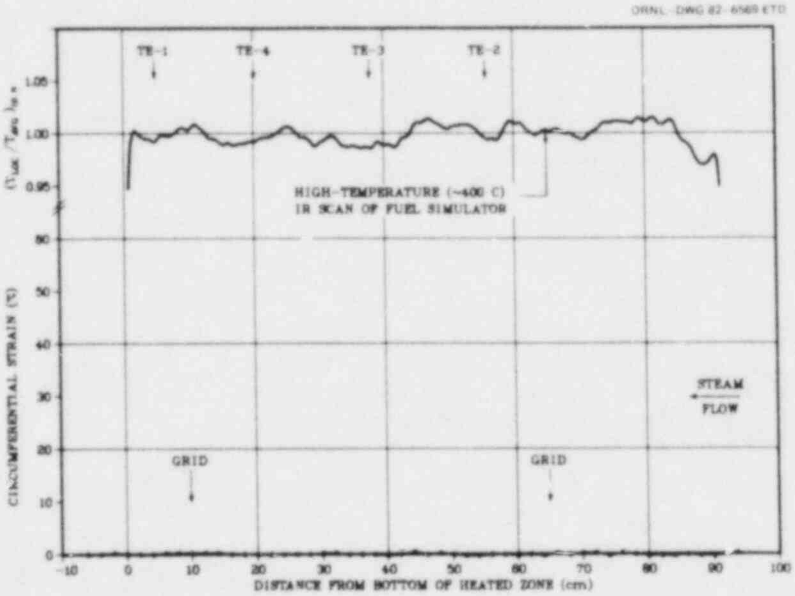


Fig. 111. Deformation profile of tube 16 in B-4 test. Rod 16 was unpressurized and unheated (electrically) during test.

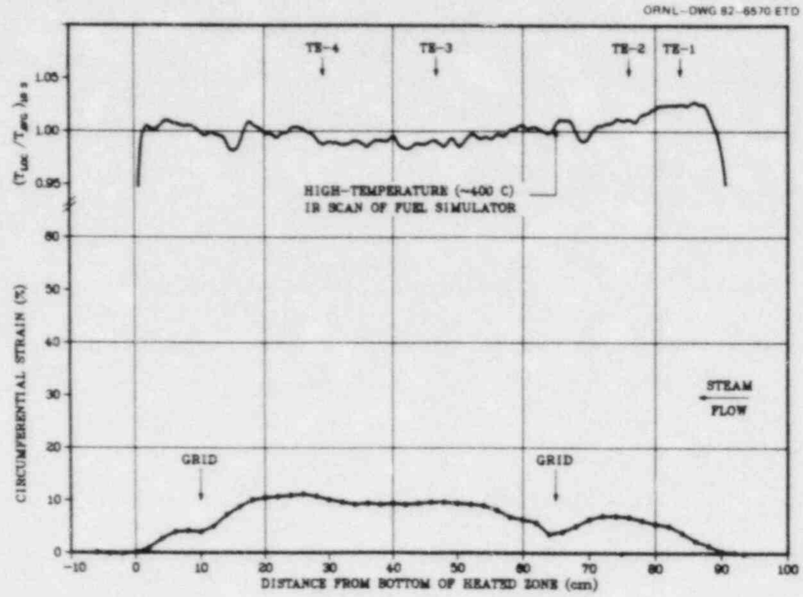


Fig. 112. Deformation profile of tube 17 in B-4 test.

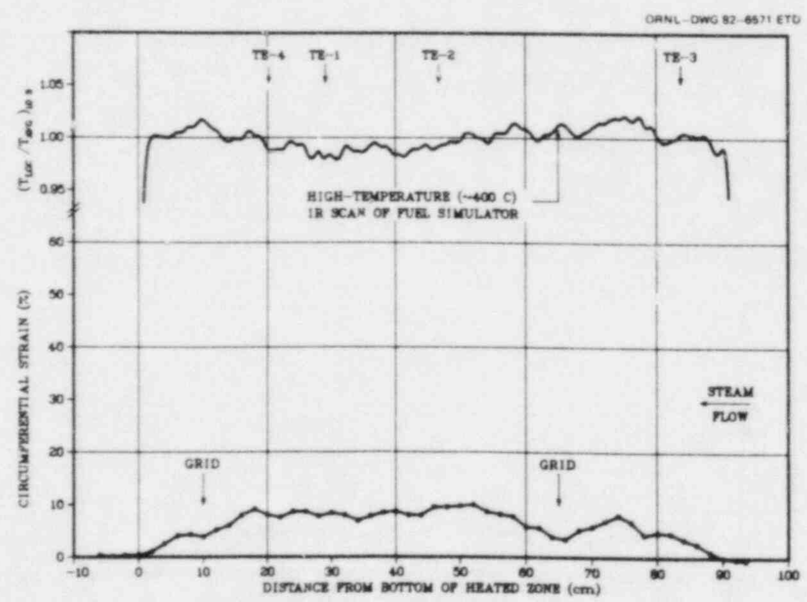


Fig. 113. Deformation profile of tube 18 in B-4 test.

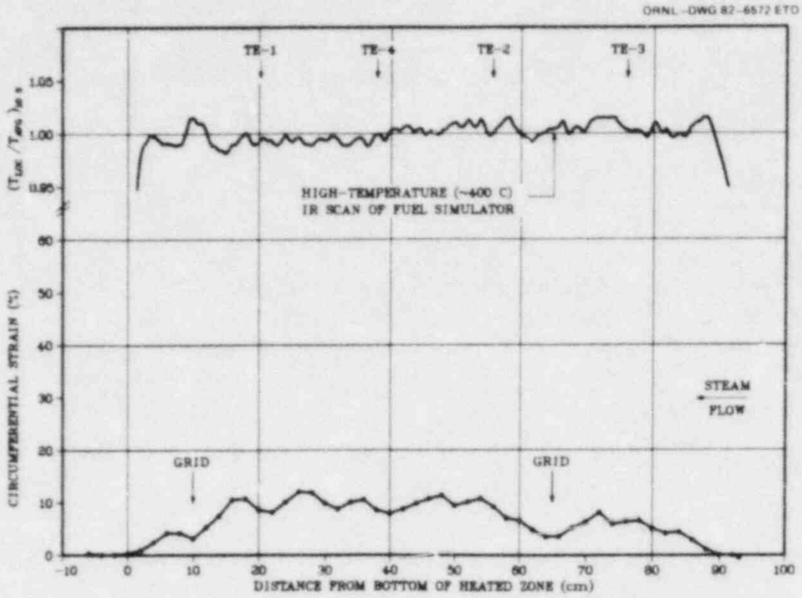


Fig. 114. Deformation profile of tube 19 in B-4 test.

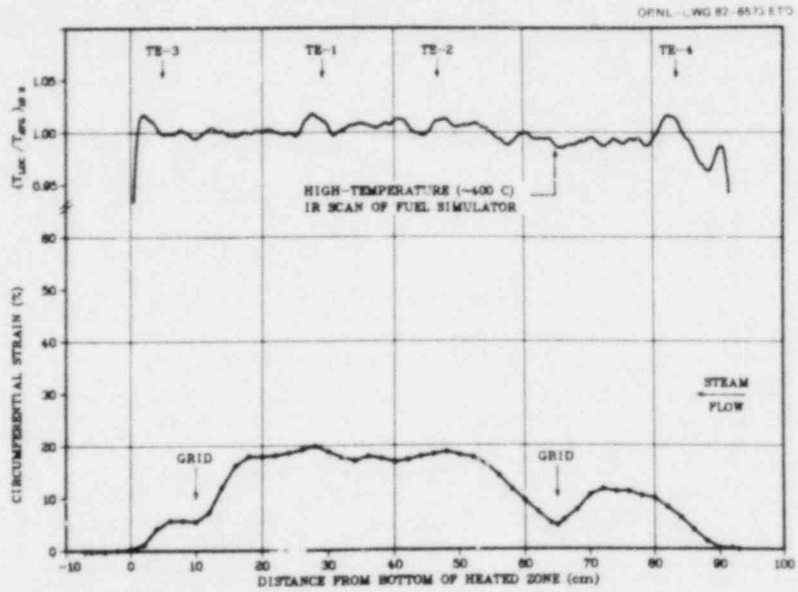


Fig. 115. Deformation profile of tube 20 in B-4 test.

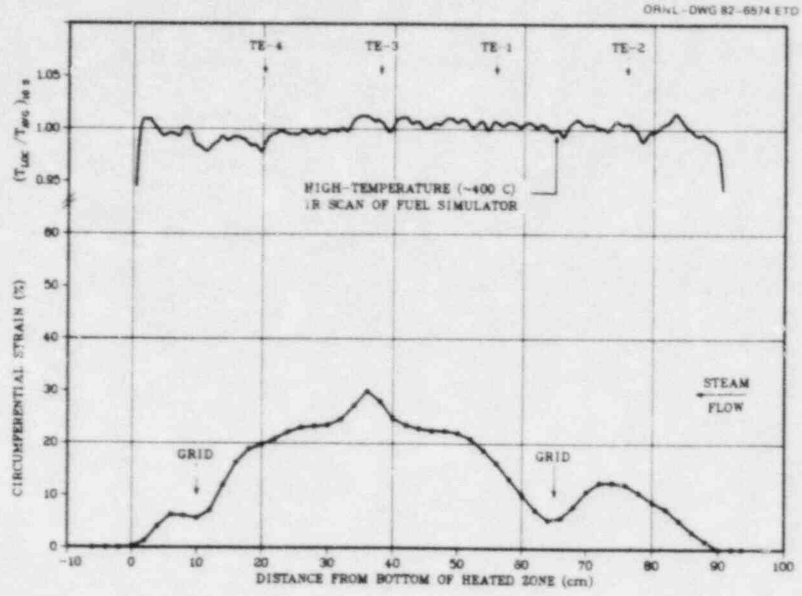


Fig. 116. Deformation profile of tube 21 in B-4 test.

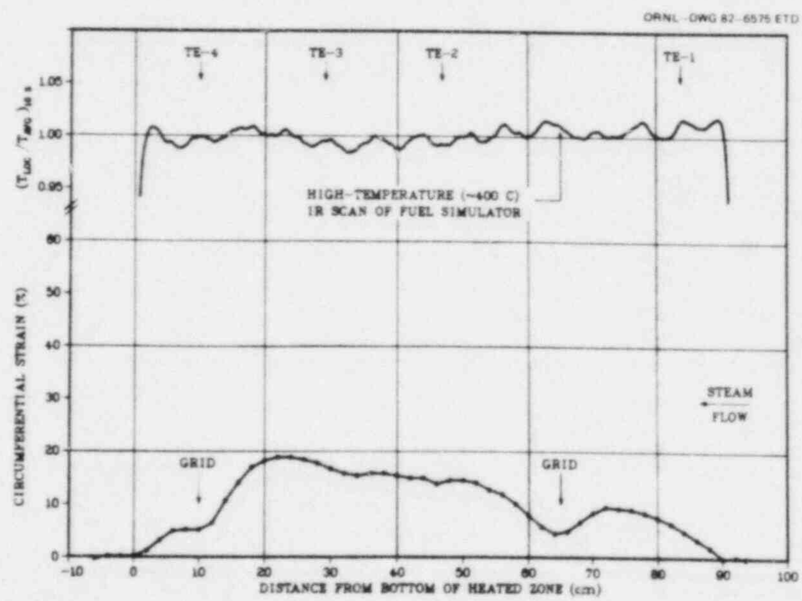


Fig. 117. Deformation profile of tube 22 in B-4 test.

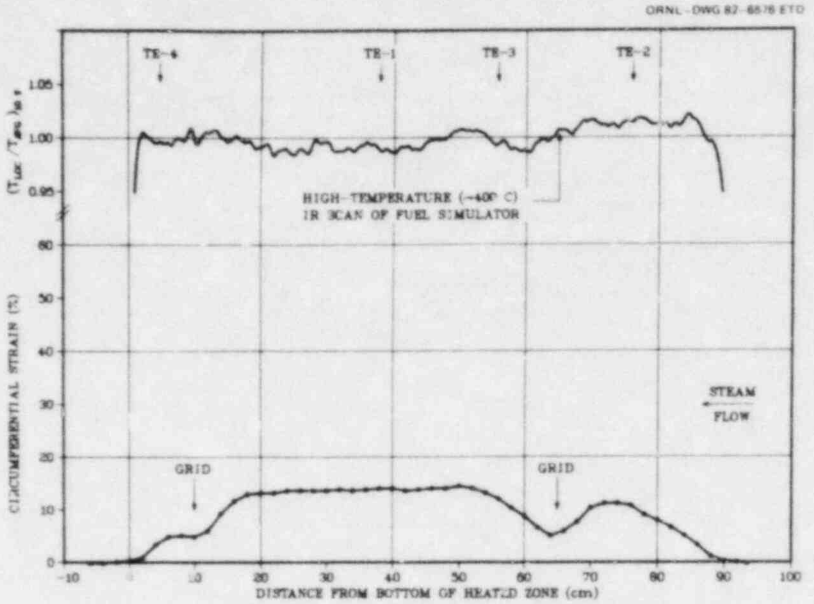


Fig. 118. Deformation profile of tube 23 in B-4 test.

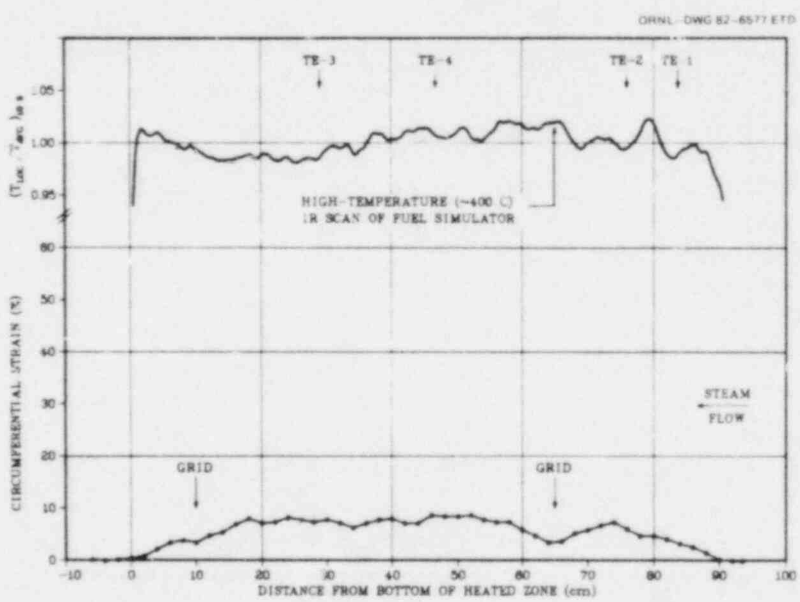


Fig. 119. Deformation profile of tube 24 in B-4 test.

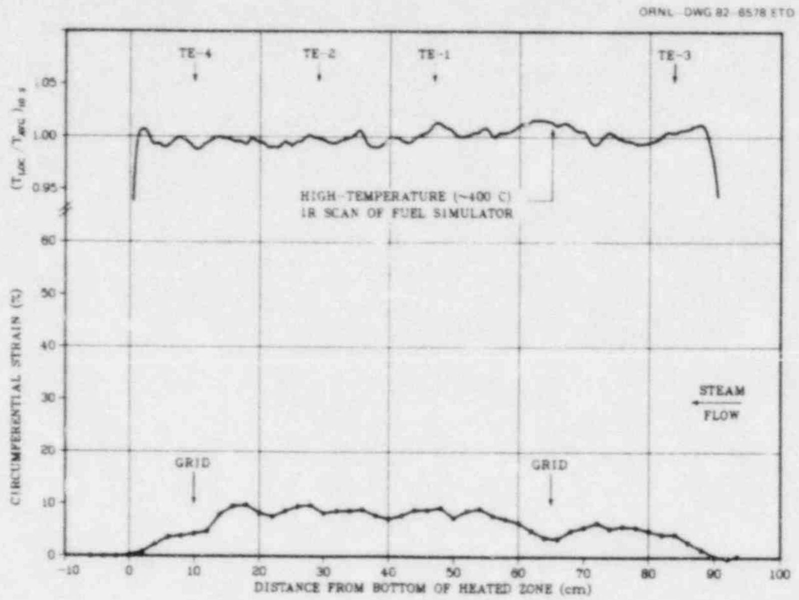


Fig. 120. Deformation profile of tube 25 in B-4 test.

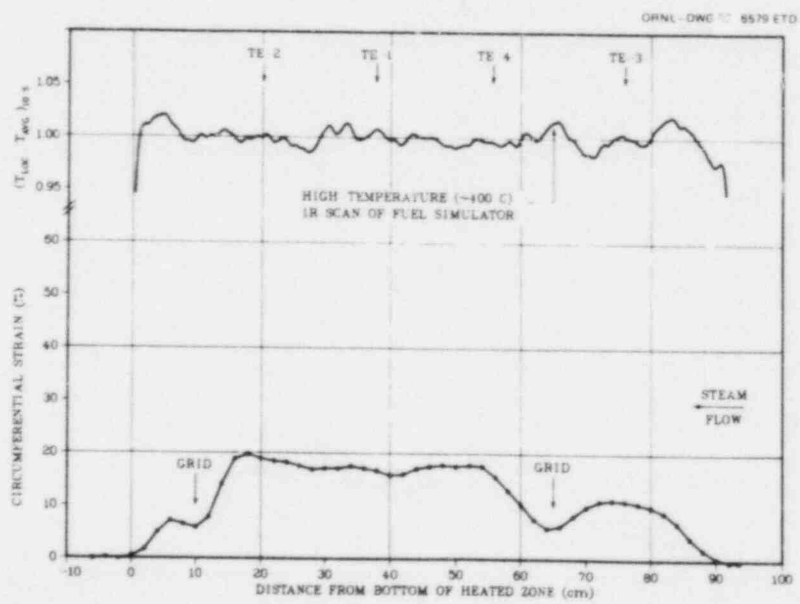


Fig. 121. Deformation profile of tube 26 in B-4 test.

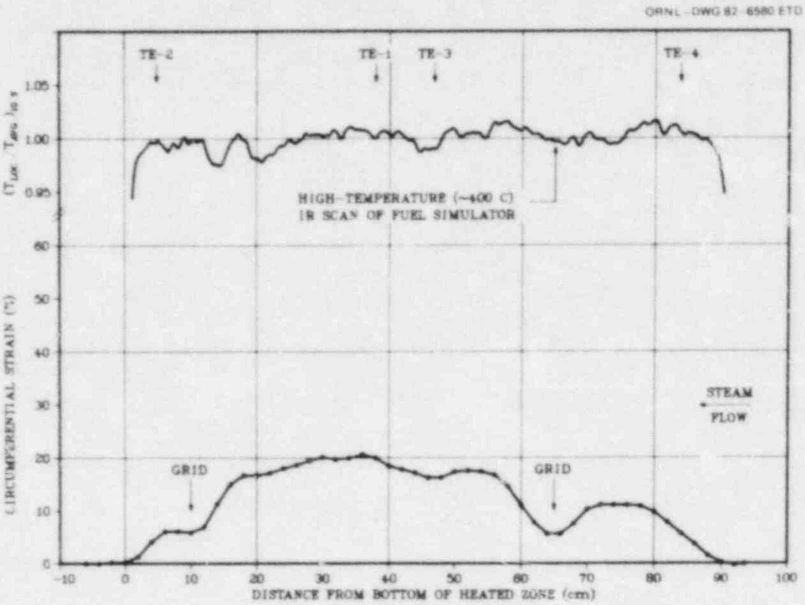


Fig. 122. Deformation profile of tube 27 in B-4 test.

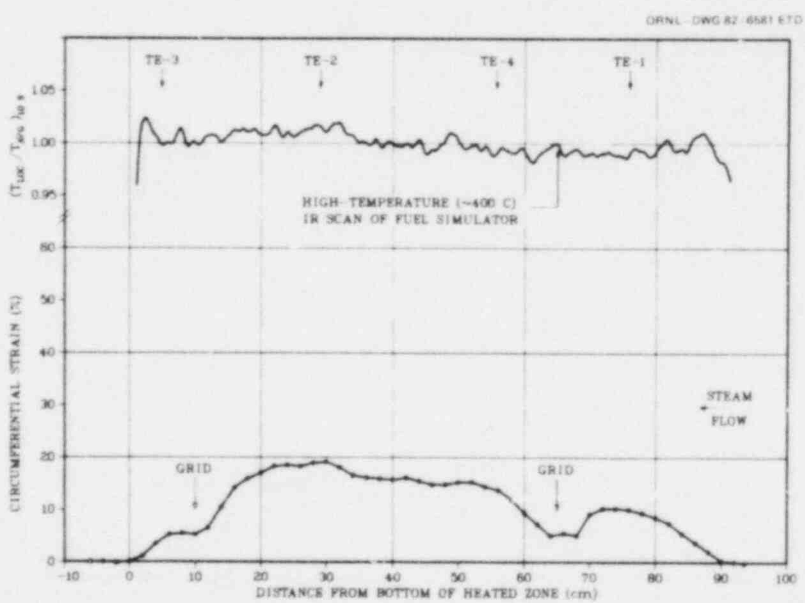


Fig. 123. Deformation profile of tube 28 in B-4 test.

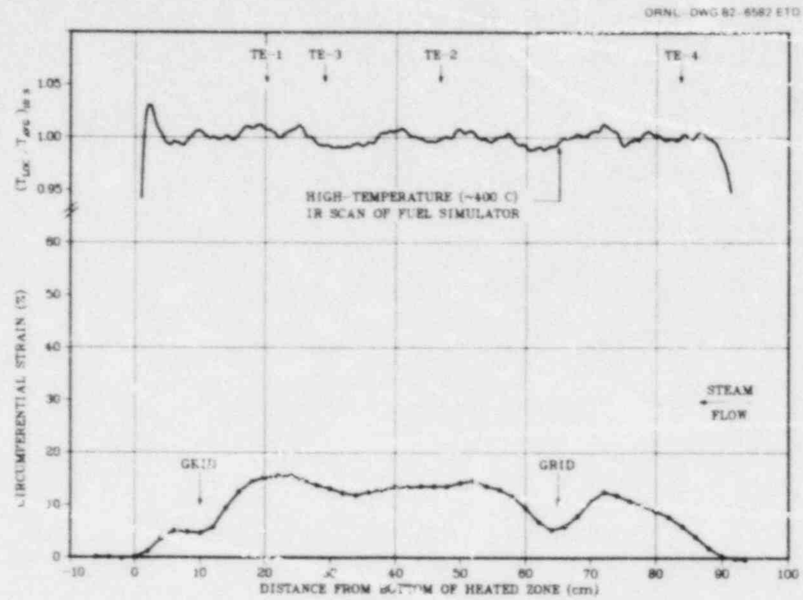


Fig. 124. Deformation profile of tube 29 in B-4 test.

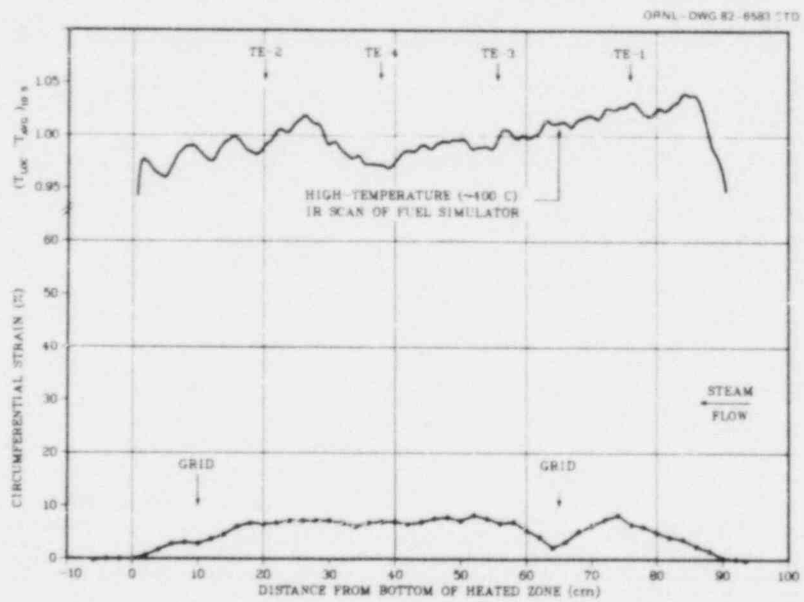


Fig. 125. Deformation profile of tube 30 in B-4 test.

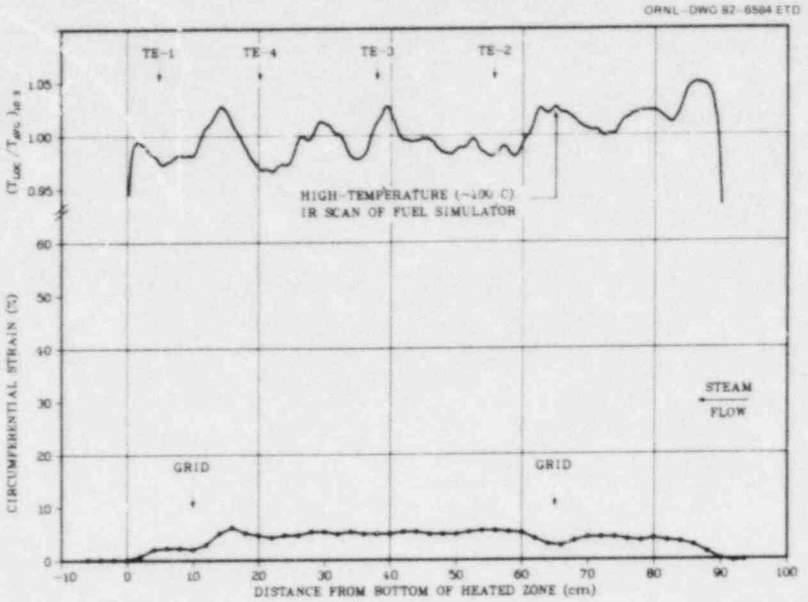


Fig. 126. Deformation profile of tube 31 in B-4 test.

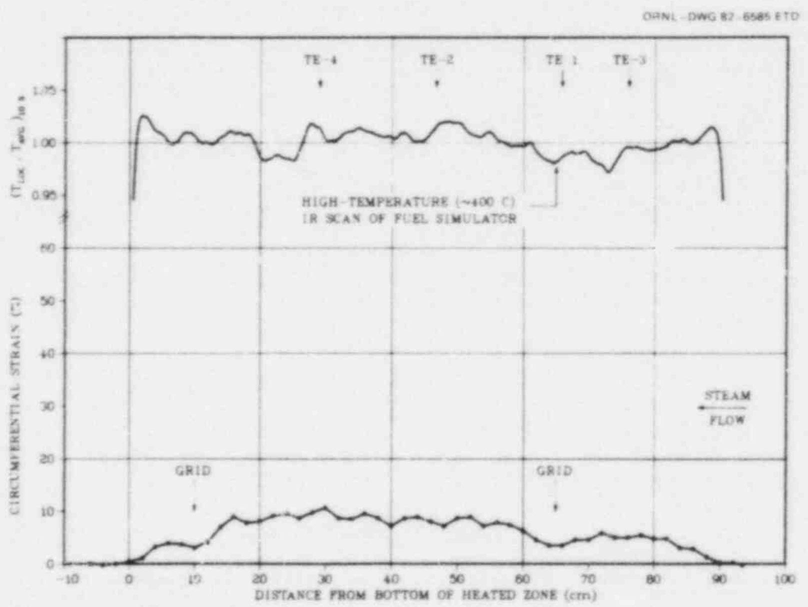


Fig. 127. Deformation profile of tube 32 in B-4 test.

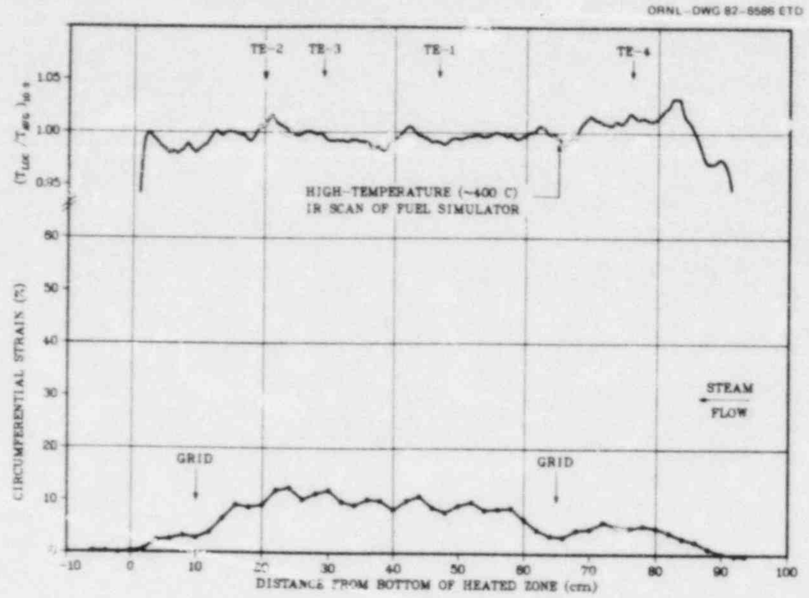


Fig. 128. Deformation profile of tube 33 in B-4 test.

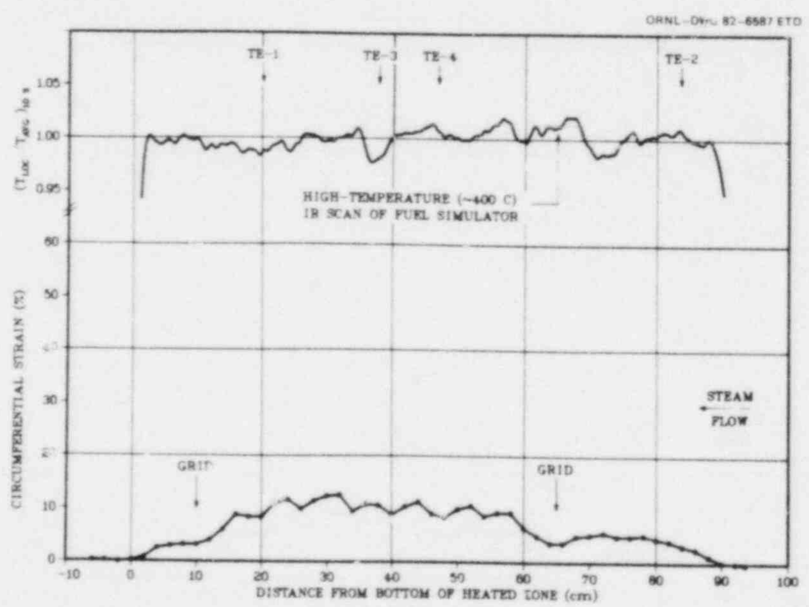


Fig. 129. Deformation profile of tube 34 in B-4 test.

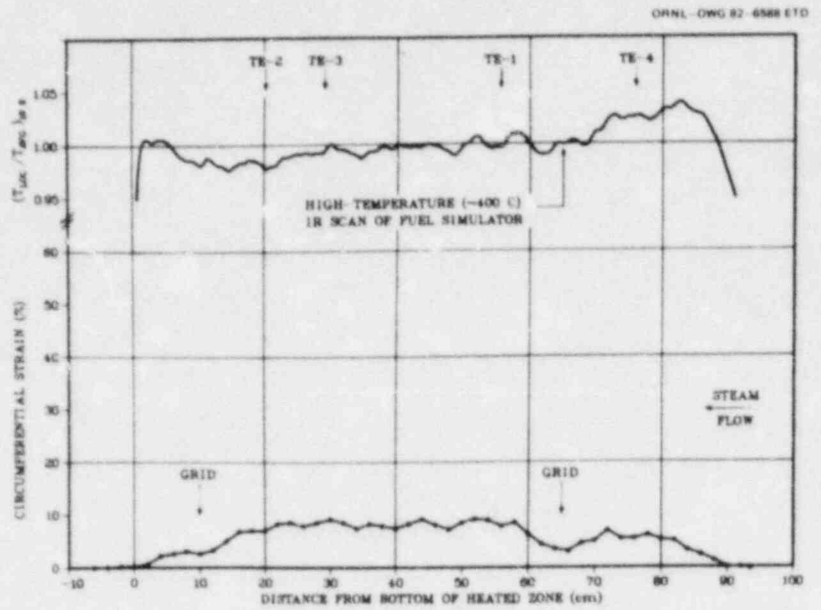


Fig. 130. Deformation profile of tube 35 in B-4 test.

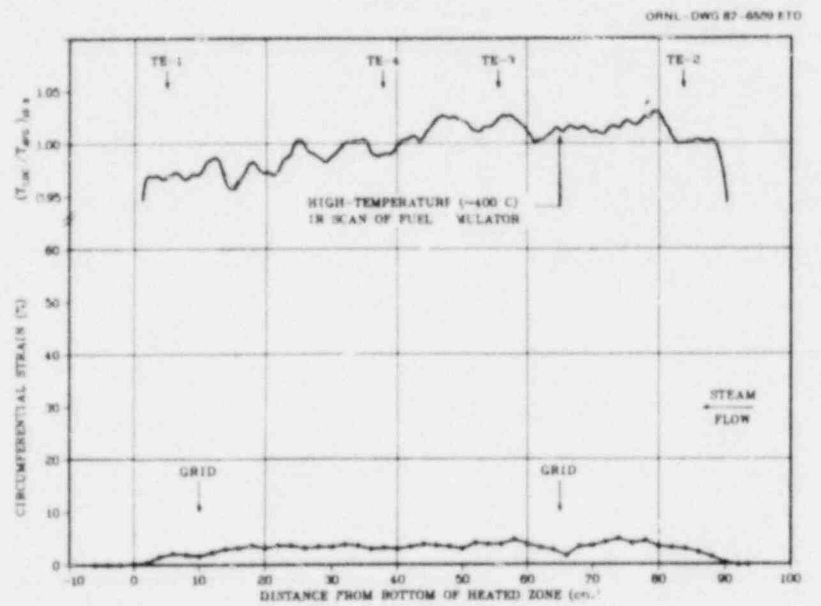


Fig. 131. Deformation profile of tube 36 in B-4 test.

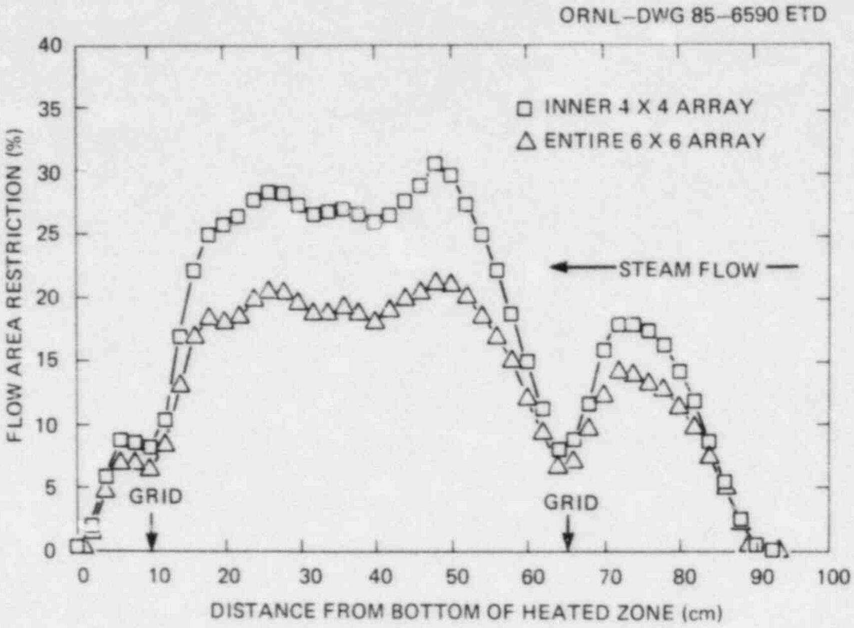


**Fig. 132. Coolant channel flow area restriction in B-4 test.**

NUREG/CR-2968
ORNL/TM-8509
Dist. Category R3

## Internal Distribution

1-5. R. H. Chapman
6. J. L. Crowley
7. D. S. Griffith
8. D. O. Hobson
9-13. A. W. Longest
14. A. L. Lotts
15. H. E. Trammell
16. Patent Office
17. Nuclear Safety Information Center
18. Central Research Library
19. Document Reference Section
20-21. Laboratory Records Department
22. Laboratory Records (RC)

## External Distribution

23. Office of Assistant Manager for Energy Research and Development, DOE, ORO, Oak Ridge, TN 37830
24. Chief, Fuel Behavior Branch, Office of Nuclear Regulatory Research, Nuclear Regulatory Commission, Washington, DC 20555
25. Chief, Core Performance Branch, Office of Nuclear Reactor Regulation, Nuclear Regulatory Commission, Washington, DC 20555
26. R. Van Houten, Fuel Behavior Branch, Office of Nuclear Regulatory Research, Nuclear Regulatory Commission, Washington, DC 20555
27. G. P. Marino, Fuel Behavior Branch, Office of Nuclear Regulatory Research, Nuclear Regulatory Commission, Washington, DC 20555
28. R. A. Adamson, Mail Code V-03, General Electric Company, Vallecitos Atomic Laboratory, P.O. Box 846, Pleasanton, CA 94566
29. D. L. Burman, Westinghouse Nuclear Fuel Division, P.O. Box 355, Pittsburgh, PA 15230
30. C. E. Crouthamel, Exxon Nuclear, Inc., 2955 George Washington Way, Richland, WA 99352
31. F. J. Erbacher, Project Nukleare Sicherheit, Kernforschungszentrum Karlsruhe, Postfach 3640, 75 Karlsruhe, Federal Republic of Germany
32. J. Gittus, UKAEA Atomic Energy Research Establishment, Harwell, Didcot, Oxfordshire, OX11 ORA, England
33. D. L. Hagrman, EG&G Idaho, Inc., INEL, Idaho Falls, ID 83401
34. T. Healey, GEGB Berkeley Nuclear Laboratories, Berkeley, Gloucestershire, GL13 9PB, England
35. T. Hoshi, Japan Atomic Energy Research Institute, Tokai-Mura, Naga-Gum, Ibaraki-Ken, Japan
36. T. Howe, EG&G Idaho, Inc., INEL, Idaho Falls, ID 83401
37. E. T. Laats, EG&G Idaho, Inc., INEL, Idaho Falls, ID 83401
38-39. W. Lowenstein, Electric Power Research Institute, 3412 Hillview Avenue, P.O. Box 10412, Palo Alto, CA 94304
40. A. L. Lowe, Babcock and Wilcox Company, P.O. Box 1260, Lynchburg, VA 24505

41. C. L. Mohr, Pacific Northwest Laboratories, P.O. Box 999, Richland, WA 99352
42. M. Murillo, Electric Power Research Institute, 3412 Hillview Avenue, P.O. Box 10412, Palo Alto, CA 94304
43. H. Rininsland, Projekt Nukleare Sicherheit, Kernforschungszentrum Karlsruhe, Postfach 3640, 75 Karlsruhe, Federal Republic of Germany
44. P. A. Smerd, Combustion Engineering, Inc., 1000 Prospect Hill Road, Windsor, CT 06093
45. W. Spencer, EG&G Idaho, Inc., INEL, Idaho Falls, ID 83401
46-47. Technical Information Center, DOE, Oak Ridge, TN 37830
48-362. Distribution as shown for NRC category R3 (NTIS-10)

☆U.S. GOVERNMENT PRINTING OFFICE 1982-646-055/222

120555078877 1 ANR3
US NRC
ADM DIV OF TIDC
PDR NUREG COPY
POLICY & PUBLICATNS MGT BR
LA 212
WASHINGTON DC 20555